REVIEW

Check for updates

Recent advances in enzymatic carbon–carbon bond formation

Hua Zhao [ID]

Enzymatic carbon–carbon (C–C) bond formation reactions have become an effective and invaluable tool for designing new biological and medicinal molecules, often with asymmetric features. This review provides a systematic overview of key C–C bond formation reactions and enzymes, with the focus of reaction mechanisms and recent advances. These reactions include the aldol reaction, Henry reaction, Knoevenagel condensation, Michael addition, Friedel–Crafts alkylation and acylation, Mannich reaction, Morita–Baylis–Hillman (MBH) reaction, Diels–Alder reaction, acyloin condensations *via* Thiamine Diphosphate (ThDP)-dependent enzymes, oxidative and reductive C–C bond formation, C–C bond formation through C1 resource utilization, radical enzymes for C–C bond formation, and other C–C bond formation reactions.

1. Introduction

Enzymatic carbon–carbon (C–C) bond formation reactions (such as the Michael addition, Friedel–Crafts alkylation, and the aldol, Mannich, Morita–Baylis–Hillman, Henry, and Diels–Alder reactions) often lead to asymmetric molecules that are essential to the synthesis of many pharmaceutical ingredients such as monoterpene indole [MIAs] and benzylisoquinoline alkaloids.[1–6] As an example, asymmetric Michael reaction is a key step for the preparation of pharmaceutical ingredients (Fig. 1) such as marine alkaloid (–)-nakadomarin A (an anti-cancer, antifungal and antibacterial compound),[7] hydro-dibenzofuran alkaloids such as (–)-galanthamine (treating Alzheimer's disease),[8] and (+)- and (–)-trigonoliimine A (anti-HIV and anti-cancer activities).[9] Michael reactions often require complex and expensive chiral organocatalysts to achieve high enantioselectivities, which can be easily accomplished by judicious selection and design of enzymes. It is very important to point out that in addition to their natural catalytic activities, some enzymes could catalyze completely different types of reactions, which is known as catalytic promiscuity.

Over the past decade, there have been several excellent general reviews on related topics focusing on the formation of tetrasubstituted carbon stereocenters catalyzed by aldolases (including those accepting fluoropyruvates as nucleophiles[10]), hydroxynitrile lyases, and thiamine diphosphate (ThDP)-dependent enzymes,[11] and promiscuous enzyme activities of hydrolases (*e.g.*, lipases, proteases, and trypsin), trans-glutaminase, hydroxynitrile lyases, 4-oxalocrotonate tautomerase, transketolases, ThDP-dependent enzymes, as well as those

acylases-catalyzed aldol condensation, Michael addition, Knoevenagel condensation, Mannich reaction, and Henry reactions.[12–14] This review intends to provide a more systematic overview of key C–C bond formation reactions and enzymes with more recent examples, and focus on catalytic mechanisms. However, it is not the main goal of this review to discuss C–C bond formations through biosynthesis[15] such as DNA methylation,[16] polyketide *C*-methylation,[17] biosynthesis of L-sorbose and L-psicose using biocatalytic aldol addition in the *Coryne-bacterium glutamicum* strain,[18] biosynthetic pathway of the phosphonate phosphonothrixin,[19] and cytochrome P450 enzymes-catalyzed biosynthesis of mycocyclosin and guatyr-omycine,[20] *etc.* To provide a high-level glance of this comprehensive topic, Table 1 presents key reaction types and enzymes with examples of recent advances in the field.

2. Aldol reaction

2.1. Aldolases

Aldol addition catalyzed by different aldolases is a power tool to facilitate C–C bond ligations and form up to two asymmetric centers as depicted by earlier reviews.[13,14,21,23,24,70–78] In particular, formaldehyde as an emerging C1 source can be converted to valuable β- and γ-hydroxycarbonyl compounds (especially carbohydrates) by aldolases and thiamine diphosphate (ThDP)-dependent enzymes.[79] Aldolases belong to a subset of lyases (EC 4), and promote the addition of a ketone donor (nucleophile) to an aldehyde acceptor stereoselectively. Aldolases abstract α-proton of the carbonyl group to produce a carbon nucleophile bound at the active site, which attacks the acceptor component (*i.e.*, electrophile) such as aldehyde's carbonyl carbon. Based on the reaction mechanism (Fig. 2), there are two types of aldolases, where Type I (known as lysine-dependent; found in animals and

Department of Bioproducts and Biosystems Engineering, University of Minnesota, St. Paul, MN 55108, USA. E-mail: zhao1822@umn.edu; huazhao98@gmail.com
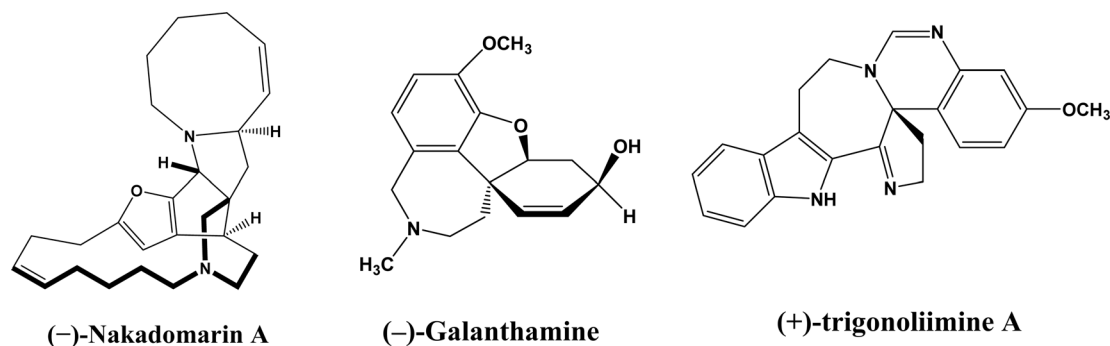
Fig. 1 Structures of several pharmaceutical ingredients.

plants) promotes the enamine formation from an imine (a Schiff base) between carbonyl group and lysine residue of the enzyme, and Types II (known as metal-dependent; found in bacteria and fungi) forms an enolate *via* chelation to a Lewis-acidic transition metal cation (usually Zn^{2+}).[21,23,70,72] Conversely, based on their donor specificity, aldolases can be categorized into five types based on different donor substrates:[23,24,71,72,74,80,81] (a) pyruvate, phosphoenolpyruvate, oxaloacetate, or 2-oxobutyrate, (b) dihydroxyacetone phosphate (DHAP), (c) dihydroxyacetone (DHA) and other unphosphorylated analogues (*e.g.*, D-fructose-6-phosphate aldolase), (d) pyridoxal 5′-phosphate (PLP) (also known as threonine aldolases or glycine/alanine-dependent; threonine aldolases and serine hydroxymethyltransferase catalyze the addition of glycine/alanine to aldehydes),[24] and (e) acetaldehyde [*i.e.* 2-deoxy-D-ribose 5-phosphate aldolase (DERA)]. It is interesting to note that 4-fluorothreonine transaldolase from *Streptomyces* sp. MA37 (FTaseMA) possesses both serine hydroxymethyltransferase and aldolase catalytic domains to catalyze transaldol reactions, and the aldolase domain is Zn^{2+}-dependent; basically, this is the PLP-dependent enzyme fused with a metal-binding domain.[82] Since the forementioned review articles have discussed various types of aldolases and their applications, this paper intends not to duplicate the effort but rather to focus on recent advances in several areas.

2.1.1 Aldolase donors and acceptors. Aldolases have high substrate specificity for donor structures, but are more tolerant to various aldol acceptor structures.[72] For this reason, one bottleneck of aldolase-catalyzed C–C bond formation is the limited choice of donors.[23] One solution is to rely on direction evolution, protein engineering, and computational *de novo* enzyme design to develop more robust and more substrate-tolerant aldolases [*e.g.*, the transaldolase family[84,85] and the discovery of fructose-6-phosphate aldolase (FSA) by serendipity[86,87]].[21–24] Meanwhile, several aldolases have been identified to take ketones as acceptors in enzymatic aldol addition. Wang and co-workers[27] reported that 4-hydroxy-4-methyl-2-oxoglutarate/4-carboxy-4-hydroxy-2-oxoadipate (HMG/CHA) aldolase from *Pseudomonas putida* F1 in the presence of Mg^{2+} or Mn^{2+} could catalyze the homo-aldol addition of pyruvate, or the addition of pyruvate to 4-hydroxy-2-keto acids including oxaloacetate (Fig. 3). In another study,[28] DHAP-dependent L-rhamnulose-1-phosphate aldolase (RhaD) from

Bacteroides thetaiotaomicron in the presence of Co^{2+} is capable of stereoselectively catalyzing the aldol reaction between DHAP and several α-hydroxylated ketones (*e.g.*, hydroxyacetone, 1-hydroxybutanone, hydroxypyruvate, and L-erythrulose) affording optically pure tertiary alcohols with 76–95% yields, although no reaction was observed for non-activated ketones such as acetone, butanone, cyclopentanone, and 4-hydroxybutan-2-one. Yang *et al.*[29] examined the catalytic behavior of L-rhamnulose-1-phosphate aldolase (RhaD) and L-fuculose-1-phosphate aldolase (FucA) from *Escherichia coli* in the aldol reaction of DHAP and DHA, and the subsequent catalysis by acid phosphatase (AP) to remove phosphate group and also form dendroketose (Fig. 4). A more recent study[30] indicated that D-fructose-6-phosphate aldolase (FSA) catalyzed the oxidation and then aldol addition of hydroxyacetone or 1-hydroxy-2-butanone to form diketones, and suggested the likely mechanism being that hydroxy groups in hydroxyketones are oxidized to aldehydes (2-oxoaldehydes), which act as acceptors to react with hydroxyketones to form aldol products (Fig. 5).

2.1.2 DHAP-dependent aldolase mechanism. To elucidate the catalytic mechanism of DHAP-dependent rhamnulose-1-phosphate aldolase (RhuA)-catalyzed aldol reaction in Fig. 6, electronic structure calculations *via* the DFT method were completed by considering the substrate molecules, Zn^{2+}, and 13 neighboring residues.[31] The calculations led to a five-step mechanism for the aldol cleavage as illustrated in Fig. 7: (1) the substrate R1P binds with Zn^{2+} through points of Zn–O interactions, and is stabilized by H-bonds and polar attraction with amino acid residues; (2) there is a proton transfer from –OH to E171′ causing the cleavage of C3–C4 bond, where the activation energy is estimated to be 24.2 kcal mol^{-1}; (3) the release of LLA and proton transfer from E171′ to a residue E117; (4) the protonation of DHAP moiety at C-3 by E117, which requires a low activation energy of 4.8 kcal mol^{-1}; and (5) the release of DHAP. Among these five steps, the C–C bond cleavage (E_a = 24.2 kcal mol^{-1}) and the DHAP deprotonation (E_a = 22.0 kcal mol^{-1}) are rate-controlling steps for retro- and aldolic reactions, respectively. Several amino acid residues (*i.e.*, E117, E171′, G31, and N29) and the Zn^{2+} co-factor are key players in the mechanism; in particular, E117 and E171′ act as two acid/base catalytic residues, and E171′ is directly involved in the C–C bond formation.

Table 1 Summary of enzymatic carbon–carbon (C–C) bond formation reactions

Type of reaction	Enzyme	Examples of recent advances

Aldol addition	**Aldolases**
	Based on mechanisms (Fig. 2):
	  (a) Type I aldolases (known as lysine-dependent)
	  (b) Types II aldolases (known as metal-dependent)
	Based on their donor specificity:
	  (a) Pyruvate, phosphoenolpyruvate, oxaloacetate, or 2-oxobutyrate
	  (b) Dihydroxyacetone phosphate (DHAP)
	  (c) Dihydroxyacetone (DHA) and other unphosphorylated analogues (*e.g.*, D-fructose-6-phosphate aldolase)
	  (d) Pyridoxal 5′-phosphate (PLP) (also known as threonine aldolases or glycine/alanine-dependent)
	  (e) Acetaldehyde [*i.e.* 2-deoxy-D-ribose 5-phosphate aldolase (DERA)]
	Non-aldolases: lipases and proteases
		• Threonine aldolase from *Pseudomonas* sp. was mutated to improve or invert its stereoselectivity towards aromatic aldehydes[32]
		• Protein engineering and computational *de novo* enzyme design to develop more robust and more substrate-tolerant aldolases[21–24]
		
		• Ketones were used as acceptors in aldol addition.[27–30]
		
		• DHAP-dependent aldolase mechanism was illustrated through electronic structure calculations *via* the DFT method[31]
		
		• Lipases catalyzed the aldol reaction between benzaldehyde derivatives with acetone[33]
		• Alcalase (protease from *Bacillus licheniformis*) catalyzed the aldol addition of 4-nitrobenzaldehyde and acetone[34]
		• Porcine pancreas lipase (PPL) favored the aldol product (*vs.* olefin products) especially in more hydrophobic deep eutectic solvent (DES)[35]

	Henry reaction (nitroaldol addition): hydroxy nitrile lyases, transglutaminase, lipases, and D-aminoacylase	• Alcalase was able to catalyze the Henry reaction between 4-nitrobenzaldehyde and nitromethane[34] • Enzymatic Henry reaction in in TX-100/H$_2$O/[BMIM][PF$_6$] microemulsions was examined[36] • Gelatin and collagen proteins showed great potential as catalysts for Henry reactions[37]
Knoevenagel condensation	Lipases, α-amylase, protease, papain, D-aminoacylase, Baker's yeast, ene-reductase (NerA), and bovine serum albumin (BSA)	• Immobilized lipase B from *Candida antarctica* (CALB) catalyzed decarboxylative aldol reactions of aromatic aldehydes and β-ketoesters[38] • But no promiscuous catalytic activity for the decarboxylative aldol addition and Knoevenagel reaction between 4-nitrobenzaldehyde and ethyl acetoacetate catalyzed by CALB[39] • PPL displayed higher reaction rates and yields for Knoevenagel condensation in water-mimicking ionic liquids (ILs) than *tert*-butanol, glymes, and [BMIM][Tf$_2$N]. But tertiary amide solvents allowed 8.2–11.1 folds of increases in the initial reaction rate than dual-functionalized ILs[40] • Baker's yeast as the whole cell biocatalyst catalyzed the Knoevenagel condensations between aryl aldehydes and malononitrile (or ethyl cyanoacetate, or 2,4-thiazolidinedione)[41]
Michael addition (1,4-addition)	Lipases, proteases, D-aminoacylase, duplex DNA, G-quadruplex DNA, and DNA/RNA-derived hybrid catalysts	• CALB mutant exhibited much faster Michael addition rates than the wild type[42] • Acetamide acted as co-catalyst of CALB to promote Michael additions of aromatic nitroolefins and less-activated ketones[43] • In contrast to other studies, one study[44] reported no stereoselectivity for lipase-catalyzed Michael additions • Hydroxy-functionalized ionic liquids (ILs) led to higher Michael addition yields than longer alkyl chain-substituted ILs[45]
Friedel–Crafts alkylation and acylation	Peptides, methyltransferases, dimethylallyl-tryptophan synthases, biosynthetic enzyme CylK, squalene hopene cyclases (SHCs), artificial metalloenzyme, and acyltransferase (ATase)	• Several methyltransferases originally found in bacteria catalyzed Friedel–Crafts alkylations of coumarins, naphthalenediols, and aromatic amino acids[46–49] • The artificial LmrR metalloenzyme promoted the enantioselective Friedel–Crafts alkylation[50] • A mutant of ATase (known as *Pp*ATaseCH) showed five-time higher activities than the wild type[51]
Mannich reaction	Acylase, lipases, trypsin, α-amylase, and Alcalase	• Neat organic solvents resulted in the Schiff base product (>90%) instead of the Mannich product while the addition of water favored the Mannich reaction when catalyzed by lipases[52]

Table 1 (Contd.)

Type of reaction	Enzyme	Examples of recent advances
Morita–Baylis–Hillman (MBH) reaction	Lipases, esterases, and Alcalase,	• Trypsin from hog pancreas was found a more effective catalyst than lipases and α-amylase for Mannich reactions[53] • The MBH reaction catalyzed by Alcalase was non-specific protein catalysis because the denatured protease produced similar yields under the same conditions[34] • A primitive computationally designed protein acted as an efficient and enantioselective MBHase to promote the MBH reaction between activated alkenes and aldehydes[54]
Diels–Alder reaction	Diels–Alderases such as macrophomate synthase (MPS) and AbyU, solanapyrone synthase, and ribozymes	• For MPS-catalyzed Diels–Alder reactions, the C–C bond forming step was previously debated whether it is Michael-aldol process or Diels–Alder reaction.[55] Later, this step was suggested to be a stepwise Michael-aldol reaction instead of a Diels–Alder reaction[56] • A de novo computational method was used to design the active site that is suitable for catalyzing a model Diels–Alder reaction[57]
Acyloin condensations via thiamine diphosphate (ThDP)-dependent enzymes	Acetohydroxy acid synthase (AHAS, EC 2.2.1.6), benzoylformate decarboxylase (BFD, EC 4.1.1.7), benzaldehyde lyase (BAL, EC 4.1.2.38), pyruvate decarboxylase (PDC, EC 4.1.1.1), phenylpyruvate decarboxylase (PhPDC, EC 4.1.1.43), keto acid decarboxylase (EC 4.1.1.72), transketolase (TK, EC 2.2.1.1), 1-deoxy-D-xylulose 5-phosphate synthase (DXPS, EC 2.2.1.7), flavoenzyme cyclohexane-1,2-dione hydrolase (CDH, EC 3.7.1.11), flavoenzyme YerE, Bacillus stearothermophilus acetylacetoin synthase, and ThDP-dependent PigD and MenD	• Two new ThDP-dependent enzymes, SeAAS from Saccharopolyspora erythraea and HapD from Hahella chejuensis were identified to catalyze intermolecular Stetter reactions and benzoin condensation with high enantioselectivity[58] • Benzaldehyde lyase (BAL) in mixtures of deep eutectic solvents (DES) and water exhibited high activities and good enantioselectivities (27–99% ee) for carboligation reactions of aldehydes[59] • A subclass of (myco)bacterial ThDP-dependent enzymes (e.g., ErwE and MyGE) could extend the donor substrate range from achiral α-keto acids and simple aldehydes to customized chiral α-keto acids[60]
Oxidative and reductive C–C bond formation	Cytochrome P450 enzymes, redG, nonheme iron mono- and dioxygenases, flavoproteins (such as berberine bridge enzyme), radical S-adenosylmethionine enzymes, laccase, and peroxidases Flavin-dependent 'ene'-reductases (EREDs), the 'ene'-reductase from Caulobacter segnis (CsER), and wild-type ene-reductases from the Old Yellow Enzyme (OYE)	• A nonheme iron enzyme, 2-oxoglutarate/Fe(II)-dependent dioxygenase (2-ODD), promoted the oxidative cyclization in the etoposide biosynthetic pathway[61] • The wild-type ene-reductases from the Old Yellow Enzyme (OYE) family favored the C=C double bond reduction instead of carbocyclization; however, single-site replacement of the critical proton donor Tyr residue (e.g., Tyr190 in OPR3, Tyr169 in YqjM) with a non-protic Phe or Trp led to more cyclization products[62]
C–C bond formation through C1 resource utilization	Formaldehyde to valuable chiral molecules by using aldolases and ThDP-dependent enzymes, CO2 conversions using carboxylases, formaldehyde transformations using C–C ligases, CO and formate conversions via C–C ligases, CO2 and succinyl coenzyme A (SCoA) conversion to 2-oxoglutarate and CoA	• Formaldehyde was converted to glycolaldehyde by formolase or its variants, and glycolaldehyde was further converted to erythrulose (C4 sugar) by another formolase variant[63] • CO2 was converted to a bis(boryl)acetal compound first, followed by selective enzymatic reactions to afford C3 (dihydroxyacetone, DHA) by using a formolase (FLS), or optically pure C4 (L-erythrulose) through a cascade reaction using FLS and D-fructose-6-phosphate aldolase (FSA) A129S variant[64]
Radical enzymes for C–C bond formation	Radical S-adenosylmethionine (SAM) enzymes such as pyruvate-formate lyase (PFL), spore photoproduct lyase (SPL), and benzylsuccinate synthase (BSS), O2-sensitive and hydrocarbon activating glycyl radical enzymes (GREs) including a subset known as x-succinate synthases [e.g., benzylsuccinate synthase (BSS), 4-isopropylbenzylsuccinate synthase (IBSS), hydroxybenzylsuccinate synthase (HBSS), naphthyl-2-methylsuccinate synthase (NMSS), and 1-methylalkylsuccinate synthase (MASS)], cytochrome P450	• Cytochrome P450 could be engineered to have a fine control of the radical addition step and the halogen rebound step during stereoselective atom-transfer radical cyclization (ATRC)[65] • Recent examples include SAM for enzymatic redox reactions in C–C bond formation,[66] the benzylic radical/carbocation intermediate initiating the C–C bond formation for a nonheme iron enzyme called 2-oxoglutarate/Fe(II)-dependent dioxygenase (2-ODD),[61] and the formation of nitro radical anion during 'ene'-reductase CsER-catalyzed cross-electrophile couplings (XECs) between alkyl halides and nitroalkanes[67]

Table 1 (Contd.)

Type of reaction	Enzyme	Examples of recent advances
Other C–C bond formation mechanisms	PLP-dependent enzymes such as CndF and Fub7, hydroxynitrile lyases (HNLs) or oxynitrilases, NAD(P)H-dependent ActVA-ORF4, cytochrome P411, ketosynthase, deoxypodophyllotoxin synthase, *cis*-isoprenyl diphosphate synthase, carboxymethylproline synthase, engineered SAM-dependent sterol methyltransferase	• CndF catalyzed the C–C coupling of *O*-acetyl-L-homoserine with 3-oxobutanoic acid to form (*S*)-2-amino-6-oxoheptanoate, which equilibrates with a cyclic Schiff base; a further reduction by a stereoselective imine reductase CndE gave (2*S*, 6*S*)-6-methyl pipecolate[68] • Engineered SAM-dependent sterol methyltransferase for *C*-methylation of unactivated alkenes in mono-, sesqui- and diterpenoids to yield C_{11}, C_{16} and C_{21} derivatives with high chemo- and regioselectivity[69]

2.1.3 Threonine aldolases. As PLP-dependent enzymes, threonine aldolases (TAs) catalyze C–C coupling with various aldehydes through C–H bond activation (Fig. 8) although wild-type threonine aldolases accommodate few D-amino acids as donors. Both wild-type L-threonine aldolase from *Aeromonas jandaei* and D-threonine aldolase from *Pseudomonas* sp. were evaluated in aldol addition reactions of D- or DL-alanine with various of aliphatic and aromatic aldehydes, producing a large pool of β-hydroxy-α,α-dialkyl-α-amino acids with conversions up to >80%; in general, D-threonine aldolase showed higher diastereoselectivities than L-threonine aldolase.[88] Three L-threonine aldolases (*i.e.*, *Aeromonas jandaei* L-allothreonine aldolase, *Escherichia coli* L-threonine aldolase, and *Thermotoga maritima* L-allo-threonine aldolase) were evaluated for the addition of glycine to various aldehyde acceptors; it was identified that *A. jandaei* L-allo-TA gave the best conversion and diastereomeric excess, and preparative-scale reactions (2.0 mmol of aldehyde and 10 mmol glycine) led to 16–50% isolated yields.[89] The Lin group[90] studied L-threonine transaldolase from *Pseudomonas* sp. in *Escherichia coli* whole cells for catalyzing *p*-methylsulfonyl benzaldehyde and L-threonine to form L-*p*-methylsulfonylphenylserine in the presence of Mg^{2+} (Fig. 9), observing 67.1% conversion and 94.5% diastereomeric excess (de) under optimized conditions. In general, when catalyzing the aldol formation of β-hydroxy-α-amino acids, threonine aldolase (LTA) has a high selectivity for the C_α position but a varied selectivity for C_β, resulting in a moderate diastereoselectivity. To further improve or invert its stereoselectivity towards aromatic aldehydes, threonine aldolase from *Pseudomonas* sp. was mutated for its amino acid residues that interact with amino and hydroxyl groups of the substrate; the change in the C_β-stereoselectivity was explained by molecular docking that the distances were modified between hydroxyl group of the substrate and imidazole groups of H133 and H89.[32] A combinatorial active-site saturation test/iterative saturation mutagenesis (CAST/ISM) was used to categorize 27 amino acid residues residing in the substrate pocket into two groups based on their functional region prior to the combinatorial mutation of L-threonine aldolase. One of the variants, known as RS1 (mutations Y8H, Y31H, I143R, and N305R), enabled an improved synthesis of L-*syn*-3-[4-(methylsulfonyl)phenylserine] in a 20 L reactor with 99.5% diastereomeric excess (de) and

73.2% yield; this variant also improved the diastereoselectivity for other aromatic aldehydes (Fig. 10).[91]

2.1.4 Other recent advances. Prior to the development of biosynthesis of L-sorbose and L-psicose using biocatalytic aldol addition in the *Corynebacterium glutamicum* strain, Yang *et al.*[18] conducted the *in vitro* aldol addition of DHAP and five different aldehydes catalyzed by 1,6-diphosphate aldolases (FruA) or tagatose 1,6-diphosphate (TagA) aldolases, and noticed that some aldolases lost their stereoselectivity when L-glyceraldehyde was the acceptor, producing both L-sorbose and L-psicose. This group collaborated with other groups[92] to further develop *in vitro* synthesis of 2-deoxy-D-ribose and rare ketoses (*e.g.*, D-allulose, L-tagatose, D-sorbose, L-fructose, and D-xylulose) from aldol reaction of D-glyceraldehyde 3-phosphate (or DHAP) with various aldehydes catalyzed by 2-deoxy-D-ribose 5-phosphate aldolase, D-fructose 1,6-bisphosphate aldolase (FruA), or L-rhamnulose 1-phosphate aldolase (RhaD); D-glyceraldehyde 3-phosphate and DHAP were produced from starch and pyrophosphate by using six artificial ATP-free cascade enzymatic reactions. 2-Deoxy-D-ribose and rare ketoses could be produced with >80% yields from high concentrations of substrates. A thermophilic recombinant aldolase, knowns as rhamnulose 1-phosphate aldolase from *Thermotoga maritima* activated by Co^{2+} as a divalent metal ion cofactor, was identified to show a maximum activity at 95 °C and its half-life time was 44 h and 33 h respectively at 80 and 95 °C; this aldolase maintained 90% of its initial activity in 40% acetonitrile, almost 100% of its activity in 20% DMSO, 50% of the activity in 25% DMF, and about 40% of the activity in 10% isopropanol and THF.[93] This aldolase could be suitable for aldol reactions conducted under extreme conditions.[94]

The Clapés group[95] employed Co^{2+}-dependent 3-methyl-2-oxobutanoate hydroxymethyltransferase (KPHMT, EC 2.1.2.11) and its variants to catalyze aldol additions of 3,3-disubstituted 2-oxoacids to aldehydes (Fig. 11) forming 3,3,3-trisubstituted 2-oxoacids, which were further converted to 2-oxolactones, 3-hydroxy acids, and ulosonic acid derivatives carrying *gem*-dialkyl, *gem*-cycloalkyl, or spirocyclic quaternary centers. Many of these chiral precursors are important to the preparation of medicinal molecules. As a type of pyruvate-dependent aldolases, sialic acid aldolases [also referred as *N*-acetylneuraminate pyruvate lyases (NPL)] promoted the reversible reaction of
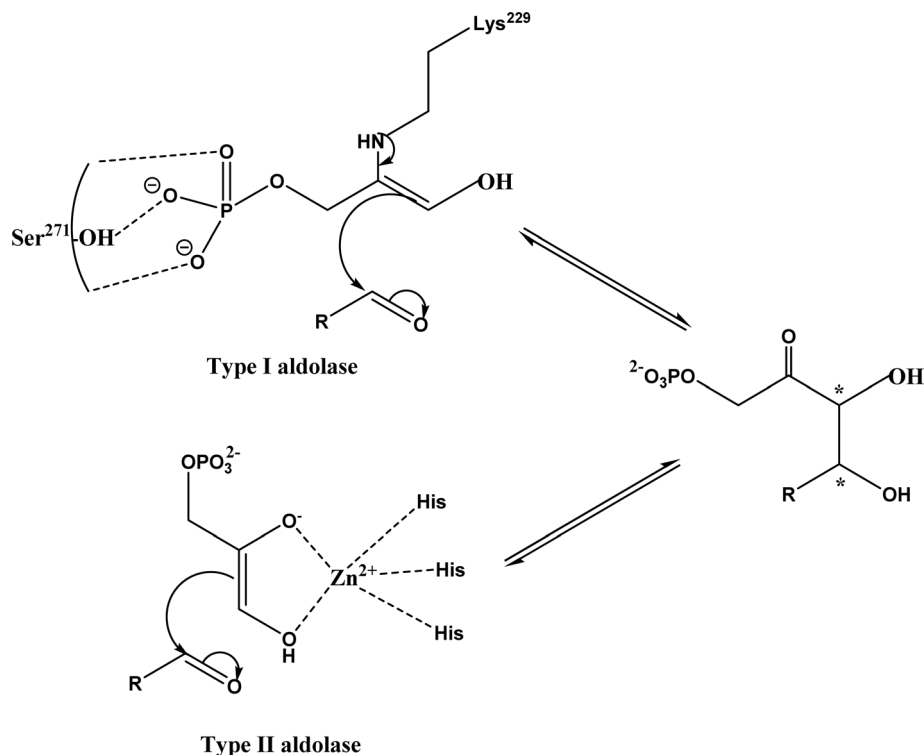
Fig. 2 Aldol addition mechanisms by Type I and II aldolases (dihydroxyacetone phosphate (DHAP)-dependent enzyme as an example).[23,72,83]
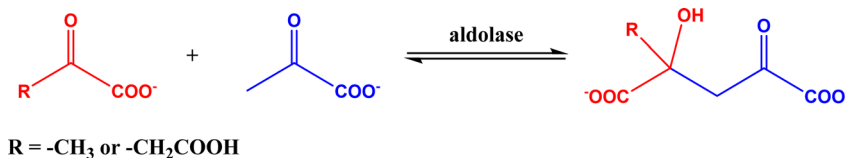

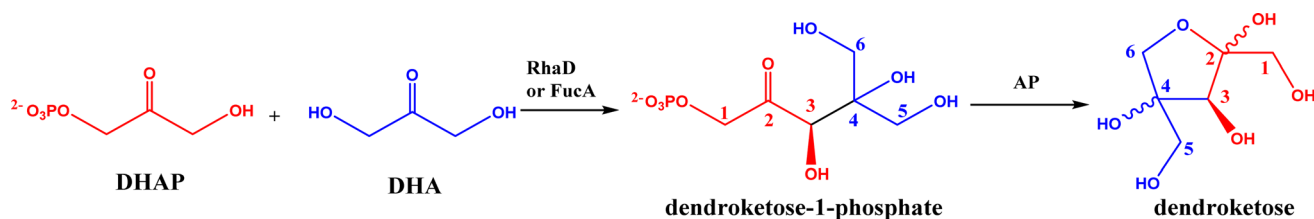**Fig. 3** HMG/CHA aldolase-catalyzed aldol addition.

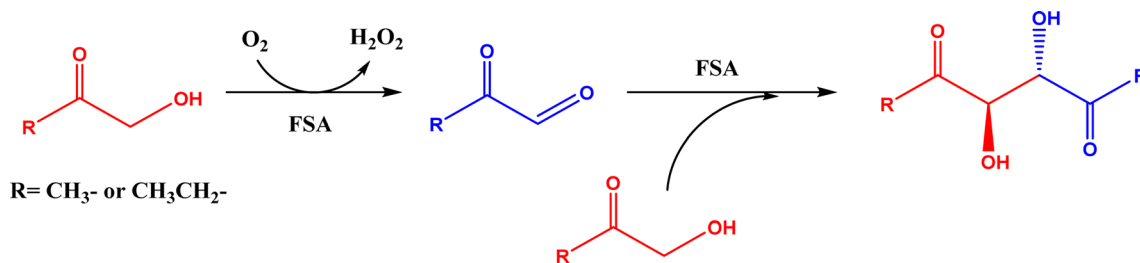**Fig. 4** Aldol addition of DHAP with DHA to form dendroketose.

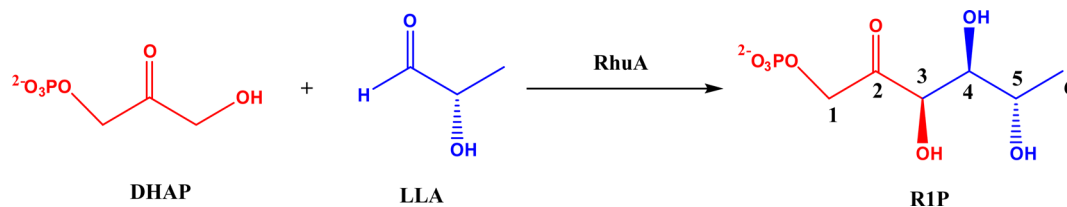**Fig. 5** Aldol reaction of hydroxyketones catalyzed by D-fructose-6-phosphate aldolase (FSA).

Fig. 6 Aldol addition of dihydroxyacetone phosphate (DHAP) and LLA = (S)-lactaldehyde to form L-rhamnulose-1-phosphate (R1P) catalyzed by dihydroxyacetone phosphate (DHAP)-dependent rhamnulose-1-phosphate aldolase (RhuA).

pyruvate and aldose to sialic acids. When catalyzing the reaction of pyruvate with D-mannose (or D-galactose), recombinant sialic acid aldolase originated from freshwater snail *Biomphalaria glabrata* (sNPL) displayed a different diastereoselectivity from sialic acid aldolase from chicken (chNPL).[96] In addition, the wild-type sNPL could catalyze the aldol reaction of pyruvate with

different aliphatic aldehydes to produce 4-hydroxy-2-oxoates with 21–78% yields, while chNPL could not. The Clapés group[97] converted various L-α-amino acids to 2-substituted 3-hydroxycarboxylic acid derivatives *via* a cascade enzymatic reaction method, which involved the oxidative deamination of L-α-amino acids to 2-oxoacid intermediates by L-α-amino acid

Fig. 7 Schematic view of catalytic mechanism of rhamnulose-1-phosphate aldolase (RhuA)-catalyzed retro- and aldolic reaction. These structures are geometrically optimized at the DFT level (B3LYP/LANL2DZ). The estimated activation energies are given in kcal mol⁻¹. DHAP = dihydroxyacetone phosphate, R1P = L-rhamnulose-1-phosphate, and LLA = (S)-lactaldehyde [Reprinted/adapted with permission from reference (Fig. S11 in its ESI data).[31] Copyright 2020 Elsevier].
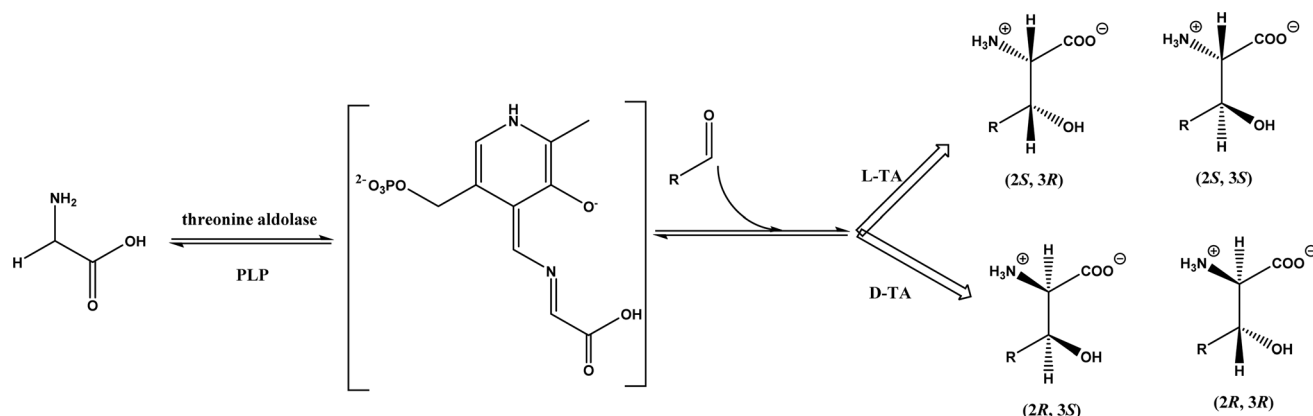
Fig. 8 Threonine aldolase (TA)-catalyzed aldol addition of glycine with aldehyde.
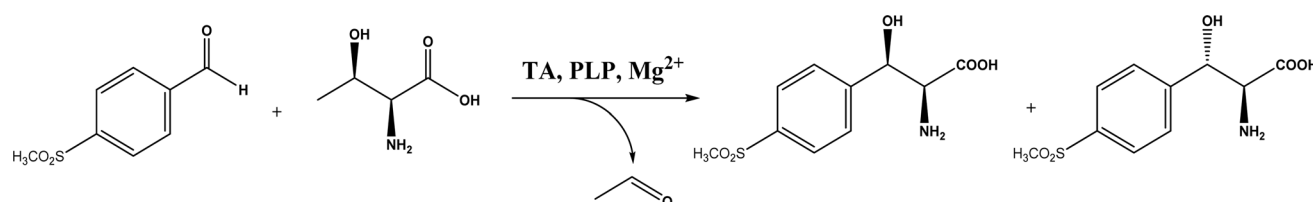

Fig. 9 L-p-Methylsulfonylphenylserine synthesis catalyzed by threonine aldolase (TA).

Six key sites in two functional regions R and S, directed evolution by CAST/ISM
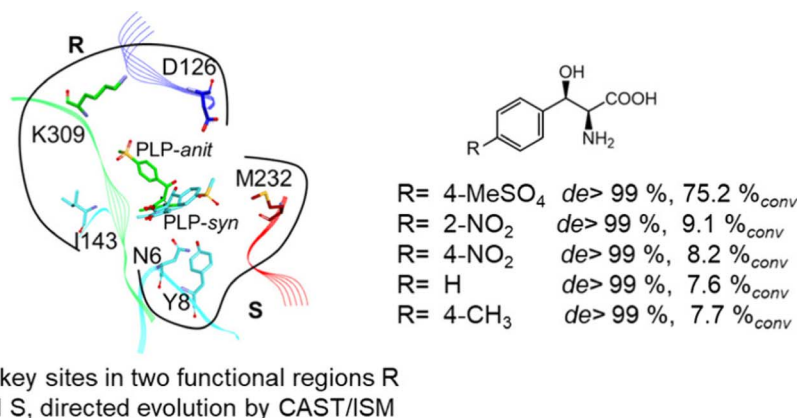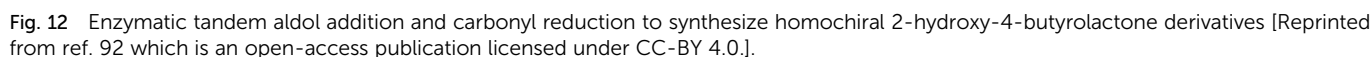
Fig. 10 Directed evolution of L-threonine aldolase leading to improved diastereoselectivity [Reprinted with permission from ref. 83 Copyright 2021 American Chemical Society].

deaminase from *Cosenzaea myxofaciens*, followed by the aldol addition reaction with formaldehyde to form (*R*)- or (*S*)-3-substituted 4-hydroxy-2-oxoacids (36–98% yields and 91–98% ee for each enantiomer) when mediated by metal-dependent carboligases known as 2-oxo-3-deoxy-L-rhamnonate aldolase (YfaU) and ketopantoate hydroxymethyltransferase (KPHMT), respectively. Similar cascade approach involving enzymatic aldol addition was used to prepare γ-hydroxy-α-amino acid derivatives,[98] and (*R*)- or (*S*)-2-substituted 3-hydroxycarboxylic esters.[99] Moreno and co-workers[100] developed a two-step strategy for synthesizing 2-hydroxy-4-butyrolactone derivatives (Fig. 12): in the first step, different chiral aldol adducts were prepared from 2-oxoacids and aldehydes by using different aldolases including

3-methyl-2-oxobutanoate hydroxymethyltransferase (KPHMT), 2-keto-3-deoxy-l-rhamnonate aldolase (YfaU), and *trans-o*-hydroxybenzylidene pyruvate hydratase-aldolase from *Pseudomonas putida* (HBPA); in the second step, 2-oxogroup of the aldol adduct was reduced by ketopantoate reductase and Δ1-piperidine-2-carboxylate/Δ1-pyrroline-2-carboxylate reductase with promiscuous ketoreductase ability. This enzymatic tandem reaction approach produced two enantiomers of 2-hydroxy-4-butyrolactone (>99% ee), twenty one (2*R*, 3*S*), (2*S*, 3*S*), (2*R*, 3*R*), or (2*S*, 3*R*)-2-hydroxy-3-substituted-4-butyrolactones [with diastereomeric ratio (d.r.) ranging from 60 : 40 to 98 : 2], and six (2*S*, 4*R*)-2-hydroxy-4-substituted-4-butyrolactones (with d.r. ranging from 87 : 13 to 98 : 2). In addition, the

Fig. 11 Aldol addition of 3,3-disubstituted 2-oxoacids to aldehydes catalyzed by 3-methyl-2-oxobutanoate hydroxymethyltransferase (KPHMT).

Fig. 12 Enzymatic tandem aldol addition and carbonyl reduction to synthesize homochiral 2-hydroxy-4-butyrolactone derivatives [Reprinted from ref. 92 which is an open-access publication licensed under CC-BY 4.0.].

diastereoselectivity of aldolases could be tuned *via* protein engineering.[25,26] Mutants of L-threonine aldolase from *Cellulosilyticum* sp were constructed by the combinatorial active-site saturation test/iterative saturation mutation method to improve the *syn* addition diastereoselectivity from 37.2% to 99.4%, or to invert the reaction to *anti* addition with 97.2% diastereoselectivity.[101]

2.2. Non-aldolase enzymes

Non-aldolase biomolecular catalysts [such as lipases and proteases,[24] and catalytic antibodies[72]] have been developed to overcome the issues with aldolases. Several lipases especially lipase from porcine pancreas (PPL) were able to catalyze the aldol reaction between benzaldehyde derivatives with acetone in the presence of 20 v% water, producing aldol products with yields up to 96.4% but relatively low enantiomeric excesses (ees, 9.4–43.6%).[33] The mechanism is depicted in Fig. 13: acetone interactions with the Asp–His dyad and the oxyanion, proton transfer from acetone to His residue forming an enolate, proton transfer to aldehyde and C–C bonding formation with acetone, and the release of aldol adduct from the oxyanion hole.[33] Alcalase (protease from *Bacillus licheniformis*) could catalyze the

aldol addition of 4-nitrobenzaldehyde and acetone with 20% water at 45 °C (see Fig. 14) producing 68% aldol product (with 13% ee and 94% selectivity of aldol product *vs.* the condensation product).[34] The Holtmann group[35] conducted the aldol reaction of 4-nitrobenzaldehyde with acetone (see Fig. 15) in several deep eutectic solvents (DES), and found that bovine serum albumin (BSA) showed no specificity for aldol and olefin products; however, PPL favored the aldol product especially in more hydrophobic DES although the initial reaction rate was faster in hydrophilic DES (*i.e.*, choline chloride/glycerol at 1 : 1.5 molar ratio). One drawback of DES in this application is the low solubility of 4-nitrobenzaldehyde in DES (0.2–1.3 M). The study did not report the configuration of asymmetric center.

Nuclease p1 from *Penicillium citrinum* was found capable of catalyzing aldol reactions between benzaldehyde derivatives and cyclic ketones, resulting in higher ee and diastereomeric ratio under solvent-free condition than in organic solvents and water.[102] UstD is a PLP-dependent enzyme that is engaged in the biosynthesis of Ustiloxin B (an inhibitor of microtubilin polymerization). In an aldol reaction shown in Fig. 16, UstD eliminates carboxyl group (C–C activation) from L-aspartic acid to form a nucleophilic enamine intermediate, which attacks the
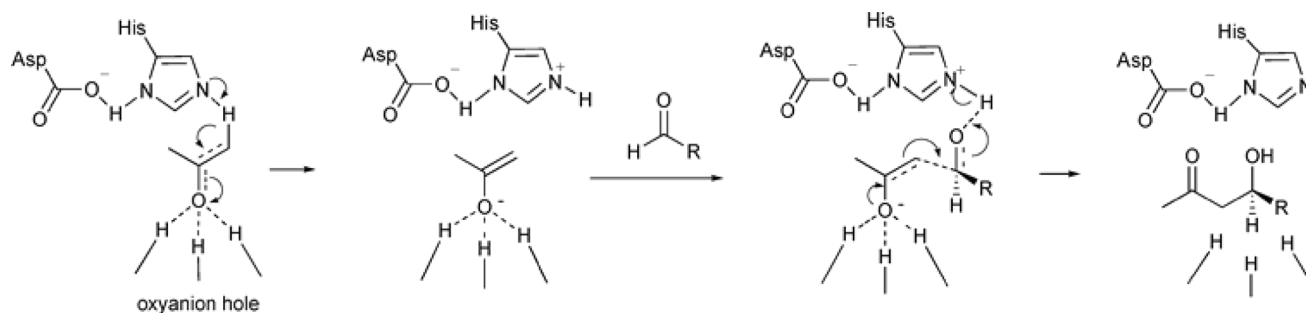
Fig. 13 Mechanism of lipase-catalyzed aldol reaction [Reprinted with permission from ref. 33 Copyright 2004 Royal Society of Chemistry].
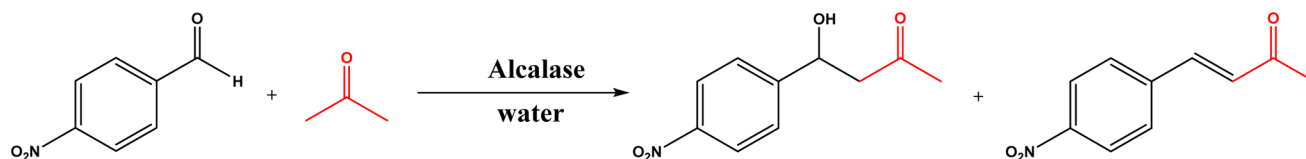

Fig. 14 Aldol addition and condensation of 4-nitrobenzaldehyde with acetone.
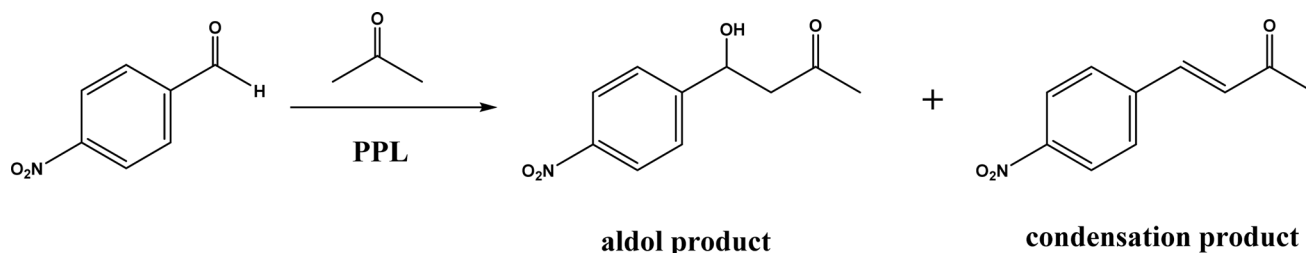

Fig. 15 Aldol addition and condensation of 4-nitrobenzaldehyde with acetone.

aldehyde to yield γ-hydroxy α-amino acid.[103] The decarboxylation step produces CO_2, which makes this aldol reaction irreversible. This mechanism is fundamentally different from classic Type I aldolase, where an enamine nucleophile is formed from the tautomerization of an imine. This enzyme UstD showed high stereoselectivities for aromatic and aliphatic aldehydes even on gram-scale.[103,104]

Henry Reaction, also known as nitroaldol addition, is the nucleophilic addition of nitroalkanes to aldehydes or ketones to synthesize β-nitro alcohols, which can be further manipulated to biologically active compounds. This reaction is usually promoted by base catalysts such as hydroxides, alkoxides, carbonates, bicarbonates, amines, and LiAlH₄, *etc.*[105] As an extension of Henry reaction, the addition of nitroalkanes to imines (called aza-Henry reaction) forms β-nitroamine derivatives.[106] Strong base catalysts often produce byproducts from side reactions and chiral catalysts are required to generate enantioselective products. On the other hand, various enzymes (*e.g.*, hydroxy nitrile lyases, transglutaminase, lipases, and D-aminoacylase) are mild catalysts to produce enantipure β-nitro alcohols as detailed in a 2012 review.[107] This section provides a more recent update, or studies that were not covered in the earlier review. Alcalase's active site was found capable of

catalyzing the Henry reaction between 4-nitrobenzaldehyde and nitromethane at 45 °C forming racemic nitroalcohol with 70% yield and 72% selectivity (Fig. 17).[34] Whole-cell baker's yeast is an affordable and effective catalyst for Henry reactions of substituted benzaldehydes and nitromethane in ethanol, resulting in 55–90% products (although enantioselectivities were not reported).[108] Acylase from *Aspergillus oryzae*, various lipases, and BSA were evaluated in TX-100/H₂O/[BMIM][PF₆] microemulsions for their catalytic capabilities in Henry reaction of 4-nitrobenzaldehyde with nitromethane at 30 °C, and the reaction produced 62% yield in the absence of enzyme suggesting the catalytic role of this solvent system (without the solvent system and enzyme, the yield was 24%); the acylase gave the highest overall yield of 88% for this reaction, and 28–87% yields for other substituted benzaldehydes.[36] Interestingly, gelatin and collagen proteins showed great potential as catalysts for Henry reactions of substituted benzaldehydes and nitromethane in DMSO or aqueous solution containing tetra-*n*-butylammonium bromide as the phase transfer catalyst (with up to 70–92% yields for those benzaldehyde derivatives containing electron-withdrawing –NO₂ or –CN groups); among different gelatins, porcine skin type-A (PSTA) gelatin, bovine skin type-B (BSTB) gelatin, and cold-water fish skin (CWFS)

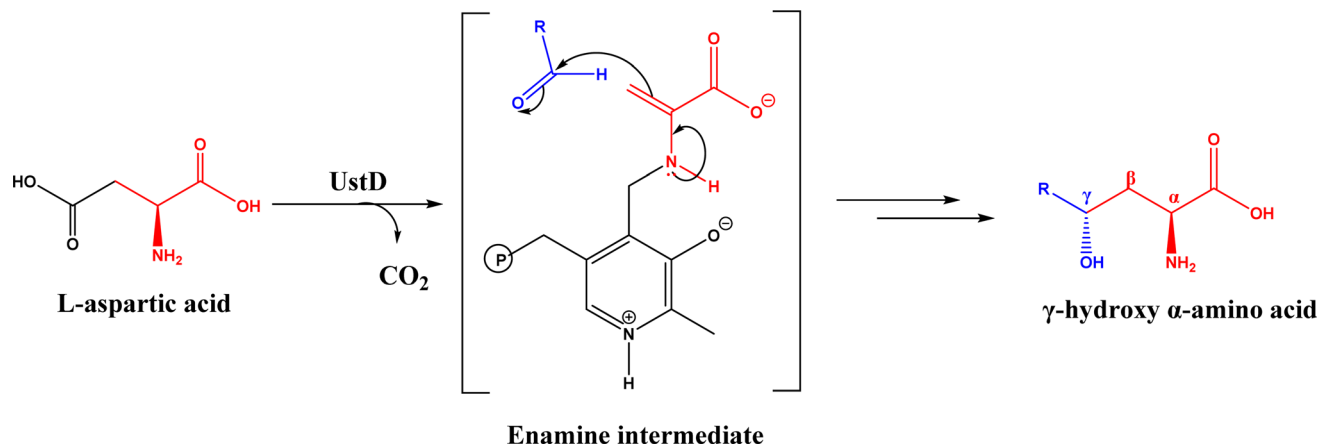**Fig. 16** Decarboxylative aldol reaction of L-aspartic acid with aldehyde catalyzed by UstD.
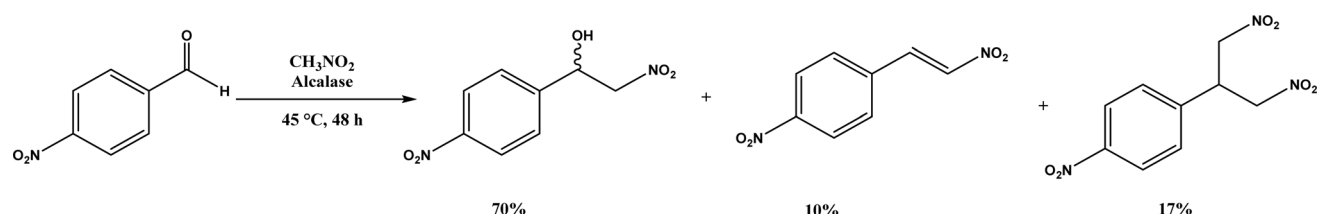

Fig. 17 Henry reaction between 4-nitrobenzaldehyde and nitromethane.

gelatin showed high catalytic activities; the first-order rate constant increased in the order of chitosan < gelatin < bovine serum albumin (BSA) < collagen.[37] CALB immobilized on hydrophobic PS-DVB (polystyrene-divinylbenzene) beads improved the enzymatic activity in water by 15–18 times when compared with the commercial Novozym 435; the Henry reaction of 4-nitrobenzaldehyde and nitromethane catalyzed by this new lipase preparation at 40 °C obtained 87% yield in water, 40% yield in [BMIM][Tf$_2$N], and 22% yield in *tert*-butanol, but were all significantly higher than those catalyzed by Novozym 435 although no stereoselectivity was discussed.[109] However, inhibited or thermally deactivated enzyme preparation still showed a considerable amount of catalytic activity, implying a different mechanism not related to the active site of lipase is in play. FT-IR spectra indicate that α-helix and β-turn structures not related to hydrogen bonds of CALB are significantly higher in new enzyme immobilization than in Novozym 435 (54% *vs.* 15%).

3. Knoevenagel condensation

Knoevenagel condensation reaction is considered a variation of aldol condensation, which involved the nucleophilic addition of an activated methylene compound to a carbonyl group (aldehyde or ketone) followed by the dehydration (*i.e.*, condensation) step to form an alkene. Knoevenagel condensation is highly valuable for preparing active pharmaceutical ingredients (APIs), and also precursors for other reactions such as Diels–Alder addition, Michael addition, oxidative coupling, and Nazarov

cyclization.[110–112] Knoevenagel condensation is traditionally catalyzed by various amines, but also by Lewis acids, zeolites, clays, amino acids, or ionic liquids (ILs).[113–116] Alternatively, lipases and other enzymes have been investigated as efficient catalysts ('catalytic promiscuity') for Knoevenagel condensation (a few examples were discussed in reviews,[12,117] but there is no systematic review on this). Immobilized lipase B from *Candida antarctica* (CALB) was reported to mediate decarboxylative aldol reactions of aromatic aldehydes and β-ketoesters at 30 °C in acetonitrile containing 1,4,7,10-tetraazacyclododecane as an additive to give 81–97% isolated yields, while the same reactions in acetonitrile with 5 v% water and a primary amine (*e.g.*, aniline, *p*-toluidine and benzylamine) produced Knoevenagel products with 56–91% isolated yields (Fig. 18).[38] However, the Bornscheuer group[39] observed no promiscuous catalytic activity of CALB for the decarboxylative aldol addition and Knoevenagel reaction between 4-nitrobenzaldehyde and ethyl acetoacetate; what happened was the enzymatic hydrolysis of ethyl acetoacetate in the presence of water to form the corresponding acetoacetic acid, which reacted with 4-nitrobenzaldehyde to form the aldol and Knoevenagel products. In another study, CALB immobilized on chitosan-functionalized electrospun PMA-*co*-PAA membrane showed a better stability and recyclability than free enzyme, and produced up to 73% yield of 3-acetylcoumarin from Knoevenagel condensation and the cyclization of salicylaldehyde and acetoacetate (Fig. 19) in methanol/water (4 : 1, v/v) mixture.[118] In a different study, CALB, Lipozyme RMIM (immobilized lipase from *Rhizomucor miehei*), Lipozyme TLIM (immobilized lipase from *Thermomyces lanuginosus*), and

several "Amano" lipases including AK (from *Pseudomonas fluorescen*), DF (from *Rhizopus oryzae*), and AS (from *Aspergillus niger*) were evaluated in Knoevenagel–Michael cascade reactions of benzaldehyde and 1,3-cyclohexanedione in *N,N*-dimethylformamide (DMF) at 40 °C (Fig. 20), where "Amano" lipase DF gave a far better yield (89%) than other enzymes (9–29%); the extension of this reaction to other aromatic aldehydes and 1,3-cyclodiketones afforded 83–94% yields.[119] However, a separate study demonstrated that RMIM produced higher yields than other lipases (including lipase DF, PPL and Novozym 435) in water during the Knoevenagel–Michael cascade reaction of 4-chlorobenzaldehyde with 4-hydroxycoumarin (Fig. 21).[120]

PPL displayed a higher catalytic activity than other lipases (including Novozym 435) for Knoevenagel reactions of aromatic aldehydes with 1,3-dihydroindol-2-one in DMSO with 20 v% water at 45 °C (Fig. 22), resulting in 75–97% yields and different *E/Z* ratios.[121] In other Knoevenagel condensation studies, PPL also showed better performance than other lipases in *tert*-butanol with 20 v% water[122] and ethanol.[123] On the other hand, using *in situ* generated acetaldehyde from the enzymatic hydrolysis of vinyl carboxylates, chemoenzymatic tandem reaction (Fig. 23) catalyzed by Novozym 435 in *tert*-butanol or acetonitrile led to ethyl 2-aroylbut-2-enoate compounds with up to 72% yields; PPL showed a lower activity than Novozym

Fig. 18 Lipase-catalyzed decarboxylative aldol and Knoevenagel reactions.

Fig. 19 CALB-catalyzed Knoevenagel condensation and the cyclization of salicylaldehyde and acetoacetate.

Fig. 20 Lipase-catalyzed Knoevenagel–Michael cascade reactions of aromatic aldehydes and 1,3-cyclodiketones.

Fig. 21 Lipase-catalyzed Knoevenagel–Michael cascade reaction of *p*-chlorobenzaldehyde with 4-hydroxycoumarin.

Fig. 22 PPL-catalyzed Knoevenagel reactions of aromatic aldehydes with 1,3-dihydroindol-2-one.

435.[113] *Candida cylindracea* lipase and Novozyme 435 enabled higher yields (up to 50%) than PPL and other lipases when catalyzing the esterification-Knoevenagel cascade reaction of cyanoacetic acid and benzaldehyde dimethyl acetal in toluene.[124] Since Knoevenagel condensation product could react with activated methylene compound to form Michael addition byproduct, the Koszelewski group[125] developed a method by using the enzymatic hydrolysis of enol carboxylates to generate active methylene compounds *in situ* for reacting with aldehydes catalyzed by PPL in *tert*-butanol with 5 v% water (Fig. 24); this hydrolysis–Knoevenagel cascade reaction produced target compounds with 11–86% yields and high *E*/*Z* selectivities (from 82 : 18 to mostly 99 : 1). The high selectivity was explained by the enol product preferably staying in one configuration in the active site of lipase, leading to the exclusive *Z* isomer. Wang and co-workers[126] examined α-amylase from hog pancreas and PPL in different ILs and DES for Knoevenagel condensations of acetylacetone and 4-nitrobenzaldehyde (and other aromatic benzaldehydes later) at 50 °C, and found that α-amylase was most active in [HOEtMIM][NO$_3$]/H$_2$O (80 : 20, v/v) allowing 89%

yield, while PPL was mostly active in choline chloride/glycerol (1 : 2, molar ratio) affording 93% yield. Interestingly, both enzymes were found highly active in nitrate-containing ILs among all ILs evaluated (with anions of BF$_4^-$, PF$_6^-$ and NO$_3^-$) although NO$_3^-$ is known enzyme-denaturing.[127] Our group[39] conducted Knoevenagel condensation of 4-chlorobenzaldehydes and acetylacetone (Fig. 25), and reported that porcine pancreas lipase (PPL) in water-mimicking ILs containing ammonium, imidazolium and benzimidazolium cations led to higher reaction rates (up to 3.22 mM per min per g lipase) and improved yields than *tert*-butanol, glymes, and [BMIM][Tf$_2$N]. More fascinatingly, tertiary amides such as 1-methyl-2-pyrrolidone (NMP), *N*,*N*-dimethylformamide (DMF) and *N*,*N*-dimethylacetamide (DMA) enabled 8.2–11.1 times of increases in the initial reaction rate (up to 35.66 mM per min per g lipase) than dual-functionalized ILs, whose exact mechanism is under investigation although there is likely some synergistic effect of tertiary amides with the lipase.

Other enzymes have also been investigated for Knoevenagel reactions. Alkaline protease from *Bacillus licheniformis*
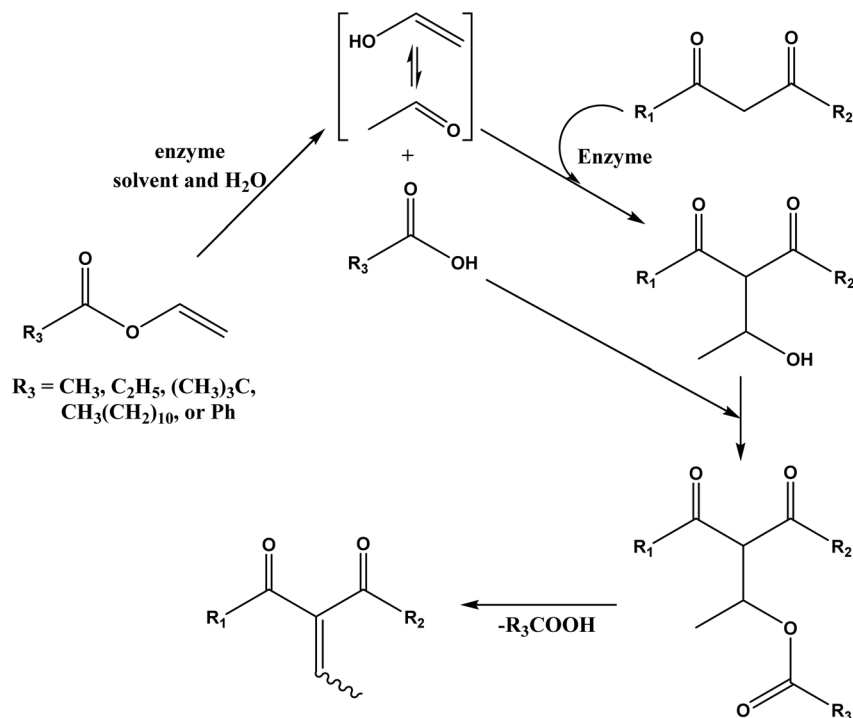
Fig. 23 Lipase-catalyzed Knoevenagel condensation using *in situ* generation of acetaldehyde (redrawn from ref. 113).
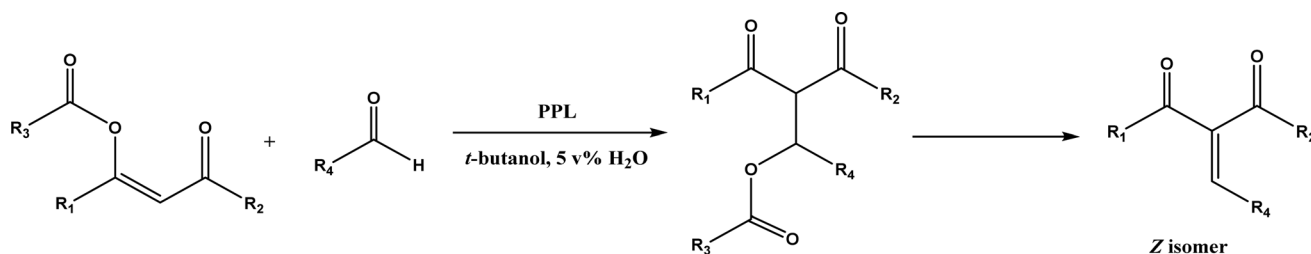

Fig. 24 Lipase-catalyzed tandem Knoevenagel reaction of enol carboxylates.

mediated Knoevenagel reactions between aromatic, hetero-aromatic, and α,β-unsaturated aldehydes with less reactive acetylacetone or ethyl acetoacetate in DMSO with 5 v% water at 45 °C, producing functionalized trisubstituted alkenes and α,β,γ,δ-unsaturated carbonyl compounds with 24–82% yields and various *E/Z* isomeric ratios.[128] With an organic salt ([BMIM]Br), bovine serum albumin (BSA) showed a similar performance as PPL in catalyzing aldol condensations of benzaldehyde derivatives with different ketones, and Knoevenagel–Doebner condensations of benzaldehyde derivatives with activated methylene compounds with good yields; in the absence of BSA or [BMIM]Br, there was little product formed.[129] It was ratio-nalized that amino acid residues (*e.g.*, lysine) in BSA and [BMIM]Br both played critical roles in the reaction as illustrated by Fig. 26. In addition, BSA was found capable of catalyzing three-component reaction of an aldehyde/ketone/isatin, malo-nonitrile, and 3-methyl-1*H*-pyrazol-5-(4*H*)-one in the ethanol/water (3 : 7) mixture at room temperature to dihydropyrano[2,3-*c*]pyrazole and spiro[indoline-3,40-pyrano[2,3-*c*]pyrazole] derivatives with 72–98% yields; BSA outperformed lipases,

trypsins, papain, and α-amylase,[130] although for Knoevenagel condensations of benzaldehyde derivatives with acetylacetone (or its analogues) in the DMSO/water mixture, papain enabled better yields (42–86% yields),[131] and papain immobilized in $Cu_3(PO_4)_2$ nanoflowers exhibited higher activities (still moderate yields of 9–53%) than free enzyme.[132] The reaction mechanism is described in Fig. 27 as three key steps: Knoeve-nagel condensation, Michael addition, and cyclization. A similar one-pot three-component condensation of aldehyde, cyanoacetamide, and 1,3-dicarnonyl compound followed same steps of Knoevenagel condensation, Michael addition, and intramolecular cyclization, where D-aminoacylase and acylase 'Amano', and Amano lipase M from *Mucor javanicus* exhibited considerably higher activities than BSA, immobilized penicillin G acylase, lipase AK 'Amano', and *Candida rugosa* lipase; 3,4-dihydropyridin-2-one derivatives were synthesized in 28–99% yields and varying diastereomeric ratios under optimum conditions.[133] Li and co-workers[134] pointed out that serine residues of lipases are not involved in Knoevenagel condensa-tion, while unspecific residues of lipases, BSA or other proton
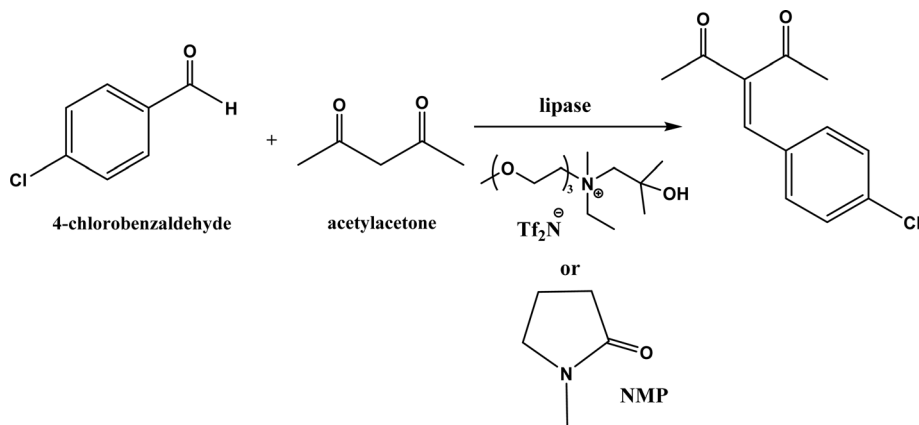
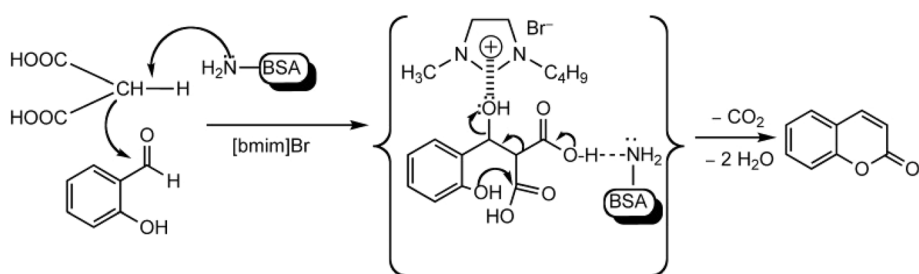**Fig. 25** Lipase-catalyzed Knoevenagel reaction between 4-chlorobenzaldehyde and acetylacetone in different solvents.

Fig. 26 Mechanism for the synthesis of coumarins *via* Knoevenagel condensation and cyclization [Reprinted with permission from ref. 129 Copyright 2011 Wiley-VCH Verlag GmbH&Co. KGaA].
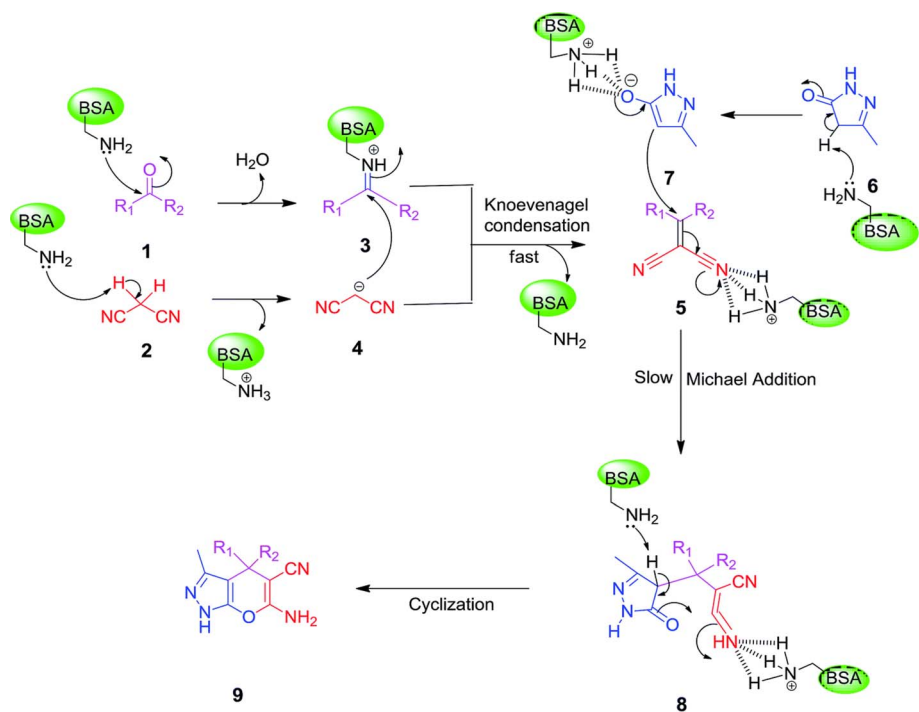

Fig. 27 Mechanism of three-component synthesis of dihydropyrano[2,3-*c*]pyrazole derivatives catalyzed by BSA in an aqueous ethanol [Reprinted with permission from ref. 130 Copyright 2016 Royal Society of Chemistry].

Fig. 28 Knoevenagel condensation of (E)-3-(4-(dimethylamino)phenyl)acrolein and ethyl 2-cyanoacetate.

Fig. 29 One-pot synthesis of coumarin-3-carboxylates using laccase/TEMPO hybrid catalyst.

Fig. 30 Tandem Knoevenagel condensation–reduction reaction of β-ketoesters using ene-reductase (NerA) (GDH = glucose dehydrogenase).

acceptors could promote the reaction. Baker's yeast as the whole cell biocatalyst effectively mediated Knoevenagel condensations between aryl aldehydes and malononitrile (or ethyl cyanoacetate, or 2,4-thiazolidinedione) in ethanol at room temperature, leading to good yields in most cases.[41] At pH 7.0, segments of RNA/DNA salts were discovered as efficient as PPL in catalyzing Knoevenagel condensations of benzaldehyde derivatives and activated methylene compounds; the catalytic rate was associated with a higher content of GC nucleosides in RNA/DNA while a higher catalytic turnover number is correlated with a longer strand of DNA.[135] Directed evolution of an artificial retro-aldolase was able to optimize its catalytic activity relying on a reactive lysine in a hydrophobic pocket to promote Knoevenagel condensations of electron-rich aldehydes and activated methylene compounds (see an example in Fig. 28), becoming >10^5-fold more proficient than BSA, and >10^8-fold more proficient than primary and secondary amines.[136] Laccase and its mediator 2,2,6,6-tetramethylpiperidin-1-oxyl (TEMPO) were co-immobilized in mesoporous silica as a hybrid catalyst to oxidize salicyl alcohols to salicylaldehydes *in situ*, followed by the Knoevenagel condensation and cyclization (trans-esterification) to form coumarin-3-carboxylates (Fig. 29) with 84–95% yields in citrate buffer (pH 4.5, 0.1 M); however, same reactions in organic solvents such as THF, DMF and acetonitrile led to no product, and 65% yield in [BMIM][PF$_6$].[137] A single ene-reductase (NerA) catalyzed the Knoevenagel condensation of β-

ketoesters first followed by a reduction to produce saturated α-substituted β-ketoesters (70–95% yields) as valuable synthons for pharmaceuticals and agrochemicals using *in situ* generation of NADH *via* glucose with glucose dehydrogenase (GDH), and it was shown that amino acid residues at the surface of NerA promoted the Knoevenagel condensation (Fig. 30),[138] which is different from an earlier study where CALB catalyzed decarboxylative aldol reactions of β-ketoesters.[38]

4. Michael addition

Michael addition (1,4-addition) typically refers to the nucleophilic addition of a carbanion to unsaturated systems (α,β-unsaturated carbonyl compounds) in conjugation with an activating group.[139] Many organocatalysts (*e.g.*, chiral diamines, chiral crown ethers, chiral alkaloids, chiral amino acids, and chiral oxazolines) and organometallic catalysts (*e.g.*, salts of amino acids, metal-diamine complexes, Schiff base-metal complexes, transition metal complexes, heterobimetallic complexes, and metal-*N,N*-dioxide complexes) have been extensively studied in asymmetric Michael addition reactions.[140] However, there is no individual catalyst that can catalyze different Michael reactions.

Several groups have reported catalytic promiscuity of lipases towards Michael addition. Svedendahl *et al.*[42] improved the reaction specificity of lipase B from *Candida antarctica* (CALB)
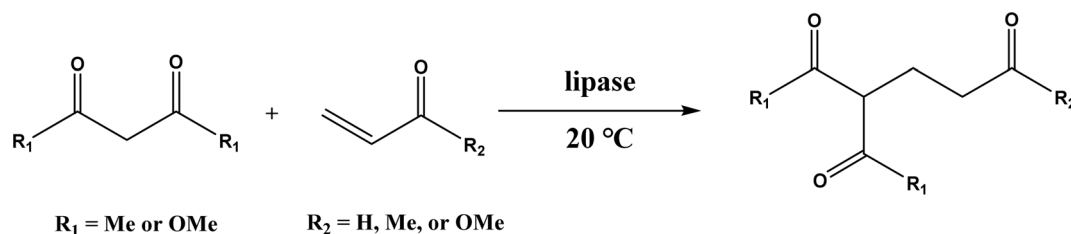
Fig. 31 Michael addition of 1,3-dicarbonyls to α,β-unsaturated carbonyl compounds.
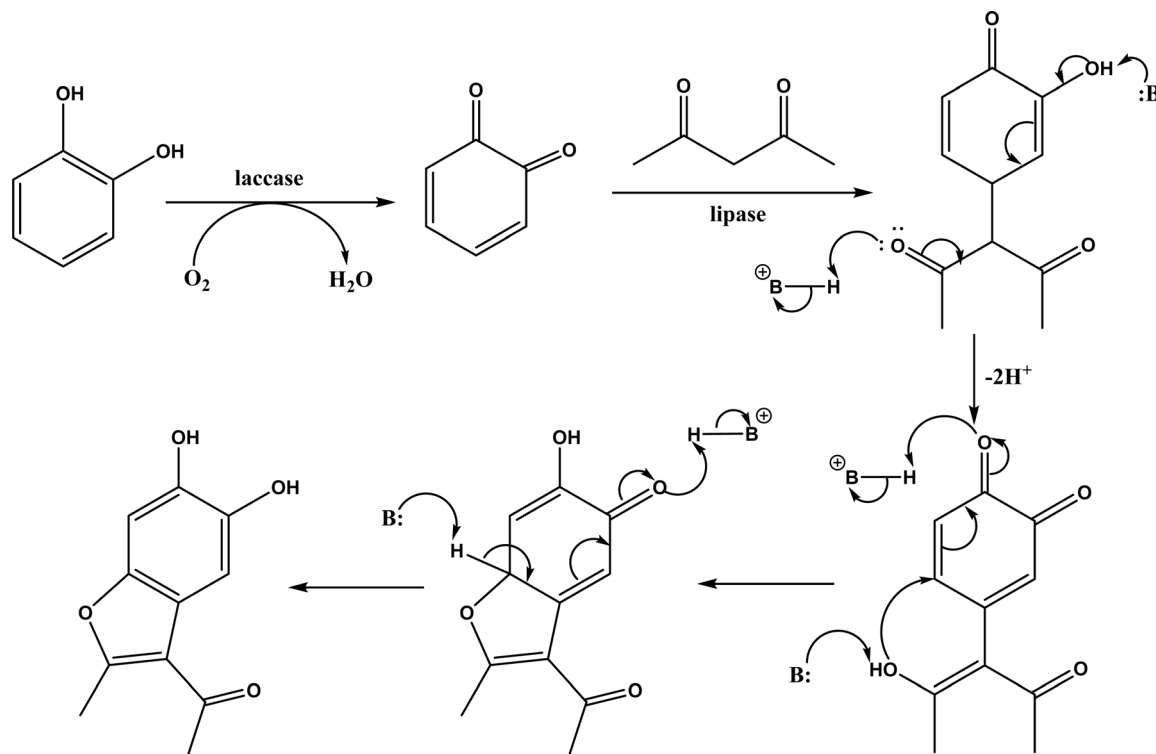

Fig. 32 Laccase/lipase catalytic Michael addition reaction of *in situ*-generated *ortho*-quinones (B: represents a base molecule such as water).

by substituting one amino acid (Ser105Ala) in the active site. They found that the lipase mutant exhibited much faster Michael addition rates (between 1,3-dicarbonyls and α,β-unsaturated carbonyl compounds, see Fig. 31) than the wild type at 20 °C. The Ragauskas group[141] suggested that lipase from *Pseudomonas cepacia* (known as lipase PS) accelerated the regioselective addition reaction between laccase-generated *o*-quinones and 1,3-dicarbonyl compounds in aqueous medium at room temperature (Fig. 32), leading to a 30–70% increase in product yield. Cai *et al.*[142] carried out the Michael addition of a wide range of 1,3-dicarbonyl compounds and cyclohexanone to aromatic and heteroaromatic nitroolefins and cyclohexanone catalyzed by various lipases (Fig. 33); they reported that lipozyme TLIM (immobilized lipase from *Thermomyces lanuginosus*) outperformed other lipases. Further, they found that DMSO (10/1, v/v, with water) was the best organic solvent in terms of generating a relatively high yield and ee. However, most yields were moderate (30–90%) and ees were relatively low (usually

below 50%). The He[143] and Hu groups[144] conducted Michael additions of 4-hydroxycoumarin with α,β-unsaturated enones promoted by PPL in aqueous organic solvents (such as DMSO), obtaining moderate to high yields (up to 95%) but low enantioselectivities (up to 28% ee). However, Chen and co-workers[43] reported that CALB alone could not catalyze Michael additions of aromatic nitroolefins and less-activated ketones (*e.g.*, cyclohexanone instead of acetylacetone), but required co-catalyst acetamide to obtain products with 25–72% yields. Other primary (1°) amides showed similar or less activation effect; the role of acetamide can be elucidated by the following mechanism (Fig. 34): the activation of cyclohexanone by acetamide and the interaction of nitroolefin with oxyanion hole, proton transfer from cyclohexanone to His residue to form an enolate (which is stabilized by acetamide), nucleophilic attack of nitroolefin by enolate, proton transfer from His residue to the product, and the product release from active site. The Griengl group[44] studied various lipases for Michael addition of β-
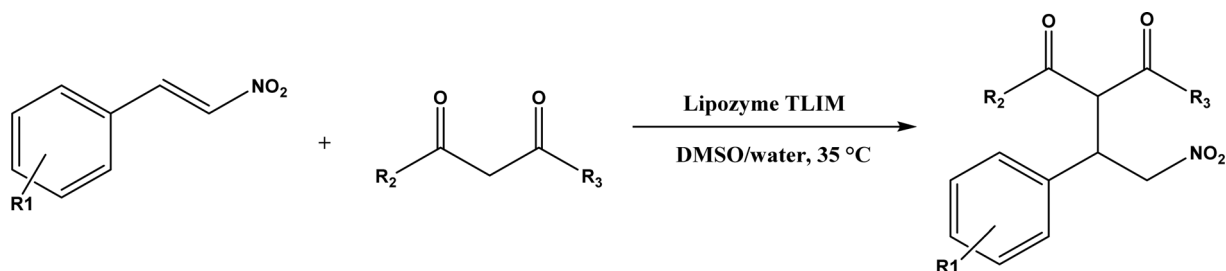
Fig. 33 Michael addition of aromatic nitroolefins and 1,3-dicarbonyl compounds catalyzed by Lipozyme TLIM.
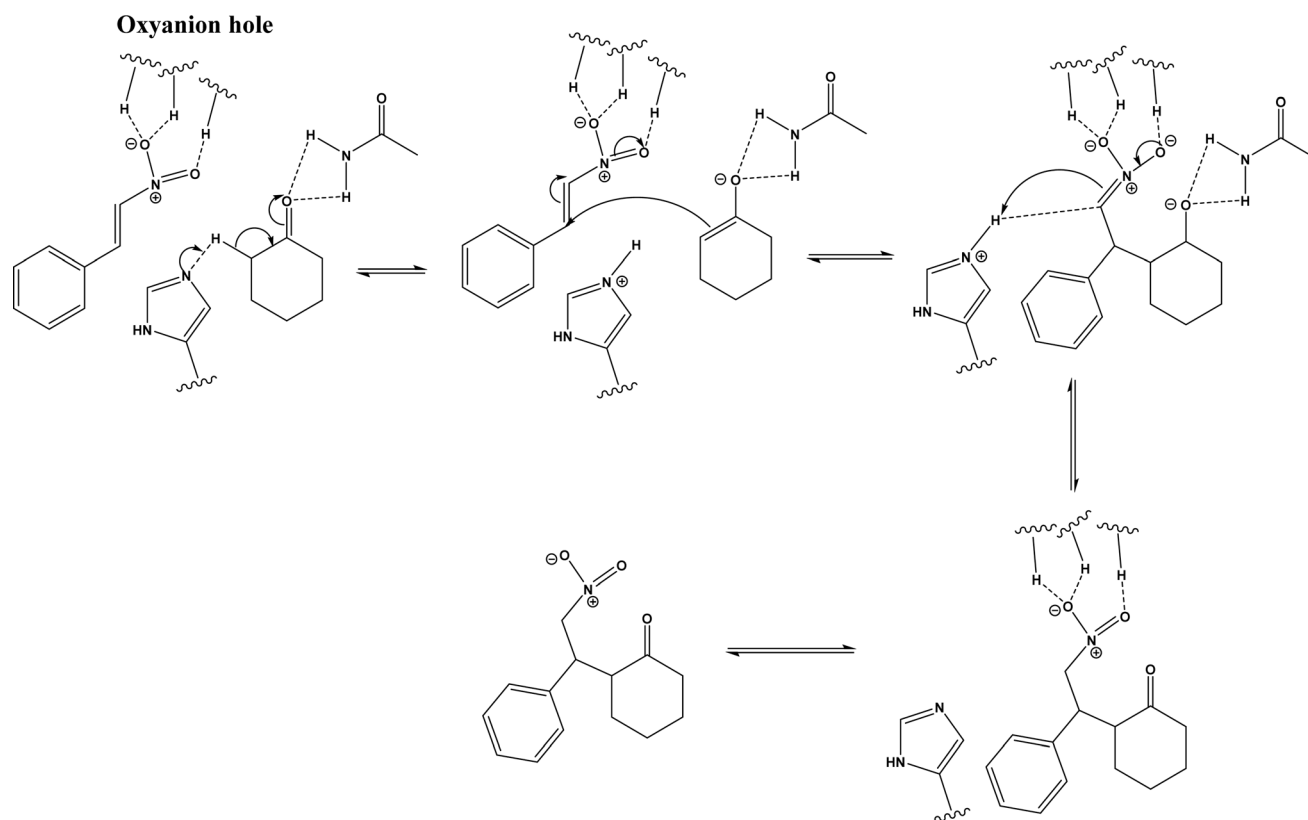

Fig. 34 Mechanism of lipase/acetamide-catalyzed Michael addition [redrawn from ref. 43].

ketoesters [methyl acetoacetate and methyl 2-(2-oxocyclopentyl) acetate] or nitroesters (methyl 2-nitropropanoate and methyl 2-nitroacetate) to 3-buten-2-one (or *trans*-β-nitrostyrene) in cyclohexane at 20 °C (Fig. 35), and identified several top-performing enzymes including *Candida antarctica* lipases A (CALA), CALB, and lipases from *Mucor miehei*, and *Thermomyces lanuginosas*. Methyl 2-nitroacetate was found the most active donor, leading to over 60–99% conversions of methyl vinyl ketone and *trans*-β-nitrostyrene in 20 h for selected lipases especially the CALB mutant; the alkene substrate requires electron withdrawing groups on it to act as the acceptor and strong nucleophilic CH-acidic donor to proceed with Michael addition. However, the enzymatic reaction between *trans*-β-nitrostyrene and acetylacetone failed. In contrast to other studies, this study[44] reported no stereoselectivity for lipase-

catalyzed Michael additions; it is suggested that the C–C-bond formation was due to the substrate activation by unique assembly of amino acids in the protein cavity. Hydroxy-functionalized ionic liquids (ILs) were evaluated as reaction media for the Michael addition synthesis of warfarin catalyzed by *Candida rugosa* lipase (Fig. 36), and it was found the hydroxy functionalization led to more hydrophilic ('water-mimicking') ILs and higher reaction yields while longer alkyl chains on ILs showed an opposite effect on the reaction; also, no stereoselectivity was observed in the reaction.[45]

Other types of hydrolases, such as proteases and D-amino-acylase, are also capable of catalyzing the Michael addition. The Lin group[145] screened various hydrolases for the Michael addition and reported that *Bacillus subtilis* protease, porcine pancreas lipase (PPL), and D-aminoacylase from *Escherichia coli*
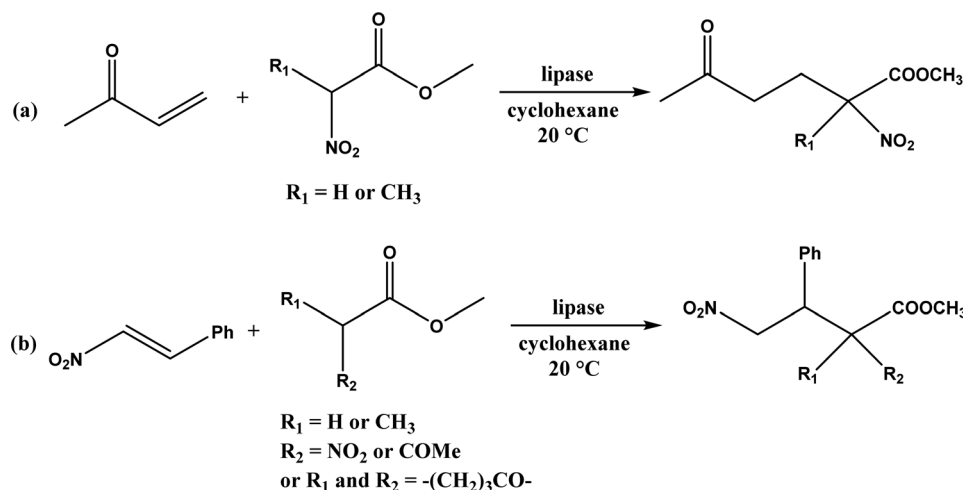
Fig. 35 Lipase-catalyzed Michael addition of (a) nitroesters to 3-buten-2-one, and (b) nitroesters or β-ketoesters to *trans*-β-nitrostyrene.
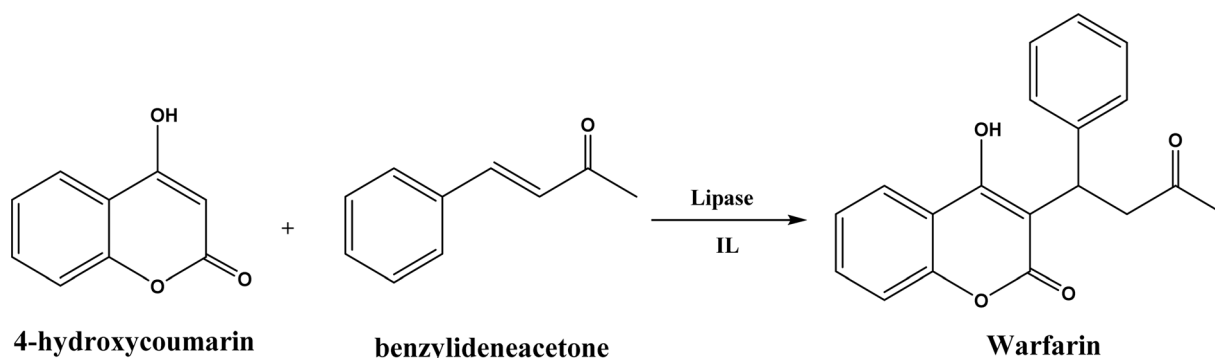

4-hydroxycoumarin   **benzylideneacetone**   **Warfarin**

Fig. 36 Lipase-catalyzed Michael addition synthesis of warfarin in ILs.
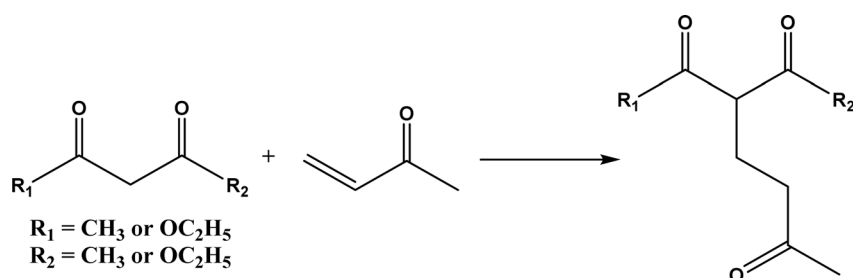

R_1 = CH$_3$ or OC$_2$H$_5$
R_2 = CH$_3$ or OC$_2$H$_5$

Fig. 37 D-Aminoacylase-catalyzed Michael addition of 1,3-dicarbonyl compounds to methyl vinyl ketone.

enabled moderate to high yields for the reactions of 1,3-dicarbonyl compounds with α,β-unsaturated compounds in 2-methyl-2-butanol and other organic solvents at 50 °C for 24 h. In another study,[146] D-aminoacylase from *Escherichia coli* as a zinc-dependent acylase was found more active than other enzymes (*e.g.*, Amano acylase from *Aspergillus oryzae*, CALB, *Candida cylindracea* lipase, and Amano lipase M) in catalyzing the Michael addition of 1,3-dicarbonyl compounds to methyl vinyl ketone (Fig. 37); tertiary alcohols (*i.e.*, 2-methyl-2-butanol and *tert*-butanol) enabled much higher yields (up to 82.1%) than more hydrophobic (*i.e.*, *n*-hexane, toluene, chloroform, and

isopropyl ether) and hydrophilic solvents (*i.e.*, THF and dioxane). The catalytic mechanism is described in Fig. 38: interactions of carbonyl groups from both substrates with Zn^{2+} near the active site, proton transfer from acetylacetone to Asp-366, nucleophilic attack of methyl vinyl ketone by acetylacetone to form an enolate, proton transfer from Asp to the enolate, and the release of final product from the active site. Wu *et al.*[147] found that protease from *Streptomyces griseus* was able to catalyze Michael additions of a variety of malonates and enones in aqueous methanol, and achieved up to 84% yields and up to 98% ee under optimum conditions. Since proline and its
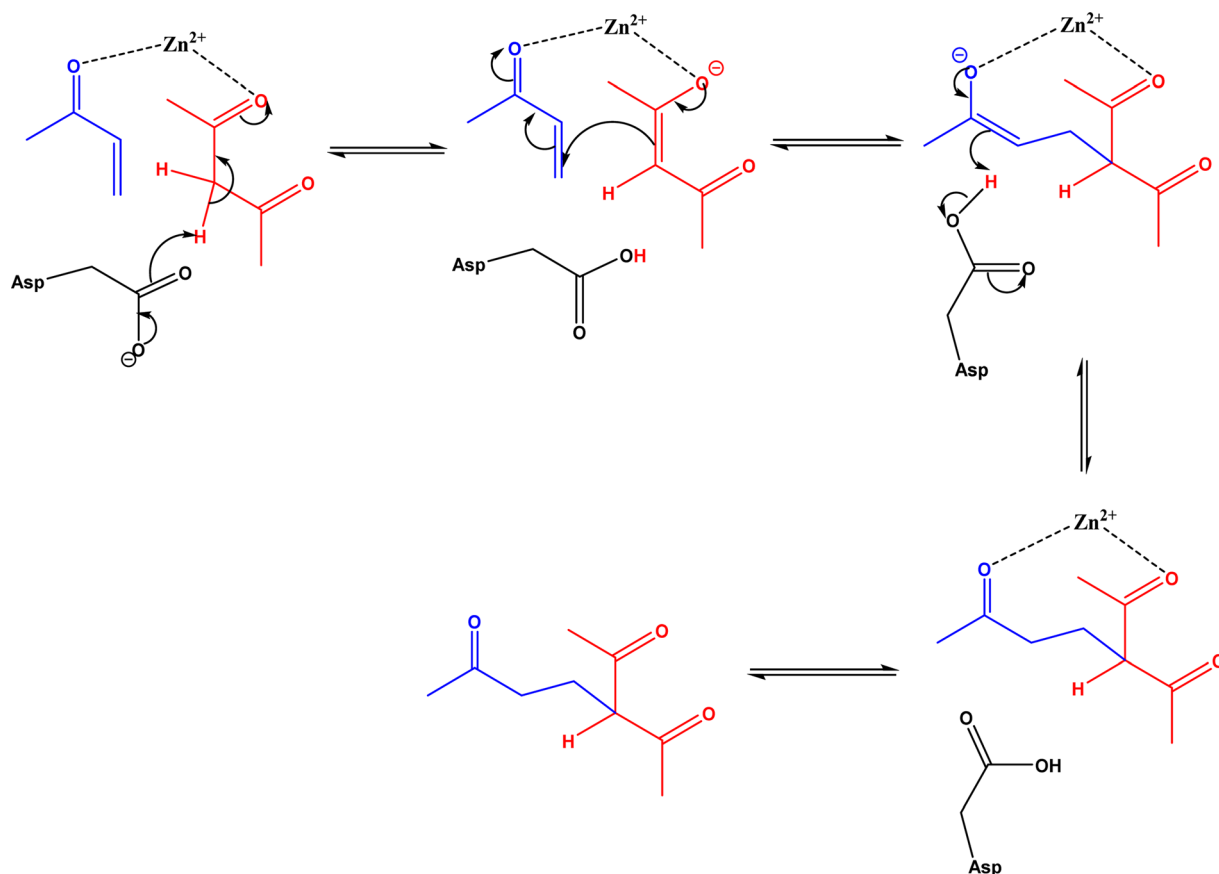
Fig. 38 Mechanism of zinc-dependent D-aminoacylase-catalyzed Michael addition.[146]
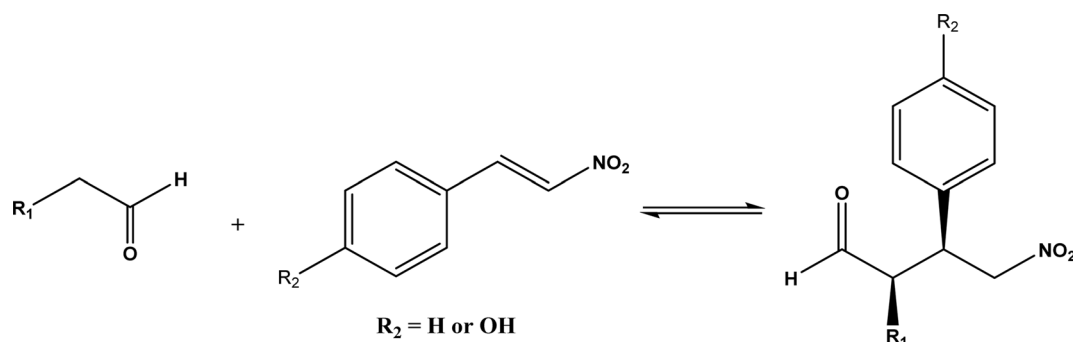

Fig. 39 Michael addition of *trans*-nitrostyrenes and linear aldehydes catalyzed by 4-oxalocrotonate tautomerase.

derivatives have been used as organocatalysts for C–C bond formations including Michael addition,[148] the Poelarends group[149,150] noted that 4-oxalocrotonate tautomerase carries a catalytic amino-terminal proline, thus could catalyze the asymmetric Michael reaction between *trans*-nitrostyrenes and linear aldehydes ranging from acetaldehyde to octanal as donors (Fig. 39) in aqueous solutions (water, or water/ethanol = 9 : 1), giving 46–92% yields, good diastereoselectivities (from 85 : 15 to 93 : 7), and fair ees (23–89%); a larger aldehyde molecule caused a lower enantioselectivity and slower reaction. The mechanism includes several steps as shown in Fig. 40: the formation of iminium ion *via* nucleophilic attach of Pro-1 to

carbonyl carbon of the aldehyde, the deprotonation of iminium ion to form enamine, Michael-type nucleophilic attack of *trans*-nitrostyrene by enamine (Arg-11 supports the correct substrate binding), proton transfer from Arg-39 to the reaction complex, and the release of final product from Pro-1.

Duplex DNA, G-quadruplex DNA, and DNA/RNA-derived hybrid catalysts have been developed for asymmetric Diels–Alder, Michael addition, and Friedel–Crafts reactions in aqueous buffers or organic solvents.[151–155] Our group conducted Michael addition in aqueous solutions of ionic liquids (ILs), deep eutectic solvents (DES), inorganic salts, glymes, glycols, and other organic solvents catalyzed by duplex DNA[156] or G-
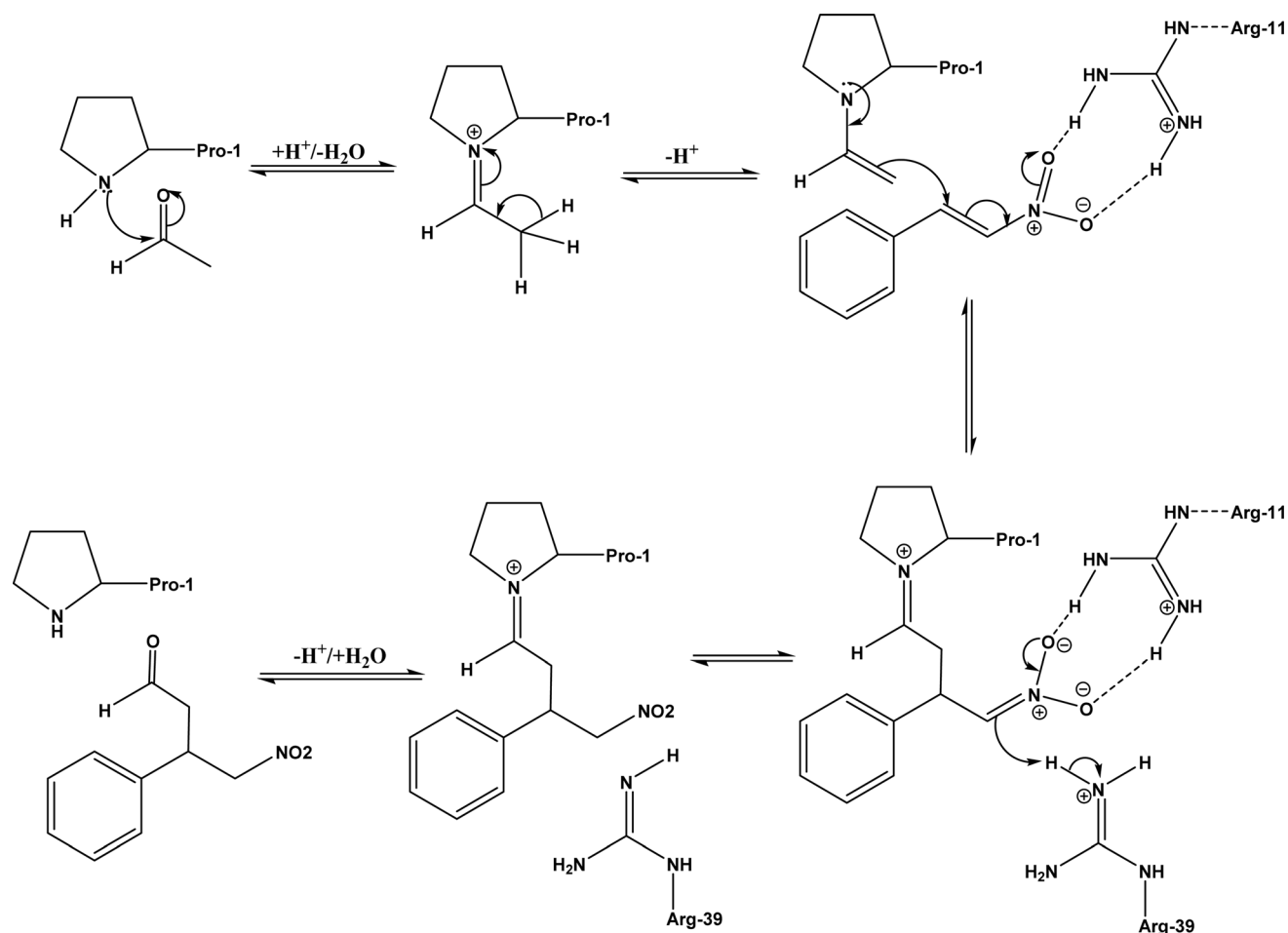
Fig. 40 Mechanism of Michael addition of *trans*-nitrostyrenes and acetaldehyde catalyzed by 4-oxalocrotonate tautomerase [redrawn from Scheme S1 in ref. 149].

quadruplex DNA-based catalysts,[157] and found that the addition of glycerol, glyme, or DES enabled the reaction to be conducted at room temperature while maintaining up to 94–99% ees and mostly >70–97% yields.[156]

5. Friedel–Crafts alkylation and acylation

Friedel–Crafts alkylation and acylation represent an important category of C–C bond formation reactions, traditionally catalyzed by Lewis acids such as $AlCl_3$, which leads to poor regioselectivity and multi-alkylation. Various biocatalysts pave a new avenue for regio- and chemoselective Friedel–Crafts. Recently, peptide catalysts supported on PEG-PS-resin were developed to catalyze the Friedel–Crafts alkylation shown in Fig. 41, and it was found that polyleucine in the form of –(AA)$_n$–, such as (Leu-Leu-Aib)$_n$ where n = 1, 2 or 3, was able to form an α-helical structure and thus, along with β-turn motif D-Pro-Aib, could effectively facilitate alkylation reactions.[158,159] Furthermore, the same group[160] extended the peptide catalysts to synthesize oxygen-functionalized indole or pyrrole derivatives (often seen in the structures of antibiotics) through a tandem reaction of

Friedel–Crafts-type alkylation of indole or pyrrole compounds followed by an α-oxyamination *via* laccase (an oxidative enzyme) in THF/H$_2$O (1 : 2, v/v) mixture (see Fig. 42), leading to 70–79% *syn* products with 91–98% ee; the stereochemistry of the α-oxyamination step is primarily controlled by the peptide catalyst. In nature, methyltransferases catalyze the transfer of a methyl group in living cells such as DNA and RNA methylation; (*S*)-adenosyl-L-methionine (SAM, Fig. 43) is the most common methyl donor, which acts as the co-factor for the enzyme.[161] Several methyltransferases originally found in bacteria such as NovO, CouO, SfmM2, and Orf19 from *Streptomyces* species, SibL from *Streptosporangium sibiricum*, and SacF from *Pseudomonas fluorescens*, could promote Friedel–Crafts alkylations of coumarins, naphthalenediols, and aromatic amino acids using SAM or non-natural SAM analogues (Fig. 43), resulting in excellent regioselectivity and various conversions.[46–49] Dimethylallyl-tryptophan synthases (a type of as "aromatic prenyltransferases") can catalyze Friedel–Crafts alkylations of various aromatic substrates (*e.g.*, indoles, naphthalenes, flavonoids, and phenylpropanoids), but exhibit a high specificity for dimethylallyl diphosphate (DMAPP) as the alkyl donor;[162–164] Liebhold and co-workers[165] demonstrated that
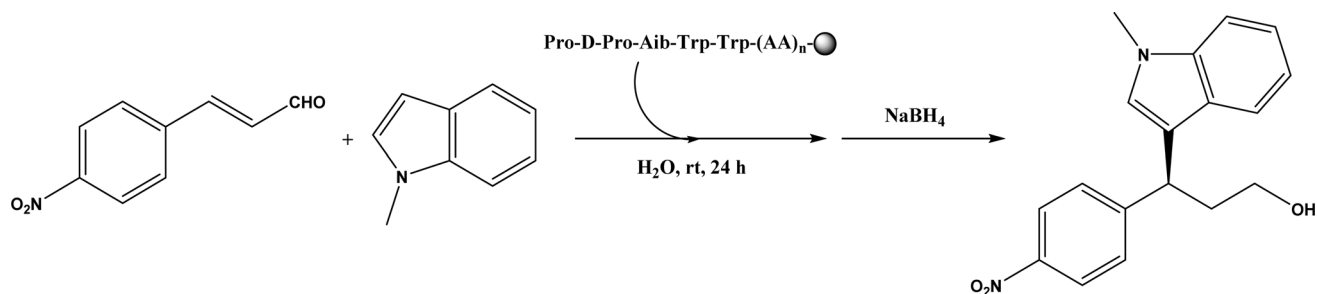
Fig. 41 Resin-supported peptide-catalyzed Friedel–Crafts alkylation (Aib = 2-aminoisobutyric acid; resin = −NH-CH$_2$−CH$_2$-PEG-PS).
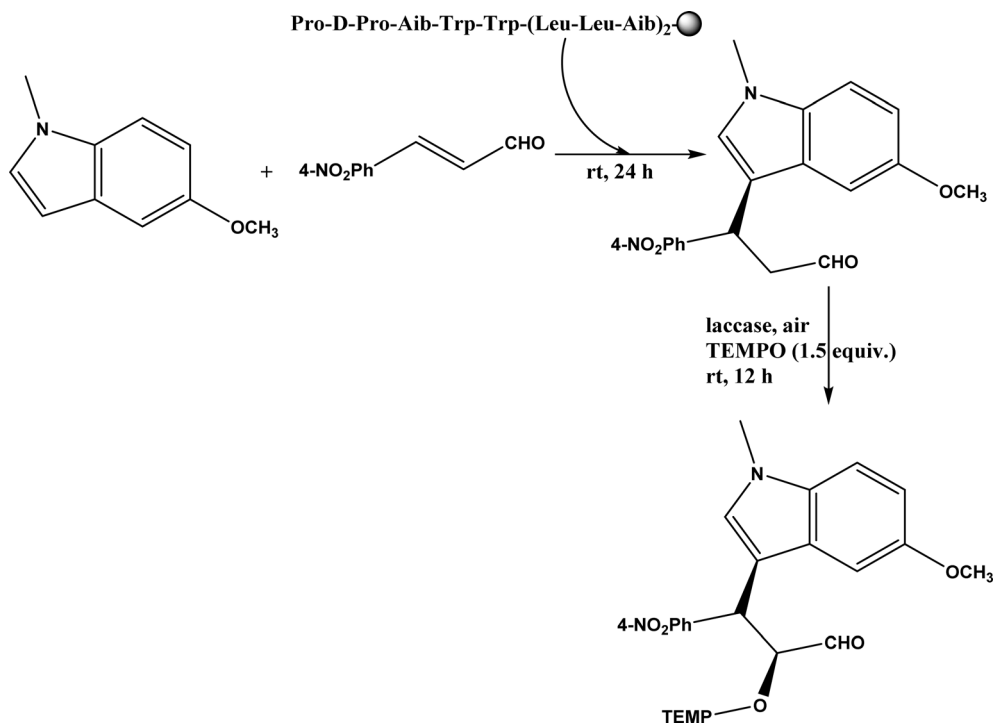

Fig. 42 One-pot sequential Friedel–Crafts-type alkylation and α-oxyamination (TEMPO = 2,2,6,6-tetramethylpiperidin-1-oxyl).

DMAPP can be modified by deleting or shifting one methyl group in DMAPP (Fig. 44) while still serving as alkyl donors for prenyltransferases, however, the double bond at β-position is important to keep for stabilizing the carbocation formed during the enzymatic alkylation on indoles. In another study, the cylindrocyclophane biosynthetic enzyme CylK was found capable of promoting a stereospecific Friedel–Crafts alkylation of resorcinol rings at their C-2-position (Fig. 45), resulting in high conversions (70–100%) and turn over numbers (>150) in most cases.[166] Their DFT calculations point out a catalysis mechanism (Fig. 46) where CylK enables partial or full deprotonation of a hydroxyl group on the resorcinol, which acts as a nucleophile to initiate a concerted S$_{N}$2 or stepwise S$_{N}$1 reaction. α-Chymotrypsin from bovine pancreas (BPC) was found being able to catalyze Friedel–Crafts reactions between a broad range of isatins and indoles to produce 3-hydroxy-oxindoles in the presence of aprotic solvents such as 1,2-dichloroethane, or 3,3-bis(indol-3-yl)indolin-2-ones when methanol was used as

the co-solvent (Fig. 47) although no stereoselectivity was specified, which enabled the synthesis of several pharmacologically active compounds.[167] As relatively strong Brønsted acids, squalene hopene cyclases (SHCs) catalyze the regio- and stereoselective polycyclization of squalene, and could catalyze the intramolecular Friedel–Crafts alkylation of polyprenyl phenyl ethers, but showed a low catalytic activity and poor selectivity between the alkylation and hydration productions (see an example in Fig. 48); interestingly, variants of SHCs can be designed using site-directed and saturation mutagenesis to afford a high selectivity of alkylation (up to 100%) despite a moderate production formation of up to 29%.[168,169]

An artificial metalloenzyme was constructed by complexing Cu(ıı) with 1,10-phenanthroline as a ligand, which had a strong affinity with the transcription factor Lactococcal multidrug resistance Regulator (LmrR), a homodimeric protein.[50] This LmrR metallozyme was used for the enantioselective Friedel–Crafts alkylation of indoles with α, β unsaturated 2-acyl-
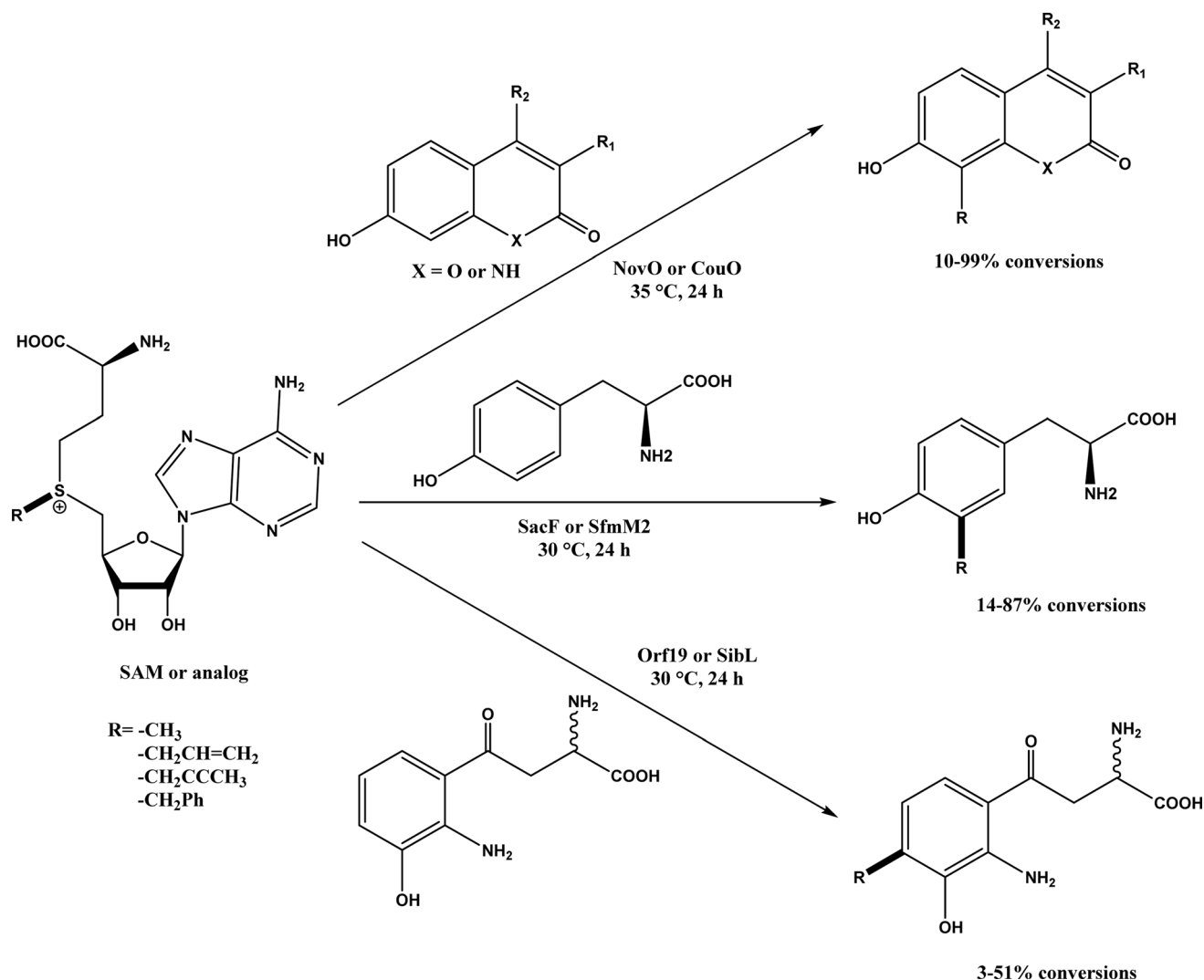
Fig. 43 Friedel–Crafts alkylation catalyzed by (S)-adenosyl-L-methionine (SAM) dependent methyltransferases.
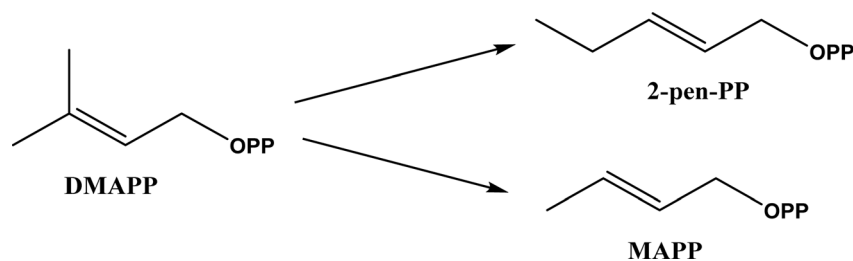

Fig. 44 Dimethylallyl diphosphate (DMAPP) and its analogues that can serve as alkyl donors for prenyltransferases.

imidazoles to afford up to 92% ee, and the tandem Friedel–Crafts alkylation/enantioselective protonation reaction (Fig. 49). The protein mutation tailored the selectivity and activity of artificial metalloenzyme. This group[170] further demonstrated that the protein's N19 and M89 positions are critical to the enzyme activity, and mutations at these locations indicate the importance of different side chains in the pocket of LmrR for controlling the reactivity and selectivity of mutants for both C–C bond formation and enantioselective protonation.

The multicomponent acyltransferase (ATase) catalyzes the *in vivo* reversible acetylation of monoacetylphloroglucinol. This activity can be extended to catalyze Friedel–Crafts acylation of resorcinols and Fries rearrangement of phenolic esters (Fig. 50). A mutant of ATase (known as *Pp*ATaseCH) showed five-fold higher activities than the wild type; polyketide 2,4-diacetyl-phloroglucinol (DAPG) and *N*-acetylimidazole were effective acyl donors leading to up to 99% product yields for regioselective Friedel–Crafts acylation.[51] This group[171] further discovered that
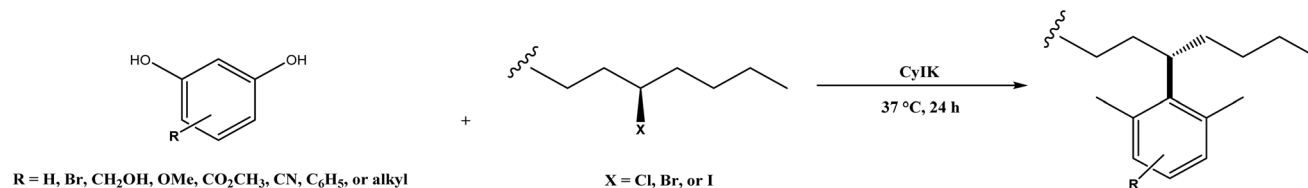
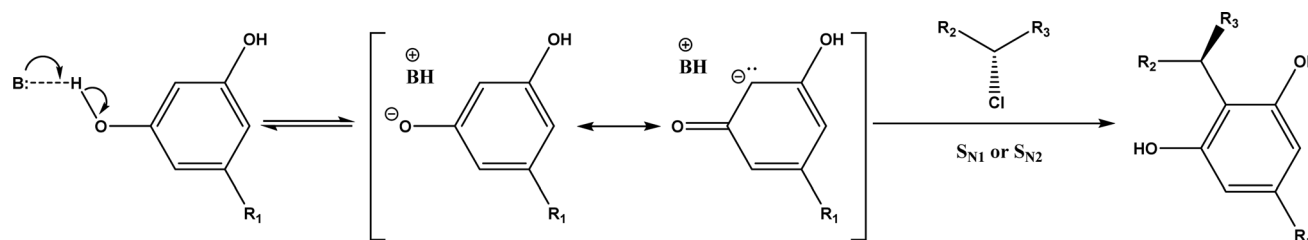**Fig. 45** CylK-mediated alkylation of resorcinols with alkyl halides.

Fig. 46 Mechanism of resorcinol nucleophilic activation through hydrogen bonding or deprotonation.
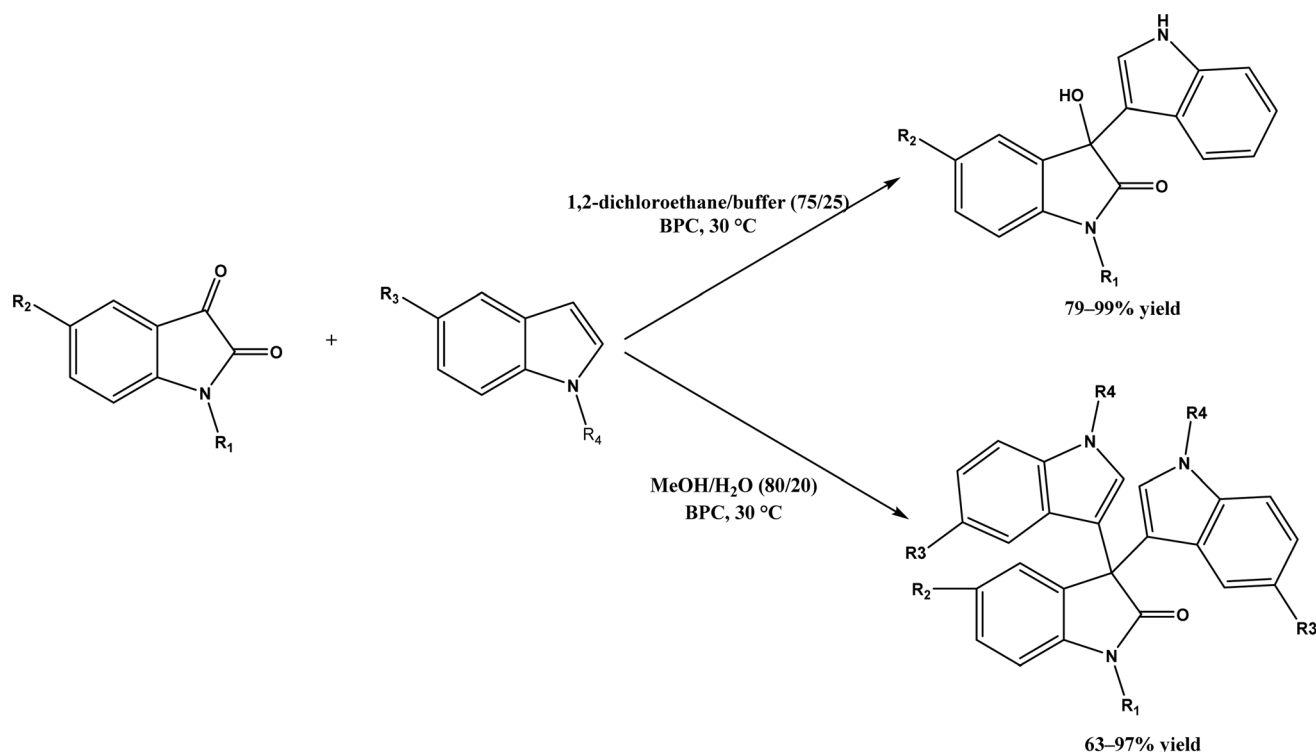

Fig. 47 Solvent-controlled Friedel–Crafts reactions between isatins and indoles catalyzed by α-chymotrypsin from bovine pancreas (BPC).

the same enzyme (*Pp*ATaseCH) promoted the C–S bond cleavage prior to C–C bond formation, thus identified ethyl thioacetate as a suitable acetyl donor for the acylation of resorcinol derivatives (Fig. 50a), achieving up to 99% conversion and 88% isolated yield. On the other hand, reverse Friedel–Crafts acylation can be accomplished by a group of co-factor independent enzymes known as retro-Friedel–Crafts hydrolases, which requires substrates with a carbonyl group. Two of these

enzymes, 2,6-diacetylphloroglucinol hydrolase (PhlG) from *Pseudomonas fluorescens* and phloretin hydrolase from *Eubacterium ramulus* (Phy), were selected to carry out the retro-Friedel–Crafts reactions shown in Fig. 51 in aqueous solutions containing organic solvents, resulting in 83% conversion in both reactions.[172] However, attempts to form C–C bonds *via* Friedel–Crafts acylation by these two enzymes in different solutions of organic solvents all failed.
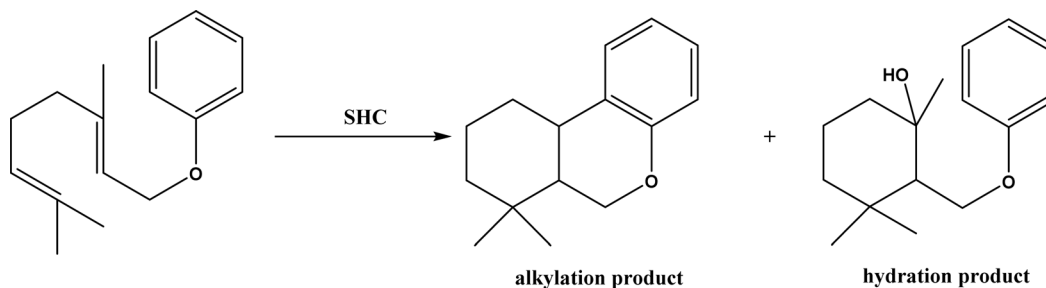
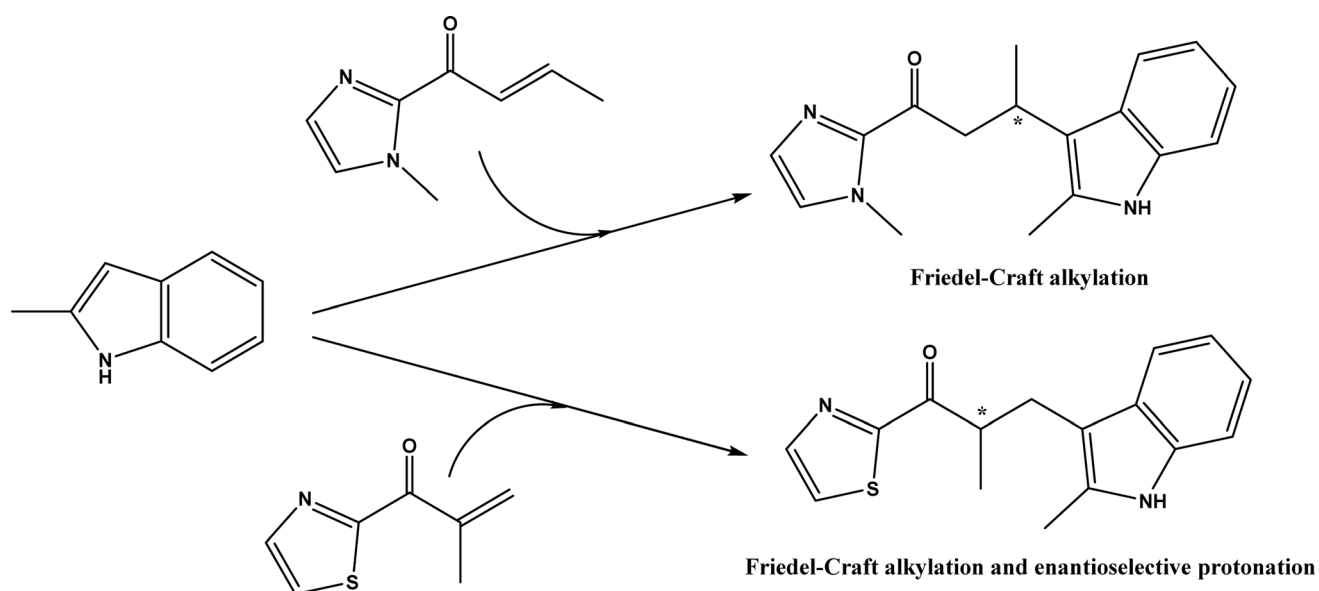**Fig. 48** Squalene-hopene cyclase (SHC)-catalyzed conversion of geranyl phenyl ether.

Fig. 49 Artificial metalloenzyme-catalyzed Friedel–Crafts and the tandem Friedel–Crafts/enantioselective protonation.
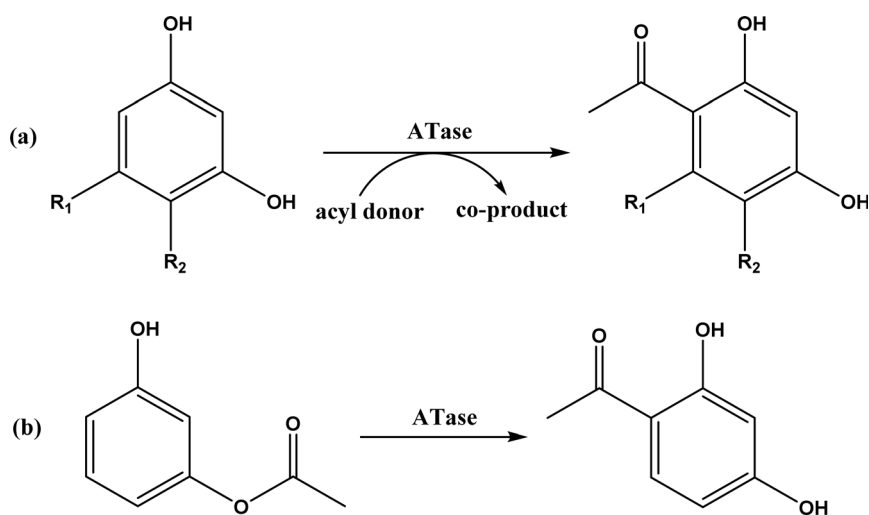
Fig. 50 Acyltransferase-catalyzed Friedel–Crafts acylation (a) and Fries rearrangement (b).
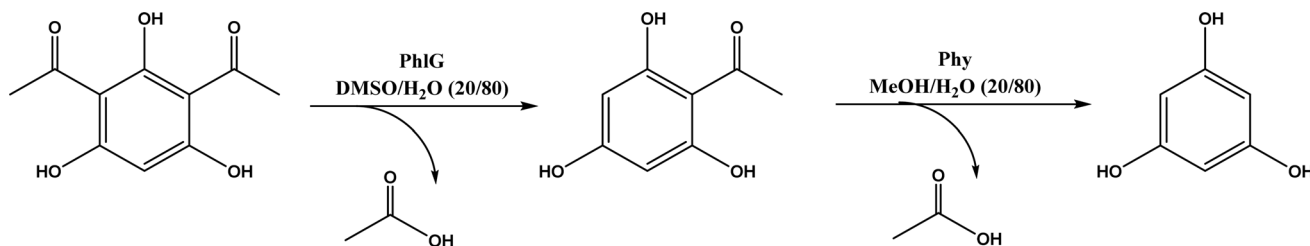
Fig. 51 PhlG and Phy-catalyzed retro-Friedel–Crafts reactions in nature.

6. Mannich reaction

Mannich reaction is a three-component reaction involving a primary or secondary amine, an enolizable carbonyl compound, and a non-enolizable aldehyde to synthesize β-amino carbonyl compounds. This reaction usually competes with the aldol condensation. The Anilkumar group[173] systematically reviewed the Mannich reaction catalyzed by various organo- and metal catalysts, along with two examples of enzyme catalysts (acylase from *Aspergillus melleus*[174] and wheat germ lipase[175]). When Mannich reactions of substituted benzaldehyde, aniline, and acetone were catalyzed by various lipases (Fig. 52),[52] it was found that *Mucor miehei* lipase led to the highest product yield (although the stereoselectivity was not specified), followed by *Candida antarctica* lipase B; in addition, neat organic solvents (*i.e.*, toluene, dichloromethane, THF, DMF and acetone) resulted in the Schiff base product (>90%) instead of the Mannich product while the addition of water favored the Mannich reaction (*e.g.*, 40–50% water mixing with acetone produced the highest yield). A lipase catalysis mechanism was described in Fig. 53:[52] a quick formation of Schiff base between aldehyde and amine, the Schiff base forming a complex with the enolate anion (from ketone as being activated by the lipase) and the His residue, new C–C bond formation *via* electron transfer from Schiff base to enolate anion to form a new carbon–carbon bond, and the release of Mannich product from the oxyanion hole. In another study, trypsin from hog pancreas was found a more effective catalyst than lipases and α-amylase for Mannich reactions among 4-nitrobenzaldehyde, *p*-anisidine, and acetone; acetone and ethanol were shown better solvents than others while water was not necessary for the reaction.[53] The Mannich reaction between 4-nitrobenzaldehyde, acetone and aniline (Fig. 54) was

catalyzed by Alcalase, producing 51% aldol product and 46% Mannich product at 45 °C (no stereoselectivity was specified) with Alcalase-CLEA® while denatured Alcalase or no enzyme favored more aldol product.[34]

7. Morita–Baylis–Hillman (MBH) reaction

The MBH reaction, also known as Baylis–Hillman reaction, is a C–C coupling reaction between activated alkene (α-carbon of a conjugated carbonyl compound) and carbon electrophile, traditionally catalyzed by a tertiary amine or phosphine.[176] The reaction mechanism typically begins with a Michael addition of the catalyst (nucleophile) at β-carbon of a conjugated carbonyl compound, continues with C–C bond formation with the electrophile, and ends with product release from the catalyst; the same mechanism is applicable to protein catalysts.[177] Lipases and esterases could only achieve 10% conversion for the MBH reaction of 4-nitrobenzaldehyde and cyclohexenone although bovine serum albumin (BSA) enable 35% conversion.[178] When the MBH reaction between 4-nitrobenzaldehyde and methyl vinyl ketone was catalyzed by Alcalase, a higher reaction temperature (30–60 °C) led to a higher conversion (up to 26%), but the reaction was non-specific protein catalysis because the denatured protease produced similar yields under the same conditions,[34] which could be explained by the nonspecific catalytic role of the histidine residue because imidazole derivatives have been shown as effective catalysts for the MBH reaction.[179] Other than the promiscuous activities of hydrolases for MBH reactions, Crawshaw and co-workers[54] employed the directed evolution to optimize a primitive computationally designed protein for the MBH reaction (BH32), and found that
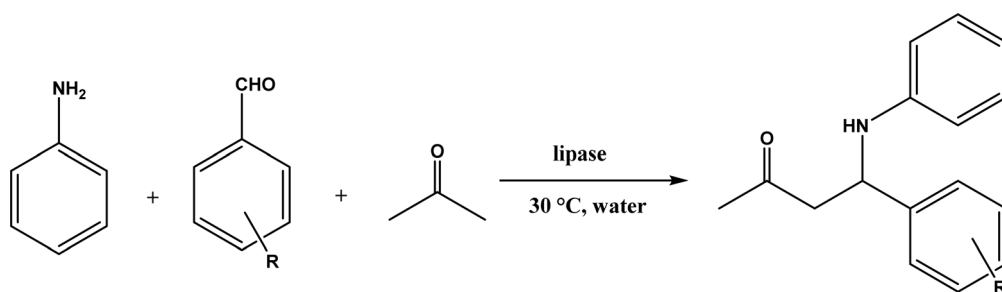

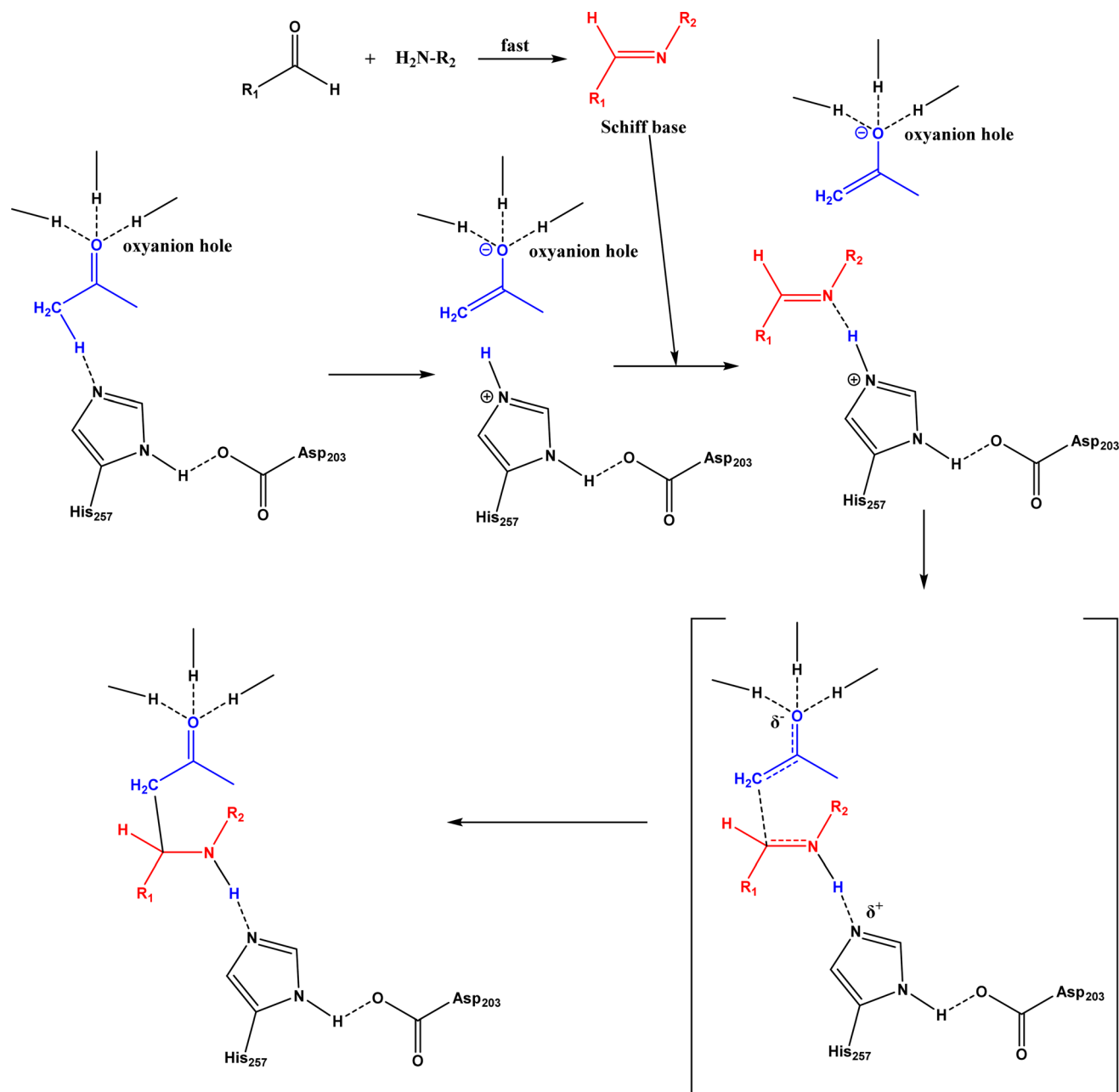**Fig. 52** Lipase-catalyzed Mannich reaction in water.

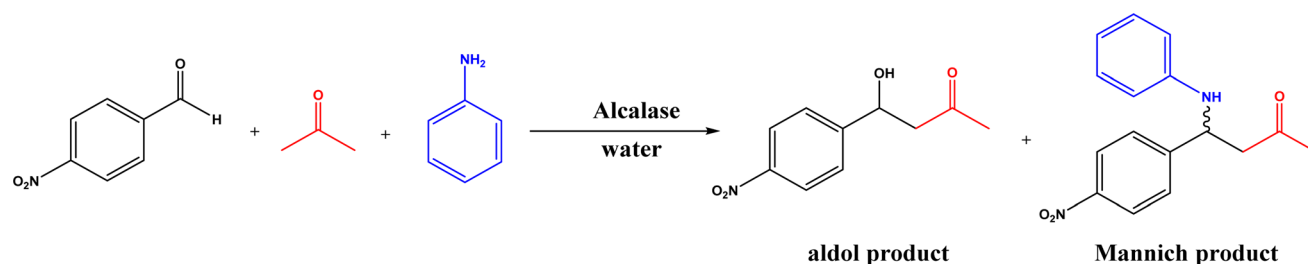**Fig. 53** Mechanism of lipase-catalyzed Mannich reaction (redrawn from ref. 52).

Fig. 54 Mannich reaction between 4-nitrobenzaldehyde, acetone and aniline.
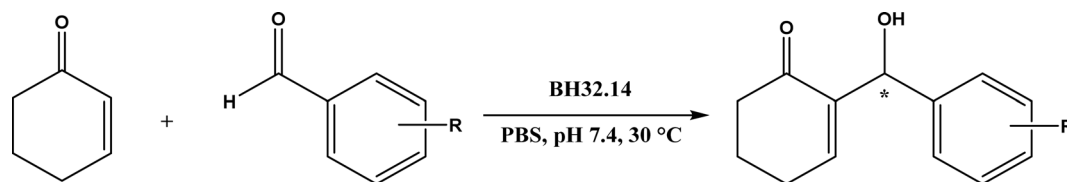
Fig. 55 Morita−Baylis−Hillman (MBH) reaction between activated alkene and aldehyde.

BH32.14 variant acted as an efficient and enantioselective MBHase to promote the reactions between activated alkenes and aldehydes with 33–99% yields and 54–99% ees in most cases (Fig. 55); the likely catalytic mechanism involved a nucleophilic His23 and a multi-functional Arg124 to accelerate the MBH reaction.

8. Diels−Alder reaction

Diels−Alder reaction, known as [4 + 2] cycloaddition, yields a six-membered ring compound with regio- and stereoselectivity through reacting a conjugated diene with a substituted alkene (as dienophile), usually catalyzed by Lewis acids such as $ZnCl_2$ and $AlCl_3$. Many natural products are biosynthetically produced through Diels−Alder reactions catalyzed by enzymes, generally categorized as Diels−Alderases,[182] for example, trans-decalin formation by Fsa2-family enzymes as shown in Fig. 56,[180] and the biosynthesis of spinosyn A involving a cyclase SpnF to catalyze [4 + 2] cycloaddition as shown in Fig. 57.[181] Several

earlier studies have identified isolated enzymes for catalyzing Diels−Alder reactions such as a crude enzyme extract of solanapyrone synthase for cycloaddition of prosolanapyroneIII to the exo adduct solanapyrone A,[183] crude lovastatin nonaketide synthase (LovB) for the cyclization of hexaketide triene esters,[3] and riboflavin synthase for the cyclization of 6,7-dimethyl-8-ribityllumazine.[184] Ose and co-workers[4] determined the 1.70 Å resolution crystal structure of Mg^{2+}-dependent fungal macrophomate synthase (MPS, a natural Diels−Alderase) in complex with pyruvate, and described the three-step catalytic mechanism for the Diels−Alder reaction of 2-pyrone and oxalacetate to form macrophomic acid (Fig. 58): decarboxylation of oxalacetate, Diels−Alder reactions of the enolate and 2-pyrones, and anti-elimination of water and decarboxylation. The C–C bond forming step was previously debated by Watanabe and co-workers[55] whether it is Michael-aldol process or Diels−Alder reaction. Later, this second step was suggested by the Jorgensen group[56] to be a stepwise Michael-aldol reaction instead of a Diels−Alder reaction (Fig. 59) based on the mixed quantum
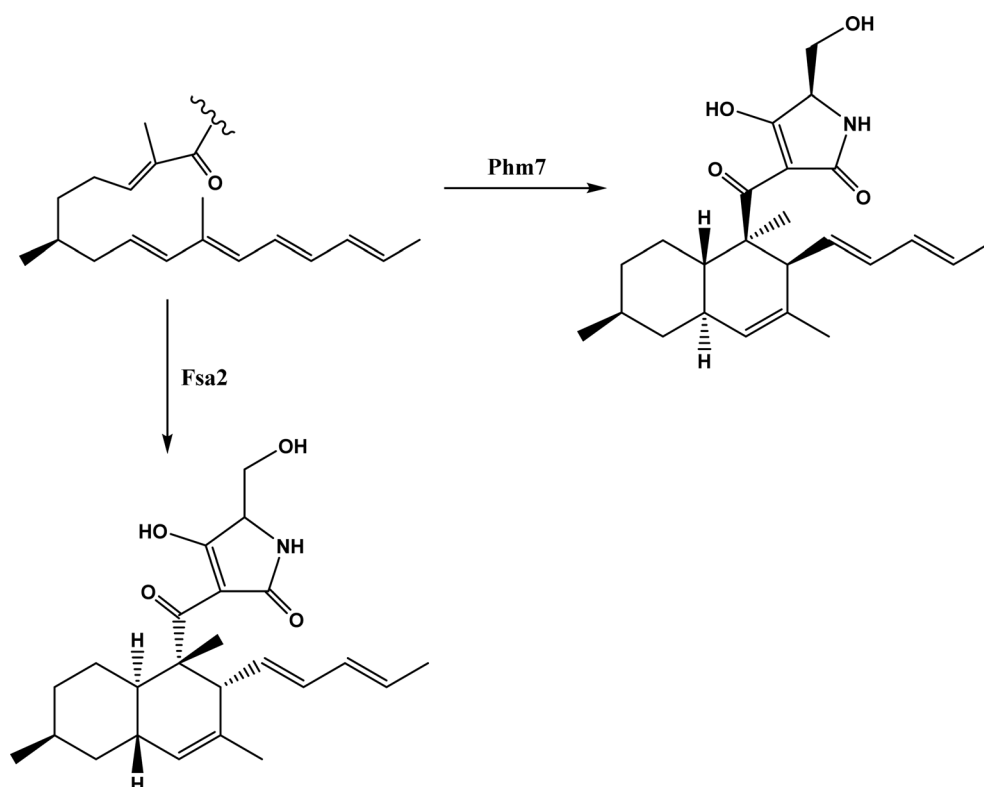

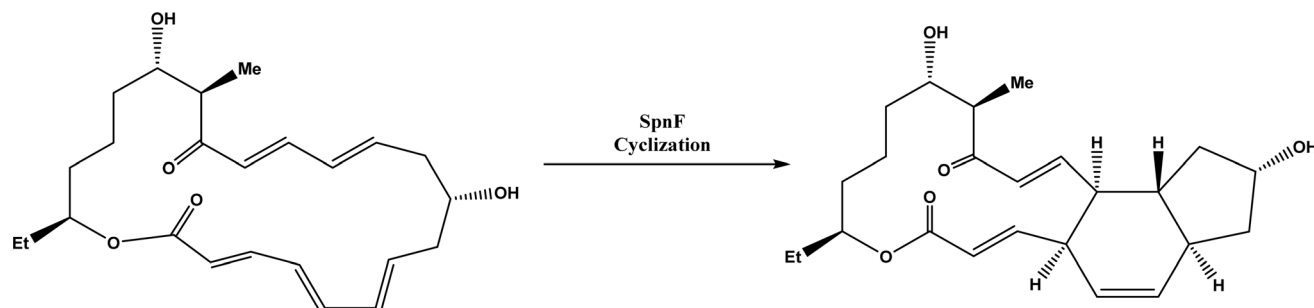**Fig. 56** Stereospecific [4 + 2] cycloaddition reactions catalyzed by decalin synthases Fsa2 and Phm7.[180]

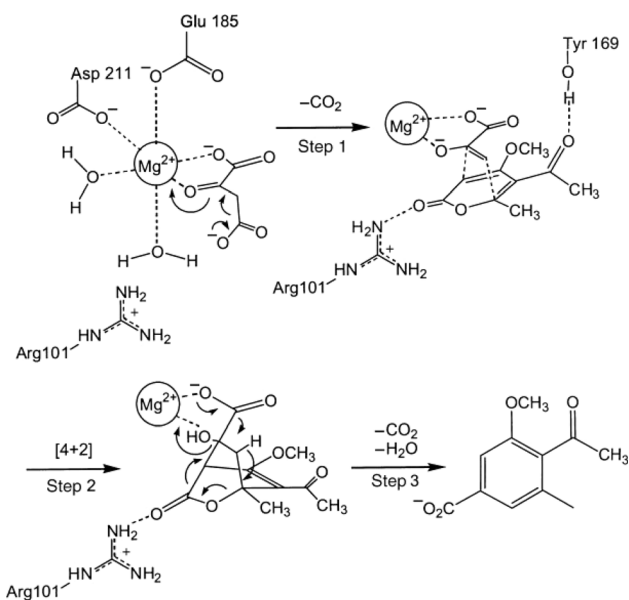**Fig. 57** Cyclase SpnF-catalyzed cyclization during the biosynthesis of spinosyn A.[181]

Fig. 58 Mechanism of macrophomate synthase-catalyzed Diels–Alder reaction of 2-pyrone and oxalacetate to synthesize macrophomic acid [Reprinted with permission from ref. 185 Copyright 2003 Wiley-VCH Verlag GmbH& Co.].
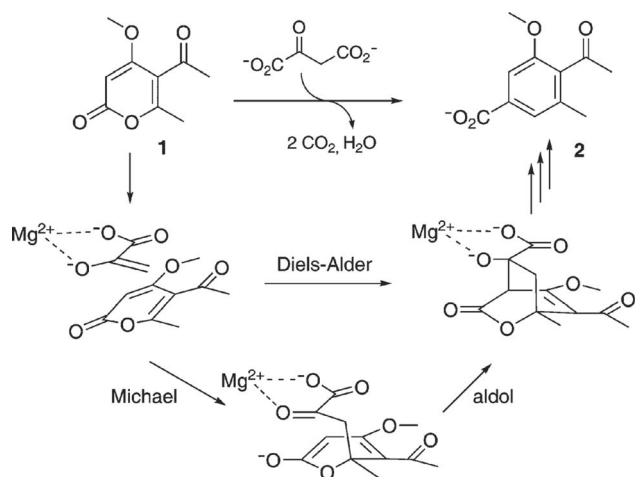

Fig. 59 Mechanism of MPS-catalyzed synthesis of macrophomate (2) from 2-pyrone (1) and oxaloacetate [Reprinted with permission from ref. 186 Copyright 2007 The Royal Society of Chemistry].

and molecular mechanics (QM/MM) in combination with Monte Carlo (MC) simulations and free-energy perturbation (FEP) computations. The free energy of Diels–Alder transition state was found over 20 kcal mol^{-1} higher than that of Michael and aldol transition states. Through site-directed mutagenesis, the Hilvert group[186] identified three amino acid residues (Arg101, Asp70, and His73) of MPS are essential to oxaloacetate decarboxylation and trapping of the enolate with a 2-pyrone. Experimentally, it was found that MPS exhibited promiscuous aldolase activity for catalyzing aldol reactions between various aldehydes and oxaloacetate although enantioselectivities were generally low.[187] However, a later study by the same group reported high aldolase activities and stereoselectivities of MPS when catalyzing the reaction between oxaloacetate and protected aldoses to synthesize protected 3-deoxysugar derivatives (28–84% yields and 8 : 1 to >19 : 1 dr) as illustrated in Fig. 60.[188] A natural cofactor-independent Diels-Alderase, AbyU, is a homodimer consisting of two eight-stranded antiparallel β-barrels; this enzyme is found in abyssomicin C biosynthetic pathway to catalyze a Diels–Alder reaction step.[189] AbyU maintained considerable catalytic activities at temperatures of up to 65 °C and in 3.0 M guanidinium hydrochloride (a protein denaturant), and >50% folding structures in up to 70% (v/v) acetonitrile and >70% folding in 80% (v/v) DMSO and methanol.[190] The Baker group[57] used *de novo* computational method to design the active site that is suitable for catalyzing a model Diels–Alder reaction between 4-carboxybenzyl *trans*-1,3-butadiene-1-carbamate and *N,N*-dimethylacrylamide (Fig. 61), searched 207 protein structures for backbone geometries that accommodate the active site and substrates, and narrowed down to test 50 enzymes, but only two of them showed measurable activities, which could be further improved *via* directed evolution. Despite its low efficiency, this method allows a rational design and search of enzyme structures for particular reactions. Quantum chemical calculations illustrated how enzyme active sites (of theozymes) accelerate the intramolecular Diels–Alder conversion of salvileucalin A to salvileucalin B; theozymes investigated contain common functional group arrays found in esters.[191] Interestingly, RNA molecules were identified as efficient as DNA in catalyzing C–C bond formation in Diels–Alder reaction.[192]

Natural ribozymes catalyze the hydrolysis and transesterification of internucleotide bonds, but *in vitro*-selected
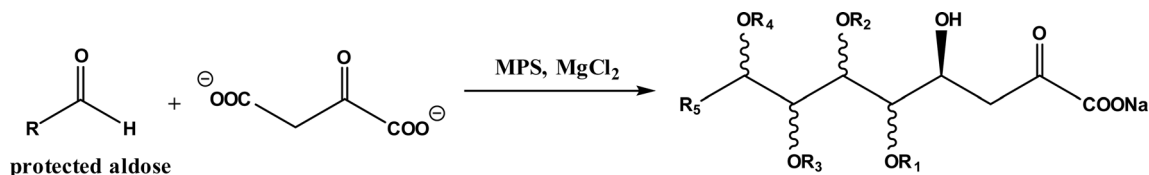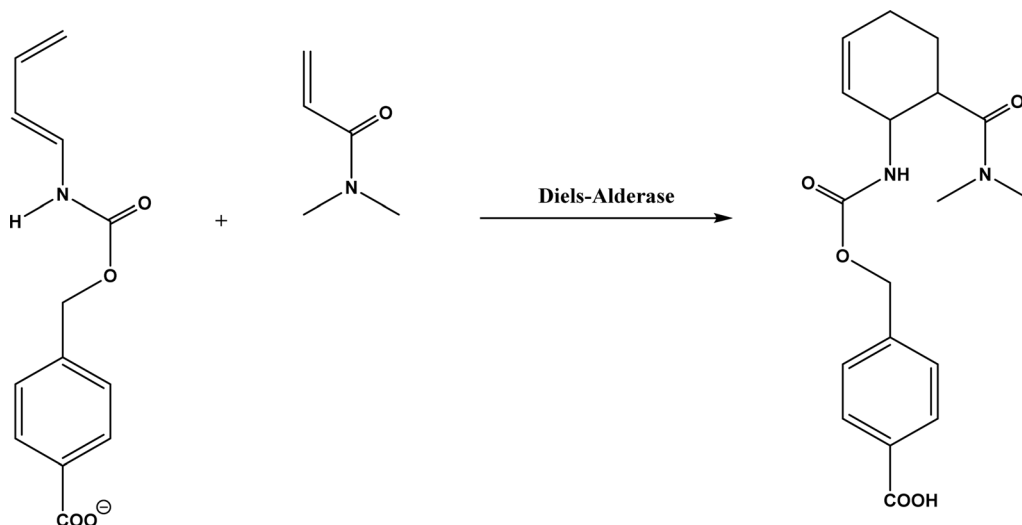
Fig. 60 MPS-catalyzed aldol reaction between oxaloacetate and protected aldoses.

Fig. 61 Diels−Alder reaction between 4-carboxybenzyl *trans*-1,3-butadiene-1-carbamate and *N,N*-dimethylacrylamide.

ribozymes could facilitate the C–C bond formation through Diels–Alder reaction.[193,194] In addition, some antibodies have been discovered for catalyzing Diels–Alder reactions.[195–197] Topics on ribozymes and nucleic acid catalysis[198] and antibody catalyzed cycloadditions[199] have been covered by other reviews. Serganov and co-workers[200] compared structural bases of these different biocatalysts: antibodies has a hydrophobic catalytic core, which is similar to natural Diels–Alderases; however, Diels–Alderases also has a co-factor Mg²⁺ cation to coordinate with carbonyl oxygens of the dienophile in addition to hydrogen bonding of the active site with substrates. The ribozyme has a wedge-shaped catalytic pocket to dictate the stereoseletivity, and its catalysis is accomplished through a combination of proximity, complementarity, and electronic effects.

9. Acyloin condensations *via* thiamine diphosphate (ThDP)-dependent enzymes

Thiamine (or thiamin) is better known as vitamin B1, a water-soluble vitamin. Its biologically active derivative, called thiamine diphosphate (ThDP) or thiamine pyrophosphate (TPP), is a cofactor of enzymes that are essential to many cellular metabolism cycles. ThDP is a natural thiazolium salt consisting of pyrimidine, thiazolium, and pyrophosphate units (Fig. 62). ThDP-dependent enzymes are known for their capabilities in forming C–C bonds *via* acyloin condensation; the general mechanism (Fig. 63) involves thiamine diphosphate cofactor

reacting with an aldehyde (donor) to form an active zwitterion, which attack the acceptor aldehyde to yield (*R*)-α-hydroxyketone after the release of the cofactor.[80] Applications of these enzymes in C–C bond formation and their specific catalytic mechanisms have been discussed in earlier reviews,[80,201–205] which include several known enzymes such as acetohydroxy acid synthase (AHAS, EC 2.2.1.6), benzoylformate decarboxylase (BFD, EC 4.1.7.7),[206] benzaldehyde lyase (BAL, EC 4.1.2.38), pyruvate decarboxylase (PDC, EC 4.1.1.1), phenylpyruvate decarboxylase (PhPDC, EC 4.1.1.43), keto acid decarboxylase (EC 4.1.1.72),[207] and transketolase (TK, EC 2.2.1.1),[208] as well as newer enzymes such as 1-deoxy-D-xylulose 5-phosphate synthase (DXPS, EC 2.2.1.7), flavoenzyme cyclohexane-1,2-dione hydrolase (CDH, EC 3.7.1.11), flavoenzyme YerE (the decarboxylation of pyruvate and the transfer of the activated acetaldehyde to aldehydes and ketones), *Bacillus stearothermophilus* acetylacetoin synthase (ketones as acceptors to form tertiary alcohols[209]), and ThDP-dependent PigD and MenD [for Stetter-type of 1,4 addition of aldehydes, or benzoin-condensation 1,2-addition[210,211]].

A few recent updates beyond previous reviews are discussed here. Other than PigD for catalyzing the Stetter reaction of α-keto acids with α,β-unsaturated ketones (Michael acceptor substrates), two new ThDP-dependent enzymes, SeAAS from *Saccharopolyspora erythraea* and HapD from *Hahella chejuensis* were identified to have 39% and 51% similarity with PigD respectively in terms of their amino acid sequences, and thus could catalyze intermolecular Stetter reactions (1,4-carboligation in Fig. 64) and benzoin condensation (1,2-carboligation in
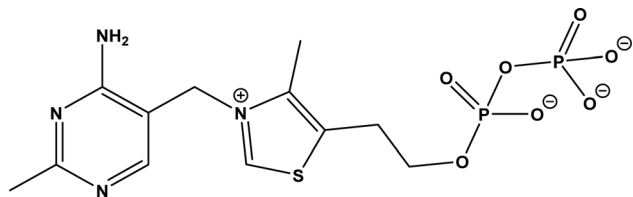
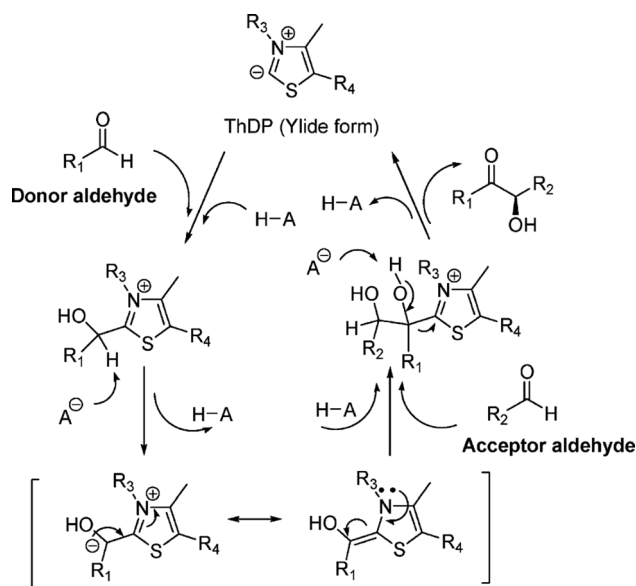Fig. 62   Structure of thiamine diphosphate (ThDP).

Fig. 63   Mechanism for ThDP-dependent lyase-catalyzed Umpolung carboligation of aldehydes [Reprinted with permission from ref. 80 Copyright 2011 American Chemical Society].

Fig. 65) with high enantioselectivity.[58] Benzaldehyde lyase (BAL) was evaluated in mixtures of deep eutectic solvents (DES) and water, and exhibited high activities (75–98% conversions) and good enantioselectivities (27–99% ee) for carboligation reactions of aldehydes conducted in a 60 : 40 (v/v) mixture of choline

chloride/glycerol (1 : 2) with phosphate buffer (pH 8.0).[59] As shown in Fig. 66, BAL promoted the enantioselective carboligation and diastereoselective condensations of benzaldehyde with a racemic aldehyde at the same time, leading to high diastereoselectivities (de up to 99%).[212] YerE is a carbohydrate-modifying enzyme from *Yersinia pseudotuberculosis*, which catalyzed the carboligation of pyruvate to (*R*)-3-methyl-cyclohexanone to produce an (*R*,*R*)-tertiary alcohol with diastereomeric ratio (dr) >99 : 1, while the similar reaction with (*R*)-3-methylcyclohexanone yielded (*S*,*S*)-tertiary alcohol with dr >99 : 1; more interestingly, the YerE-catalyzed carboligation to non-chiral acceptors (with or without structural analogy to physiological carbohydrate substrates as shown in Fig. 67(a) and (b) respectively) led to corresponding 84% and 30% ees, which implies that the substrate structure dictates its interactions with the enzyme and the stereoselectivity of YerE.[213] Along with MenD from *E. coli*, two other tricarboxylic acid (TCA) cycle-involving enzymes (with decarboxylation activity), SucA from *E. coli* and Kgd from *Mycobacterium tuberculosis*, were able to catalyze asymmetric mixed carboligation (1,2-addition) of α-ketoglutarate and different aldehydes to synthesize δ-hydroxy-γ-keto acids with moderate to excellent enantioselectivity (Fig. 68).[214] Similar, C–C carboligation between substituted benzaldehyde and glyoxylic acid was catalyzed by variants of ThDP-dependent pyruvate decarboxylase to produce 2-hydroxyacetophenone (2-HAP) and its derivatives with 0.2–92.7% yields.[215] Benzaldehyde lyase (BAL) from *Pseudomonas fluorescens biovar I* was evaluated for intramolecular benzoin reactions of dibenzaldehyde derivatives (Fig. 69), which require three-carbon linker to connect two benzaldehyde rings at 2,2′ positions *via* ether linkages; BAL also accommodated substituents (*e.g.*, Cl, Br, and OCH$_3$) at either 3 and 3′ or 5 and 5′ positions of benzaldehyde moieties, and a pyridine ring instead of benzaldehyde.[216] This BAL was further found capable of catalyzing intramolecular stereoselective Stetter reaction of ethyl (*E*)-4-(2-formylphenoxy)but-2-enoate or it analogues to form chroman-4-one derivatives (as important intermediates for synthesizing medical molecules), resulting in yields >90% and enantiomeric ratios (er) >90 : 10 in most cases.[217] In
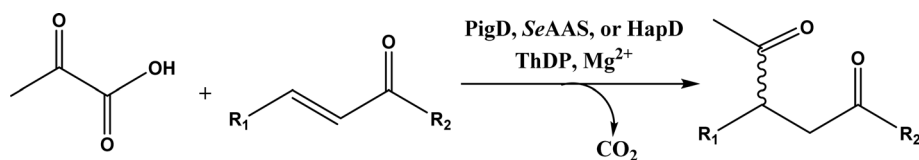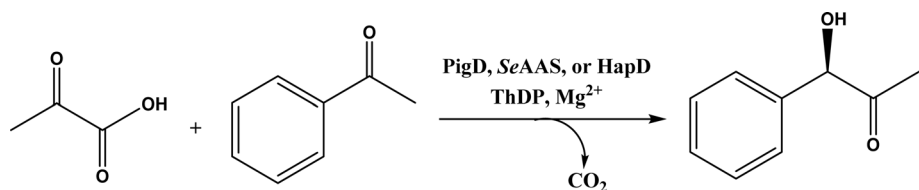

Fig. 64   1,4-Carboligation reactions of pyruvic acid with α,β-unsaturated ketones (Michael acceptors) catalyzed by PigD, *Se*AAS, or HapD.

Fig. 65   1,2-Carboligation reaction of pyruvic acid with benzaldehyde (acceptor) catalyzed by PigD, *Se*AAS, or HapD.
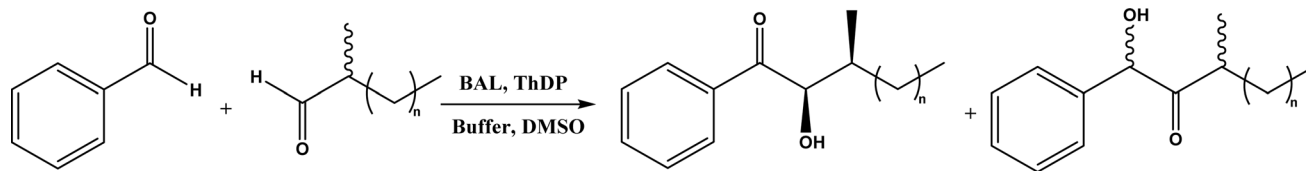
Fig. 66 BAL-catalyzed simultaneous enantioselective carboligation and kinetic resolution.
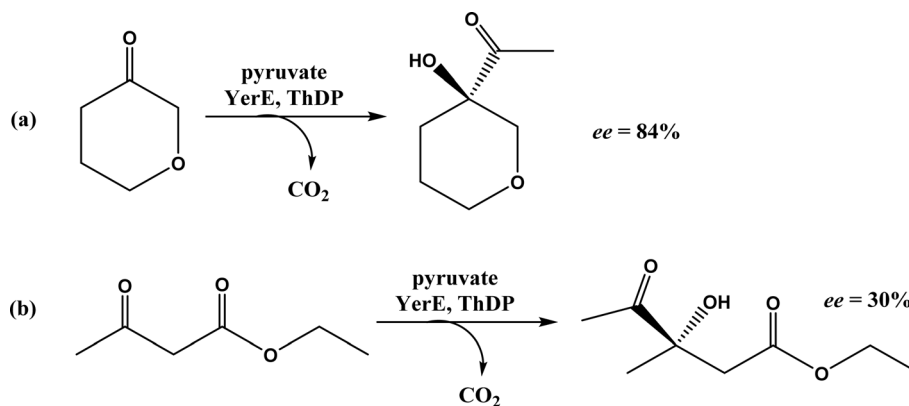
Fig. 67 YerE-catalyzed carboligation to non-chiral acceptor substrates [with or without structural analogy to physiological carbohydrate substrates as shown in (a) and (b) respectively].
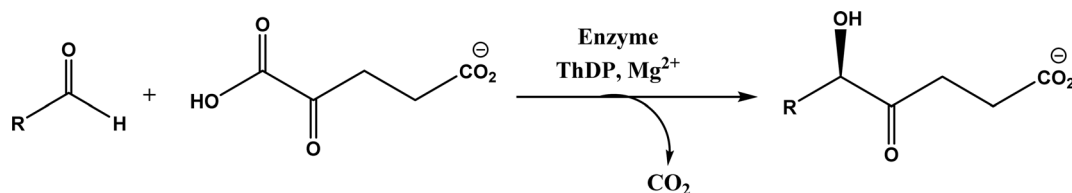
Fig. 68 Enzymatic 1,2-addition of α-ketoglutarate to aldehydes.

Fig. 69 BAL-catalyzed intramolecular benzoin reaction of dibenzaldehyde derivatives.

addition, BAL was used to promote hydroxymethylation of aldehydes followed by enzymatic reductive amination to form enantiomeric *N*-substituted 1,2-amino alcohols,[218] and the coupling of formaldehyde with 3-hydroxypropanal.[219] It was recently discovered[52] that a subclass of (myco)bacterial ThDP-dependent enzymes (*e.g.*, ErwE and MyGE) could extend the donor substrate range from achiral α-keto acids and simple aldehydes to customized chiral α-keto acids with a chain length from C_4 to C_8; as a result, enantioselectivity acyloin products were produced (Fig. 70) with 22–85% yields and >90% ees.

10. Oxidative and reductive C–C bond formation

In their 2011 review paper, the Dong group[220] described a few examples of biological dehydrogenative C–C bond formations involving cytochrome P450 enzymes, *redG*, and dioxygenases, *etc.* In a more recent review (2018), Guengerich and Yoshimoto[66] systematically surveyed enzymatic oxidation–reduction reactions and their mechanisms for forming (and breaking) C–C

Fig. 70 Benzoin condensation reaction between 2-oxoalkanoate and benzaldehyde.

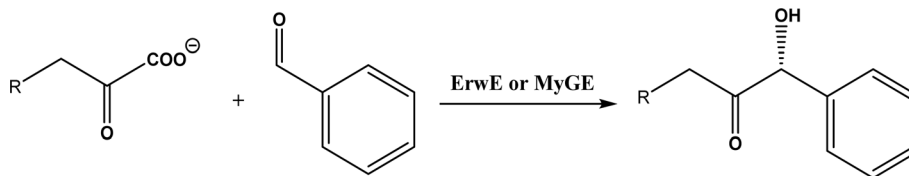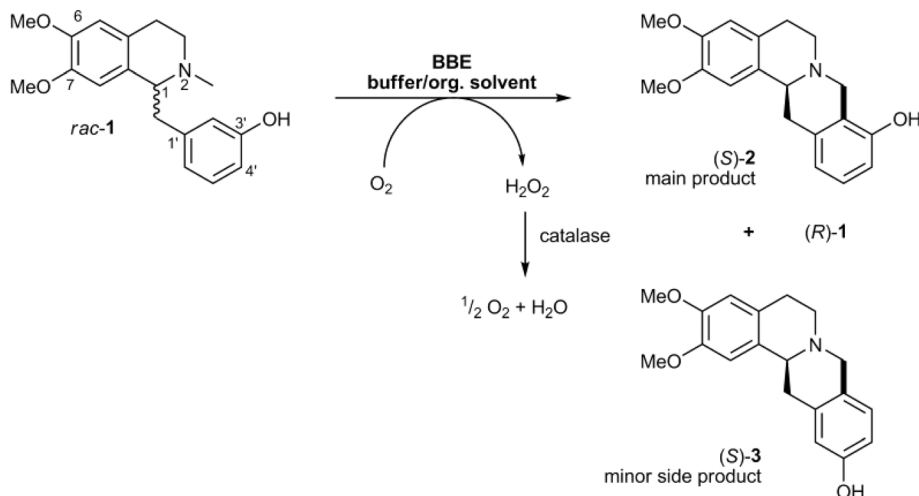**Fig. 71** Berberine bridge enzyme (BBE)-catalyzed enantioselective oxidative C–C bond formation of the non-natural racemic substrate [Reprinted with permission from ref. 221 Copyright 2011 Wiley-VCH Verlag GmbH&Co. KGaA].

bonds, which covered cytochrome P450 and variants, nonheme iron mono- and dioxygenases, flavoproteins (such as berberine bridge enzyme), radical *S*-adenosylmethionine enzymes, and peroxidases, *etc.* Berberine bridge enzyme (BBE) promoted the oxidative intramolecular C–C bond formation using a non-natural racemic substrate that is the analogue of natural substrate (*S*)-reticuline (Fig. 71); the preparative scale synthesis was performed with 500 mg substrate in 70 v% toluene and buffer (pH 9, 50 mM) using BBE and catalase (to remove H_2O_2) at 40 °C for 24 h, resulting in 42% (*S*)-**2** with >97% ee as the major product, 8% regioisomer **3** as the byproduct, and 50% (*R*)-**1** with >97% ee as the remaining reactant.[221] A nonheme iron enzyme, 2-oxoglutarate/Fe(II)-dependent dioxygenase (2-ODD), mediates the oxidative cyclization in the etoposide biosynthetic pathway; based on mechanistic probe design, *in vitro* biochemical assays, model studies, and LC-MS monitoring of 2-ODD catalyzed reactions, the reaction mechanism is likely the benzylic radical/carbocation intermediate initiating the C–C bond formation (Fig. 72), instead of previous known hydroxylated intermediate.[53] Several studies have demonstrated oxidative biaryl coupling reactions catalyzed by cytochrome P450 or laccase.[222–225]

Reductases also showed potential for forming C–C bonds. Under photoexcitation, flavin-dependent 'ene'-reductases (EREDs) can catalyze chemoselective and enantioselective cross-electrophile couplings (XECs) between various α-chloroamides and α-aryl-nitroalkanes to form C–C bonds. As illustrated by

a model reaction between 2-chloro-*N*,*N*-dimethylacetamide and (1-nitroethyl)benzene in Fig. 73, the 'ene'-reductase from *Caulobacter segnis* (CsER) selectively produced (*S*)-enantiomer with up to 92% yield and 90% ee while the ERED variant from *Gluconobacter oxydans* (GluER-T36A) preferred (*R*)-enantiomer with 51% yield and 80% ee.[67] The reaction mechanism involves the formation of nitro radical anion by combining an *in situ*-generated nitronate with an alkyl radical, followed by the formation of nitrite and an alkyl radical from the nitro radial anion; the enantioselectivity is dictated by hydrogen atom transfer (HAT) controlled by the enzyme. For α,β-unsaturated aldehydes and ketones, the wild-type ene-reductases from the Old Yellow Enzyme (OYE) family favored the C=C double bond reduction instead of carbocyclization (Fig. 74); however, single-site replacement of the critical proton donor Tyr residue (*e.g.*, Tyr190 in OPR3, Tyr169 in YqjM) with a non-protic Phe or Trp led to more cyclization products; for example, YqjM Y169F-catalyzed the reaction in Fig. 74 showed 95% selectivity of cyclization, 94% de (*trans/cis*), >99% ee of (*R,R*)-product, and −29% ee of (*S,R*)-product.[62]

11. C–C bond formation through C1 resource utilization

The biotransformation of C1 resources such as CO_2, CO, formaldehyde, and formate has become a new route for constructing C–C bonds. An earlier review[79] surveyed the enzymatic
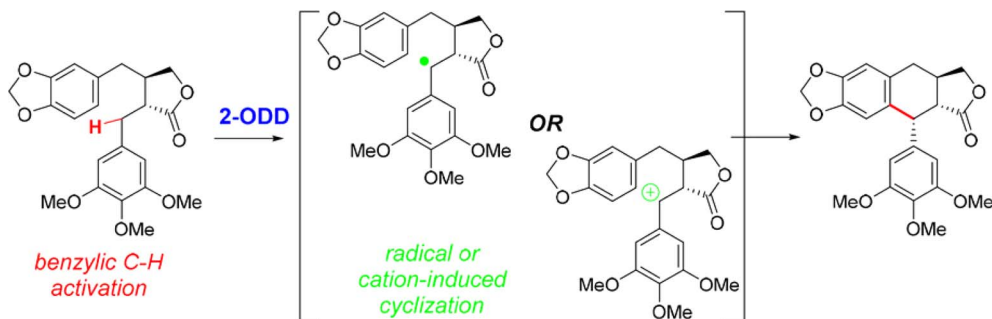
Review

Fig. 72 Mechanism of nonheme iron enzyme 2-ODD catalyzed oxidative cyclization [Reprinted with permission from ref. 53 Copyright 2019 American Chemical Society].
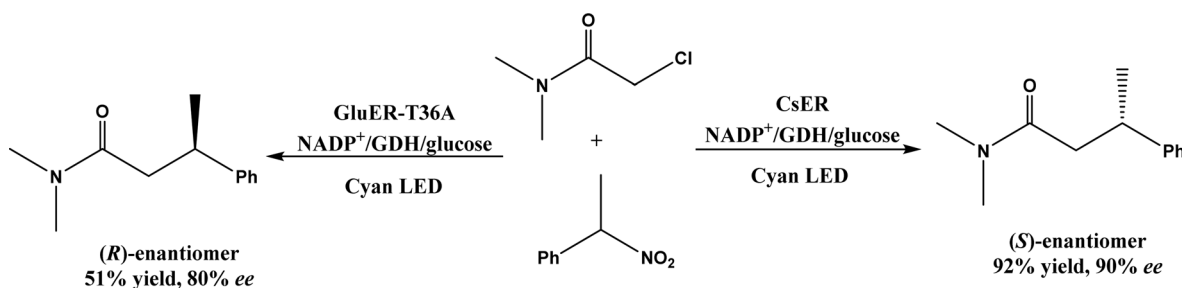
Fig. 73 Phototenzymatic asymmetric cross-electrophile couplings catalyzed by flavin-dependent 'ene'-reductases (*i.e.*, CsER and GluER-T36A) (NADP+, nicotinamide adenine dinucleotide phosphate; GDH, glucose dehydrogenase; LED, light–emitting diode).
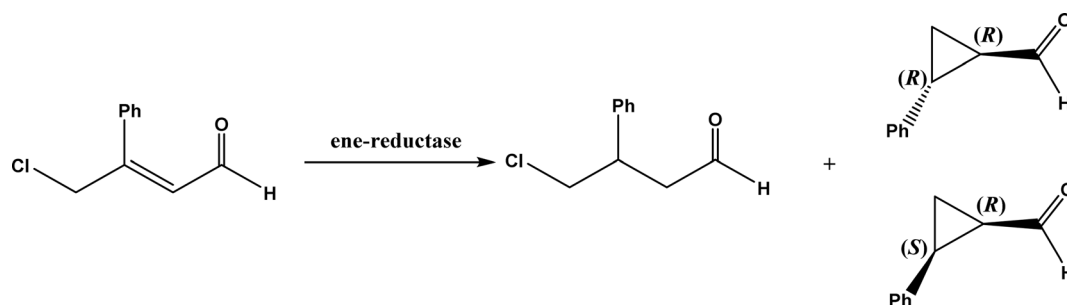
Fig. 74 Ene-reductase-catalyzed C=C double bond reduction and carbocyclization of α,β-unsaturated aldehyde.

conversions of formaldehyde to valuable chiral molecules by using aldolases and ThDP-dependent enzymes, and discussed the reaction mechanisms and enzyme discovery. Another review paper[226] focused on light-driven C–H bond activation to form new C–C bonds using CO_2 as the feedstock catalyzed by enzymes or molecular catalysts. A recent paper[227] overviewed the CO_2 conversions using carboxylases, formaldehyde transformations using C–C ligases, and CO and formate conversions *via* C–C ligases. Several more recent updates are discussed below. From CO_2 and pyruvic acid, oxaloacetic acid and malate were derived photoenzymatically with malic enzyme using the photoreduction of a 1,1′-bis(*p*-sulfonatophenyl)-4,4′-bipyridinium salt as electron mediator and water-soluble tetraphenylporphyrin tetrasulfonate (H_2TPPS) with triethanolamine (TEOA) as an electron donor.[228,229] CO_2 and succinyl coenzyme A (SCoA) can be converted to 2-oxoglutarate and CoA *via* light-

driven carbon–carbon bond formation by using 2-oxoglutarate: ferredoxin oxidoreductase and photoexcited electrons from cadmium sulfide nanorods; electron transfer efficiency is highly dependent on how SCoA is bound at the enzyme's active site.[230] The enzymatic fixation of CO_2 was realized by enzymatic reductive carboxylation of crotonyl-CoA to (2*S*)-ethylmalonyl-CoA catalyzed by NADPH-dependent crotonyl-CoA carboxylase/reductase (Ccr), which was co-immobilized within a viologen-based redox hydrogel with the co-factor (NADPH) regeneration enzyme ferredoxin NADP+ reductase (FNR) for continuous NADPH recycling (Fig. 75); electrons were transferred from the electrode to FNR through a mediated electron transfer method (2,2′-viologen-modified hydrogel; see a review[231] on viologens for enzymatic photoredox conversions of CO_2); the reaction system achieved $92 \pm 6\%$ faradaic efficiency and at a rate of 1.6 ± 0.4 μmol cm^{-2} h^{-1}.[232] Formaldehyde can be produced from
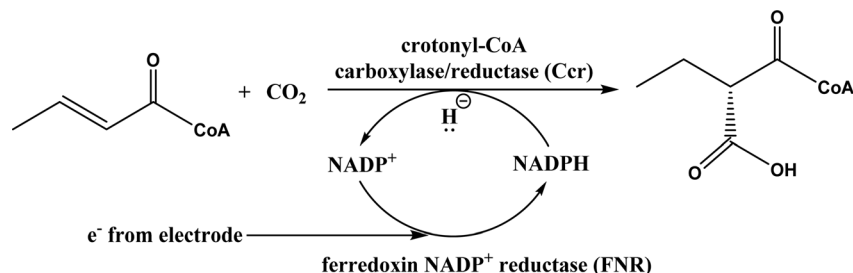
Fig. 75 Bioelectrocatalytic $NADP^+$ cofactor regeneration coupled with enzymatic CO_2 fixation.
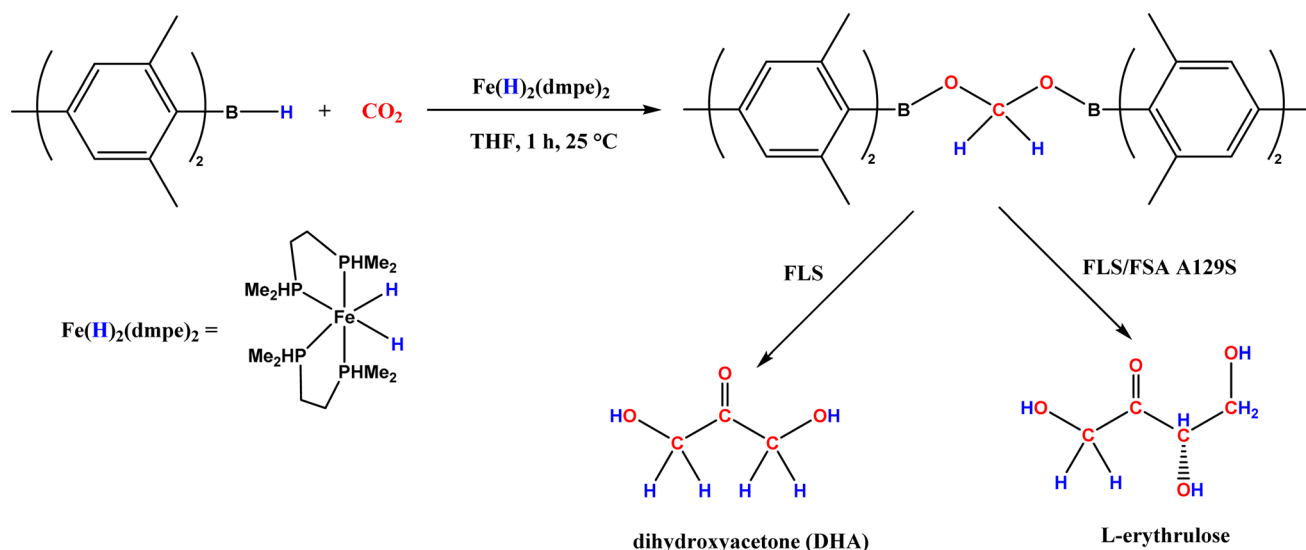

Fig. 76 Chemoenzymatic conversion of CO_2 to C_3 (dihydroxyacetone, DHA) and C_4 (L-erythrulose) carbohydrates.

sustainable C1 feedstocks; formaldehyde could be converted to glycolaldehyde by formolase or its variants, and furthermore, glycolaldehyde was converted to erythrulose (C4 sugar) with 98% yield by another formolase variant.[63] Alternatively, form-aldehyde could be transformed to glycolaldehyde through gly-colaldehyde synthase, followed by the conversions to ethylene glycol *via* alcohol or aldehyde dehydrogenases from *Gluconobacter oxydans*, to glycolic acid *via* acetaldehyde dehydrogenases, or to D-(−)-erythrose *via* 2-deoxy-D-ribose-5-phosphate aldolases (DERAs).[233] In another study,[64] CO_2 was converted to a bis(boryl)acetal compound first, followed by selective enzymatic reactions to afford C_3 (dihydroxyacetone, DHA) with up to 86% yield by using a formolase (FLS), or optically pure C_4 (L-erythrulose) with 35% yield through a cascade reaction using FLS and D-fructose-6-phosphate aldolase (FSA) A129S variant (Fig. 76).

A chemoenzymatic route to convert CO_2 to hexoses (*e.g.*, glucose and D-allulose) was designed by the Ma group:[234] chemical reduction of CO_2 to 'green' methanol by ZnO–ZrO₂ catalyst, methanol conversion to DHAP *via* multi-step strategy involving formolase, aldol condensation catalyzed by fructose-6-phosphate aldolases (FSAs), iso/epimerization, and dephosphorylation reactions. Similarly, 'green' methanol can be converted to L-alanine with 88% yield,[235] or to starch at 22

nmol min^{-1} mg^{-1} of total catalyst and proteins (an 8.5-fold faster than starch formation *via* the Calvin cycle in maize),[236] both through multi-enzyme cascade reactions under cell-free conditions.

12. Radical enzymes for C–C bond formation

Other than two electron mechanisms (involving nucleophile and electrophile), C–C bonds can be formed by free radical-mediated reactions such as those catalyzed by radical *S*-adenosylmethionine (SAM) enzymes. As discussed in a recent review,[237] radical *S*-adenosylmethionine (SAM) enzymes are involved in the biosynthesis of ribosomally synthesized and post-translationally modified peptides (RiPPs), and O_2-sensitive and hydrocarbon activating glycyl radical enzymes (GREs) include a subset known as X-succinate synthases [*e.g.*, benzyl-succinate synthase (BSS), 4-isopropylbenzylsuccinate synthase (IBSS), hydroxybenzylsuccinate synthase (HBSS), naphthyl-2-methylsuccinate synthase (NMSS), and 1-methylalkylsuccinate synthase (MASS)]. More specifically, C–C bond forming radical SAM enzymes were surveyed in terms of SPASM–twitch subfamily, radical SAM enzymes with N-terminal cofactor
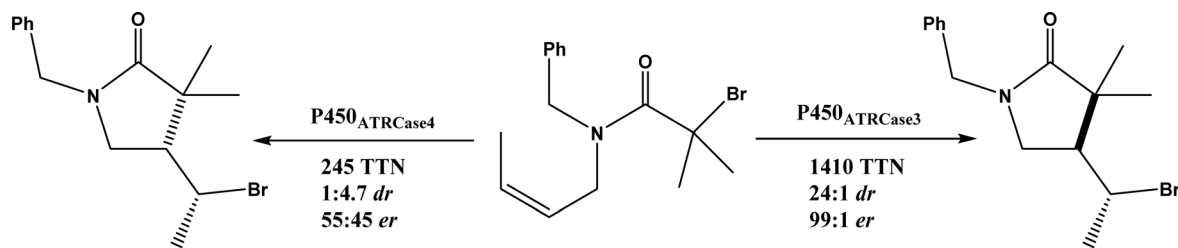
Fig. 77 Stereoselective atom-transfer radical cyclization (ATRC) with cytochrome P450 variants (TTN = total turnover number; dr = diastereomeric ratio; er = enantiomeric ratio).

binding domains, ThiH-like enzymes, and noncanonical radical SAM enzymes; additionally, three critical mechanistic factors (radical initiation, acceptor substrate activation, and radical quenching) were discussed in detail.[238] In another review,[239] mechanistic understandings are provided for C–C bond formation or cleavage reactions catalyzed by three enzymes: pyruvate-formate lyase (PFL), spore photoproduct lyase (SPL), and benzylsuccinate synthase (BSS). Our earlier sections also covered several examples of radical species during the C–C bond formation, such as radical S-adenosylmethionine enzymes for enzymatic redox reactions in C–C bond formation,[66] the benzylic radical/carbocation intermediate initiating the C–C bond formation for a nonheme iron enzyme called 2-oxoglutarate/Fe(II)-dependent dioxygenase (2-ODD),[61] and the formation of nitro radical anion by reacting nitronate with an alkyl radical during 'ene'-reductase CsER-catalyzed cross-electrophile couplings (XECs) between alkyl halides and nitroalkanes.[67] The Yang group[65] suggested that cytochrome P450

could be engineered to have a fine control of the radical addition step and the halogen rebound step during stereoselective atom-transfer radical cyclization (ATRC), affording enantio- and diastereodivergent radical catalysis (Fig. 77); as indicated by molecular dynamics (MD) and quantum mechanics/molecular mechanics (QM/MM) calculations, glutamine residue of P450 acts as hydrogen bond donor to interact with the carbonyl group of the substrate to facilitate the removal of bromine atom and control the stereoselectivity of ATRC.[240] Spectroscopy and computational studies have revealed the C–C bond formation mechanism for radical SAM enzyme (cyclase),[241] cytochrome P450,[242] and benzylsuccinate synthase.[243]

13. Other C–C bond formation mechanisms

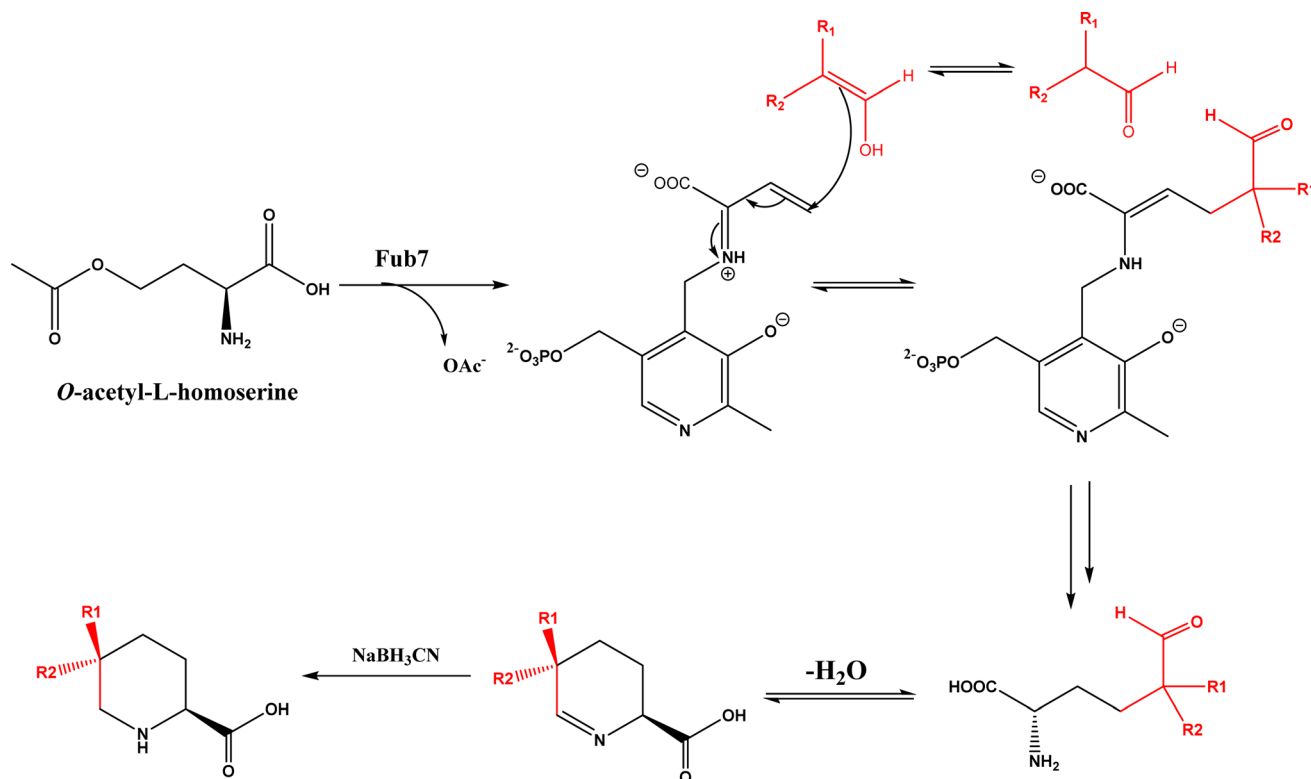Two PLP-dependent enzymes, CndF and Fub7, induce C–O activation and catalyze γ-substitution providing a new route for

Fig. 78 Fub7-catalyzed C–C bond formation to prepare substituted L-pipecolic acids.
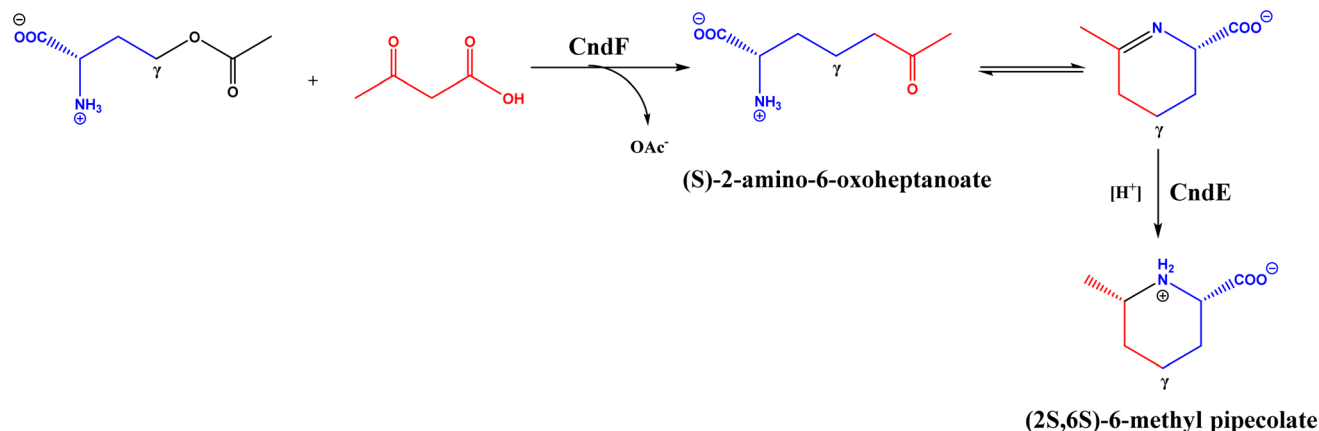
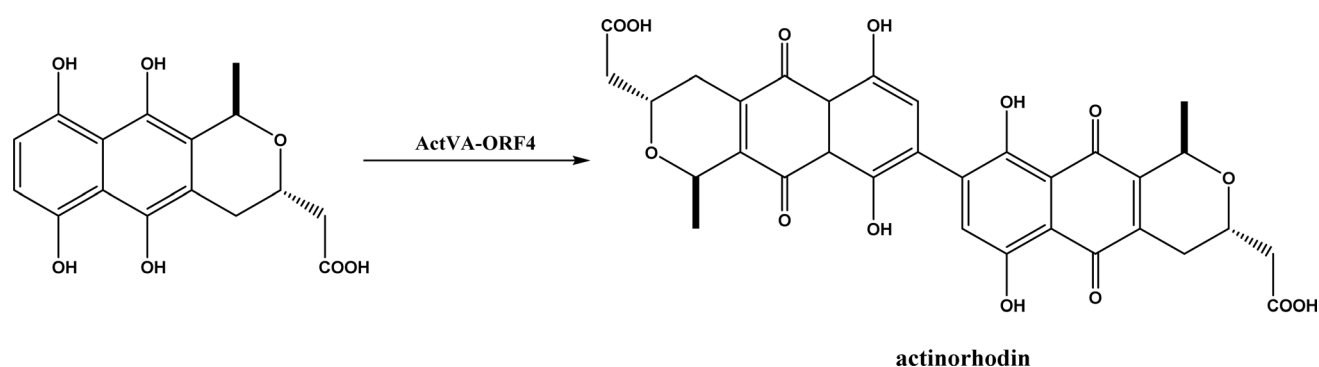**Fig. 79** Chemoenzymatic synthesis of (2S,6S)-6-methyl pipecolate using CndF.

Fig. 80 Enzymatic aryl coupling between 8-hydroxydihydrokalafungin molecules to synthesize actinorhodin.

stereoselective C–C bond formation.[68,244] A chemoenzymatic method involving Fub7 (Fig. 78) afforded 5-alkyl-, 5,5-dialkyl-, and 5,5,6-trialkyl-L-pipecolic acids with diastereomeric ratio ranging from 50:50 to 95:5.[244] CndF catalyzed the C–C coupling of O-acetyl-L-homoserine with 3-oxobutanoic acid to form (S)-2-amino-6-oxoheptanoate, which equilibrates with a cyclic Schiff base; a further reduction by a stereoselective imine reductase CndE gave (2S, 6S)-6-methyl pipecolate (Fig. 79).[68] CndF is also capable of converting β-keto ethyl esters to enamine-containing pipecolates.

Hydroxynitrile lyases (HNLs), or oxynitrilases (EC 4.1.2.x) catalyze the reversible enantioselective condensation of hydrocyanic acid (HCN) with aldehydes or ketones to produce cyanohydrins.[70,80,81,245,246] Other enzymatic C–C bond formation mechanisms include intermolecular aryl coupling between 8-hydroxydihydrokalafungin molecules to actinorhodin (Fig. 80) catalyzed by NAD(P)H-dependent ActVA-ORF4 (NmrA-family dimerizing enzyme),[247] sp^3 C–H functionalization catalyzed by iron-based catalysts derived from cytochrome P450 (to become cytochrome P411),[248] by trypsin,[249] or by tyrosine phenol lyase,[250] ketosynthase-catalyzed decarboxylative Claisen-like condensation,[251] C-nucleoside synthase ForT-catalyzed C–C bond formation,[252] carbon–carbon bond formation by deoxypodophyllotoxin synthase,[253] cis-isoprenyl diphosphate synthase-catalyzed condensation conversions of isoprene units

to produce isoprenoids or terpenoids,[254] carboxymethylproline synthase (a member of crotonase family)-catalyzed C–C bond formation,[255] and engineered SAM-dependent sterol methyltransferase for C-methylation of unactivated alkenes in mono-, sesqui- and diterpenoids to yield C_{11}, C_{16} and C_{21} derivatives with high chemo- and regioselectivity.[69]

14. Perspectives

Enzymes have shown unique and tailorable chemo-, regio- and/or stereoselectivity during the C–C bond formation through judicious engineering of enzyme structures and the optimization of reaction conditions. Enzymes discovered in the biosynthesis of C–C bond formation have a great potential to be evolved to become robust biocatalysts for asymmetric reactions in aqueous or nonaqueous environments. It is highly valuable to make carbon-based molecules through enzymatic conversions of C1 resources.

There have been some conflicting reports about the existence and extent of catalytic promiscuity of some enzymes, which require further experimental examinations. In addition, the catalytic mechanisms of enzymatic C–C bond formation are not well understood, and not fully backed by experimental and computational results. Aqueous reaction media are not always ideal for biocatalytic conversion due to insolubility of substrates

resulting in low reaction efficiency; water-miscible organic co-solvents assist with the substrate dissolution, but may cause enzyme inactivation. There is still a great need to find and optimize non-aqueous solvents (*e.g.*, ILs and DES) for enzymatic C–C formation reactions. Future efforts to address these issues will lead to more effective synthesis of stereoselective molecules with medicinal and biological significance, and a better utilization of C1 resources.

Data availability

No primary research results, software or code have been included and no new data were generated or analyzed as part of this review.

Conflicts of interest

The authors declare that they have no conflict of interest.

Acknowledgements

References

1 Z. Guan, L. Li and Y. He, *RSC Adv.*, 2015, **5**, 16801–16814.

2 L. Poppe and J. Rétey, *Angew. Chem., Int. Ed.*, 2005, **44**, 3668–3688.

3 K. Auclair, A. Sutherland, J. Kennedy, D. J. Witter, J. P. van den Heever, C. R. Hutchinson and J. C. Vederas, *J. Am. Chem. Soc.*, 2000, **122**, 11519–11520.

4 T. Ose, K. Watanabe, T. Mie, M. Honma, H. Watanabe, M. Yao, H. Oikawa and I. Tanaka, *Nature*, 2003, **422**, 185–189.

5 M. López-Iglesias, E. Busto, V. Gotor and V. Gotor-Fernández, *Adv. Synth. Catal.*, 2011, **353**, 2345–2353.

6 M. D. Patil, G. Grogan and H. Yun, *ChemCatChem*, 2018, **10**, 4783–4804.

7 P. Jakubec, D. M. Cockfield and D. J. Dixon, *J. Am. Chem. Soc.*, 2009, **131**, 16632–16633.

8 P. Chen, X. Bao, L.-F. Zhang, M. Ding, X.-J. Han, J. Li, G.-B. Zhang, Y.-Q. Tu and C.-A. Fan, *Angew. Chem., Int. Ed.*, 2011, **50**, 8161–8166.

9 T. Buyck, Q. Wang and J. Zhu, *Angew. Chem., Int. Ed.*, 2013, **52**, 12714–12718.

10 C. L. Windle, A. Berry and A. Nelson, *Curr. Opin. Chem. Biol.*, 2017, **37**, 33–38.

11 M. Müller, *Adv. Synth. Catal.*, 2012, **354**, 3161–3174.

12 Y. Miao, M. Rahimi, E. M. Geertsema and G. J. Poelarends, *Curr. Opin. Chem. Biol.*, 2015, **25**, 115–123.

13 P. Clapés, in *Organic Synthesis Using Biocatalysis*, ed. A. Goswami and J. D. Stewart, Academic Press, 2016, pp. 285–337, DOI: **10.1016/B978-0-12-411518-7.00010-X**.

14 N. G. Schmidt, E. Eger and W. Kroutil, *ACS Catal.*, 2016, **6**, 4286–4311.

15 B. T. Ueberbacher, M. Hall and K. Faber, *Nat. Prod. Rep.*, 2012, **29**, 337–350.

16 A. L. Mattei, N. Bailly and A. Meissner, *Trends Genet.*, 2022, **38**, 676–707.

17 P. A. Storm, P. Pal, C. R. Huitt-Roehl and C. A. Townsend, *ACS Chem. Biol.*, 2018, **13**, 3043–3048.

18 J. Yang, J. Li, Y. Men, Y. Zhu, Y. Zhang, Y. Sun and Y. Ma, *Appl. Environ. Microbiol.*, 2015, **81**, 4284–4294.

19 Y. Zhu, T. Shiraishi, J. Lin, K. Inaba, A. Ito, Y. Ogura, M. Nishiyama and T. Kuzuyama, *J. Am. Chem. Soc.*, 2022, **144**, 16715–16719.

20 J. Liu, L. Harken, Y. Yang, X. Xie and S.-M. Li, *Angew. Chem., Int. Ed.*, 2022, **61**, e202200377.

21 A. Bolt, A. Berry and A. Nelson, *Arch. Biochem. Biophys.*, 2008, **474**, 318–330.

22 S.-H. Lee, S.-J. Yeom, S.-E. Kim and D.-K. Oh, *Trends Biotechnol.*, 2022, **40**, 306–319.

23 S. M. Dean, W. A. Greenberg and C.-H. Wong, *Adv. Synth. Catal.*, 2007, **349**, 1308–1320.

24 P. Clapés and X. Garrabou, *Adv. Synth. Catal.*, 2011, **353**, 2263–2283.

25 G. J. Williams, S. Domann, A. Nelson and A. Berry, *Proc. Natl. Acad. Sci. U.S.A.*, 2003, **100**, 3143–3148.

26 G. J. Williams, T. Woodhall, L. M. Farnsworth, A. Nelson and A. Berry, *J. Am. Chem. Soc.*, 2006, **128**, 16238–16247.

27 W. Wang, S. Mazurkewich, M. S. Kimber and S. Y. K. Seah, *J. Biol. Chem.*, 2010, **285**, 36608–36615.

28 V. Laurent, E. Darii, A. Aujon, M. Debacker, J. L. Petit, V. Hélaine, T. Liptaj, M. Breza, A. Mariage, L. Nauton, M. Traïkia, M. Salanoubat, M. Lemaire, C. Guérard-Hélaine and V. de Berardinis, *Angew. Chem., Int. Ed.*, 2018, **57**, 5467–5471.

29 J. Yang, Y. Zhu, G. Qu, Y. Zeng, C. Tian, C. Dong, Y. Men, L. Dai, Z. Sun, Y. Sun and Y. Ma, *Biotechnol. Biofuels*, 2018, **11**, 290.

30 C. Ren, J. Yang, Y. Zeng, T. Zhang, C. Tian, Y. Men and Y. Sun, *Enzyme Microb. Technol.*, 2021, **147**, 109784.

31 A. J. Rigual, J. Cantero, M. Risso, P. Rodríguez, S. Rodríguez, M. Paulino, D. Gamenara and N. Veiga, *Mol. Catal.*, 2020, **495**, 111131.

32 Q. Chen, X. Chen, J. Feng, Q. Wu, D. Zhu and Y. Ma, *ACS Catal.*, 2019, **9**, 4462–4469.

33 C. Li, X. Feng, N. Wang, Y. Zhou and X. Yu, *Green Chem.*, 2008, **10**, 616–618.

34 M. López-Iglesias, E. Busto, V. Gotor and V. Gotor-Fernández, *Adv. Synth. Catal.*, 2011, **353**, 2345–2353.

35 S. Milker, M. Pätzold, J. Z. Bloh and D. Holtmann, *Mol. Catal.*, 2019, **466**, 70–74.

36 W.-J. Xia, Z.-B. Xie, G.-F. Jiang and Z.-G. Le, *Molecules*, 2013, **18**, 13910–13919.

37 D. Kühbeck, B. B. Dhar, E.-M. Schön, C. Cativiela, V. Gotor-Fernández and D. D. Díaz, *Beilstein J. Org. Chem.*, 2013, **9**, 1111–1118.

38 X.-W. Feng, C. Li, N. Wang, K. Li, W.-W. Zhang, Z. Wang and X.-Q. Yu, *Green Chem.*, 2009, **11**, 1933–1936.

39 A. S. Evitt and U. T. Bornscheuer, *Green Chem.*, 2011, **13**, 1141–1142.

40 H. Zhao and C. D. Campbell, *J. Chem. Technol. Biotechnol.*, 2024, **99**, 780–787.

41 U. R. Pratap, D. V. Jawale, R. A. Waghmare, D. L. Lingampalle and R. A. Mane, *New J. Chem.*, 2011, **35**, 49–51.

42 M. Svedendahl, K. Hult and P. Berglund, *J. Am. Chem. Soc.*, 2005, **127**, 17988–17989.

43 X. Chen, G. Chen, J. Wang, Q. Wu and X. Lin, *Adv. Synth. Catal.*, 2013, **355**, 864–868.

44 G. A. Strohmeier, T. Sović, G. Steinkellner, F. S. Hartner, A. Andryushkova, T. Purkarthofer, A. Glieder, K. Gruber and H. Griengl, *Tetrahedron*, 2009, **65**, 5663–5668.

45 Y. Fan, D. Cai, X. Wang and L. Yang, *Molecules*, 2018, **23**, 2154.

46 H. Stecher, M. Tengg, B. J. Ueberbacher, P. Remler, H. Schwab, H. Griengl and M. Gruber-Khadjawi, *Angew. Chem., Int. Ed.*, 2009, **48**, 9546–9548.

47 M. Tengg, H. Stecher, P. Remler, I. Eiteljörg, H. Schwab and M. Gruber-Khadjawi, *J. Mol. Catal. B: Enzym.*, 2012, **84**, 2–8.

48 M. Tengg, H. Stecher, L. Offner, K. Plasch, F. Anderl, H. Weber, H. Schwab and M. Gruber-Khadjawi, *ChemCatChem*, 2016, **8**, 1354–1360.

49 J. C. Sadler, C.-w. H. Chung, J. E. Mosley, G. A. Burley and L. D. Humphreys, *ACS Chem. Biol.*, 2017, **12**, 374–379.

50 L. Villarino, S. Chordia, L. Alonso-Cotchico, E. Reddem, Z. Zhou, A. M. W. H. Thunnissen, J.-D. Maréchal and G. Roelfes, *ACS Catal.*, 2020, **10**, 11783–11790.

51 N. G. Schmidt, T. Pavkov-Keller, N. Richter, B. Wiltschi, K. Gruber and W. Kroutil, *Angew. Chem., Int. Ed.*, 2017, **56**, 7615–7619.

52 K. Li, T. He, C. Li, X. Feng, N. Wang and X. Yu, *Green Chem.*, 2009, **11**, 777–779.

53 S. Chai, Y. Lai, H. Zheng and P. Zhang, *Helv. Chim. Acta*, 2010, **93**, 2231–2236.

54 R. Crawshaw, A. E. Crossley, L. Johannissen, A. J. Burke, S. Hay, C. Levy, D. Baker, S. L. Lovelock and A. P. Green, *Nat. Chem.*, 2022, **14**, 313–320.

55 K. Watanabe, T. Mie, A. Ichihara, H. Oikawa and M. Honma, *J. Biol. Chem.*, 2000, **275**, 38393–38401.

56 C. R. W. Guimarães, M. Udier-Blagović and W. L. Jorgensen, *J. Am. Chem. Soc.*, 2005, **127**, 3577–3588.

57 J. B. Siegel, A. Zanghellini, H. M. Lovick, G. Kiss, A. R. Lambert, J. L. St. Clair, J. L. Gallaher, D. Hilvert, M. H. Gelb, B. L. Stoddard, K. N. Houk, F. E. Michael and D. Baker, *Science*, 2010, **329**, 309–313.

58 E. Kasparyan, M. Richter, C. Dresen, L. S. Walter, G. Fuchs, F. J. Leeper, T. Wacker, S. L. A. Andrade, G. Kolter, M. Pohl and M. Müller, *Appl. Microbiol. Biotechnol.*, 2014, **98**, 9681–9690.

59 Z. Maugeri and P. Domínguez de María, *J. Mol. Catal. B: Enzym.*, 2014, **107**, 120–123.

60 J.-P. Steitz, L. Krug, L. Walter, K. Hernández, C. Röhr, P. Clapés and M. Müller, *Angew. Chem., Int. Ed.*, 2022, **61**, e202113405.

61 W.-C. Chang, Z.-J. Yang, Y.-H. Tu and T.-C. Chien, *Org. Lett.*, 2019, **21**, 228–232.

62 K. Heckenbichler, A. Schweiger, L. A. Brandner, A. Binter, M. Toplak, P. Macheroux, K. Gruber and R. Breinbauer, *Angew. Chem., Int. Ed.*, 2018, **57**, 7240–7244.

63 S. Güner, V. Wegat, A. Pick and V. Sieber, *Green Chem.*, 2021, **23**, 6583–6590.

64 S. Desmons, K. Grayson-Steel, N. Nuñez-Dallos, L. Vendier, J. Hurtado, P. Clapés, R. Fauré, C. Dumon and S. Bontemps, *J. Am. Chem. Soc.*, 2021, **143**, 16274–16283.

65 Q. Zhou, M. Chin, Y. Fu, P. Liu and Y. Yang, *Science*, 2021, **374**, 1612–1616.

66 F. P. Guengerich and F. K. Yoshimoto, *Chem. Rev.*, 2018, **118**, 6573–6655.

67 H. Fu, J. Cao, T. Qiao, Y. Qi, S. J. Charnock, S. Garfinkle and T. K. Hyster, *Nature*, 2022, **610**, 302–307.

68 M. Chen, C.-T. Liu and Y. Tang, *J. Am. Chem. Soc.*, 2020, **142**, 10506–10515.

69 B. Aberle, D. Kowalczyk, S. Massini, A.-N. Egler-Kemmerer, S. Gergel, S. C. Hammer and B. Hauer, *Angew. Chem., Int. Ed.*, 2023, **62**, e202301601.

70 W.-D. Fessner, *Curr. Opin. Chem. Biol.*, 1998, **2**, 85–97.

71 P. Clapés, W.-D. Fessner, G. A. Sprenger and A. K. Samland, *Curr. Opin. Chem. Biol.*, 2010, **14**, 154–167.

72 T. D. Machajewski and C.-H. Wong, *Angew. Chem., Int. Ed.*, 2000, **39**, 1352–1374.

73 A. K. Samland and G. A. Sprenger, *Appl. Microbiol. Biotechnol.*, 2006, **71**, 253–264.

74 P. Falcicchio, S. Wolterink-Van Loo, M. C. R. Franssen and J. van der Oost, *Extremophiles*, 2014, **18**, 1–13.

75 C. C. Aragon, J. M. Palomo, M. Filice and C. Mateo, *Curr. Org. Chem.*, 2016, **20**, 1243–1251.

76 P. Clapés, in *Green Biocatalysis*, ed. R. N. Patel, John Wiley & Sons, Inc., Hoboken, New Jersey, 2016, pp. 267–306, DOI: **10.1002/9781118828083.ch10**.

77 P. Clapés, in *Biocatalysis in Organic Synthesis*, ed. K. Faber, W.-D. Fessner and N. J. Turner, Georg Thieme Verlag KG, Stuttgart (Germany), 2015, vol. 2, pp. 31–92.

78 V. Hélaine, C. Gastaldi, M. Lemaire, P. Clapés and C. Guérard-Hélaine, *ACS Catal.*, 2022, **12**, 733–761.

79 S. Desmons, R. Fauré and S. Bontemps, *ACS Catal.*, 2019, **9**, 9575–9588.

80 W.-D. Fessner, A. Schneider, H. Held, G. Sinerius, C. Walter, M. Hixon and J. V. Schloss, *Angew. Chem., Int. Ed.*, 1996, **35**, 2219–2221.

81 M. Brovetto, D. Gamenara, P. S. Méndez and G. A. Seoane, *Chem. Rev.*, 2011, **111**, 4346–4403.

82 E. Ricca, B. Brucher and J. H. Schrittwieser, *Adv. Synth. Catal.*, 2011, **353**, 2239–2262.

83 L. Wu, M. H. Tong, A. Raab, Q. Fang, S. Wang, K. Kyeremeh, Y. Yu and H. Deng, *Appl. Microbiol. Biotechnol.*, 2020, **104**, 3885–3896.

84 A. K. Samland, M. Rale, G. A. Sprenger and W.-D. Fessner, *ChemBioChem*, 2011, **12**, 1454–1474.

85 A. K. Samland and G. A. Sprenger, *Int. J. Biochem. Cell Biol.*, 2009, **41**, 1482–1494.

86 S. Schneider, T. Sandalova, G. Schneider, G. A. Sprenger and A. K. Samland, *J. Biol. Chem.*, 2008, **283**, 30064–30072.

© 2024 The Author(s). Published by the Royal Society of Chemistry

87 M. Schürmann and G. A. Sprenger, *J. Biol. Chem.*, 2001, **276**, 11055–11061.

88 J. Blesl, M. Trobe, F. Anderl, R. Breinbauer, G. A. Strohmeier and K. Fesko, *ChemCatChem*, 2018, **10**, 3453–3458.

89 S. F. Beaudoin, M. P. Hanna, I. Ghiviriga and J. D. Stewart, *Enzyme Microb. Technol.*, 2018, **119**, 1–9.

90 L. Xu, L. Wang, X. Xu and J. Lin, *Catal. Sci. Technol.*, 2019, **9**, 5943–5952.

91 W. Zheng, H. Yu, S. Fang, K. Chen, Z. Wang, X. Cheng, G. Xu, L. Yang and J. Wu, *ACS Catal.*, 2021, **11**, 3198–3205.

92 W. Wang, J. Yang, Y. Sun, Z. Li and C. You, *ACS Catal.*, 2020, **10**, 1264–1271.

93 I. Oroz-Guinea, I. Sánchez-Moreno, M. Mena and E. García-Junceda, *Appl. Microbiol. Biotechnol.*, 2015, **99**, 3057–3068.

94 I. Oroz-Guinea, K. Hernández, F. Camps Bres, C. Guérard-Hélaine, M. Lemaire, P. Clapés and E. García-Junceda, *Adv. Synth. Catal.*, 2015, **357**, 1951–1960.

95 R. Marín-Valls, K. Hernández, M. Bolte, T. Parella, J. Joglar, J. Bujons and P. Clapés, *J. Am. Chem. Soc.*, 2020, **142**, 19754–19762.

96 Z. Hu, C. Cheng, Y. Li, X. Qi, T. Wang, L. Liu and J. Voglmeir, *ChemBioChem*, 2022, **23**, e202200074.

97 M. Pickl, R. Marín-Valls, J. Joglar, J. Bujons and P. Clapés, *Adv. Synth. Catal.*, 2021, **363**, 2866–2876.

98 C. J. Moreno, K. Hernández, S. J. Charnok, S. Gittings, M. Bolte, J. Joglar, J. Bujons, T. Parella and P. Clapés, *ACS Catal.*, 2021, **11**, 4660–4669.

99 R. Marín-Valls, K. Hernández, M. Bolte, J. Joglar, J. Bujons and P. Clapés, *ACS Catal.*, 2019, **9**, 7568–7577.

100 C. J. Moreno, K. Hernández, S. Gittings, M. Bolte, J. Joglar, J. Bujons, T. Parella and P. Clapés, *ACS Catal.*, 2023, **13**, 5348–5357.

101 W. Zheng, Z. Pu, L. Xiao, G. Xu, L. Yang, H. Yu and J. Wu, *Angew. Chem., Int. Ed.*, 2023, **62**, e202213855.

102 H. Li, Y. He, Y. Yuan and Z. Guan, *Green Chem.*, 2011, **13**, 185–189.

103 J. M. Ellis, M. E. Campbell, P. Kumar, E. P. Geunes, C. A. Bingman and A. R. Buller, *Nat. Catal.*, 2022, **5**, 136–143.

104 R. Zhang, J. Tan, Z. Luo, H. Dong, N. Ma and C. Liao, *Catal. Sci. Technol.*, 2021, **11**, 7380–7385.

105 F. A. Luzzio, *Tetrahedron*, 2001, **57**, 915–945.

106 A. M. F. Phillips, *Curr. Organocatal.*, 2016, **3**, 222–242.

107 S. E. Milner, T. S. Moody and A. R. Maguire, *Eur. J. Org Chem.*, 2012, **2012**, 3059–3067.

108 P. Shrivas, N. Punyapreddiwar, A. Wankhade, S. Zodape and U. Pratap, *Iran. J. Catal.*, 2017, **7**, 337–340.

109 D. F. Izquierdo, O. Barbosa, M. I. Burguete, P. Lozano, S. V. Luis, R. Fernandez-Lafuente and E. García-Verdugo, *RSC Adv.*, 2014, **4**, 6219–6225.

110 L. F. Tietze, *Chem. Rev.*, 1996, **96**, 115–136.

111 K. Hackelöer, G. Schnakenburg and S. R. Waldvogel, *Eur. J. Org Chem.*, 2011, **2011**, 6314–6319.

112 I. Walz, A. Bertogg and A. Togni, *Eur. J. Org Chem.*, 2007, **2007**, 2650–2658.

113 D. Koszelewski, D. Paprocki, A. Madej, F. Borys, A. Brodzka and R. Ostaszewski, *Eur. J. Org Chem.*, 2017, **2017**, 4572–4579.

114 K. van Beurden, S. de Koning, D. Molendijk and J. van Schijndel, *Green Chem. Lett. Rev.*, 2020, **13**, 349–364.

115 X. Yuan, J. Liu, Y. Wang, X. Jie, J. Qin and H. He, *Chem. Eng. J.*, 2023, **451**, 138941.

116 V. Bhaskar, R. Chowdary, S. R. Dixit and S. D. Joshi, *Bioorg. Chem.*, 2019, **84**, 202–210.

117 A. Paul, A. Maji, A. Sarkar, S. Saha, P. Janah and T. K. Maity, *Mini-Rev. Org. Chem.*, 2023, **20**, 5–34.

118 C. Wang, N. Wang, X. Liu, P. Wan, X. He and Y. Shang, *Fibers Polym.*, 2018, **19**, 1611–1617.

119 L. Jiang, B. Wang, R.-R. Li, S. Shen, H.-W. Yu and L.-D. Ye, *Chin. Chem. Lett.*, 2014, **25**, 1190–1192.

120 Y. Fu, Z. Lu, K. Fang, X. He, H. Huang and Y. Hu, *Bioorg. Med. Chem. Lett.*, 2019, **29**, 1236–1240.

121 Y. Ding, X. Xiang, M. Gu, H. Xu, H. Huang and Y. Hu, *Bioprocess Biosyst. Eng.*, 2016, **39**, 125–131.

122 Z. Wang, C.-Y. Wang, H.-R. Wang, H. Zhang, Y.-L. Su, T.-F. Ji and L. Wang, *Chin. Chem. Lett.*, 2014, **25**, 802–804.

123 H. Bavandi, Z. Habibi and M. Yousefi, *Bioorg. Chem.*, 2020, **103**, 104139.

124 M. Wilk, D. Trzepizur, D. Koszelewski, A. Brodzka and R. Ostaszewski, *Bioorg. Chem.*, 2019, **93**, 102816.

125 D. Koszelewski and R. Ostaszewski, *Chem.–Eur. J.*, 2019, **25**, 10156–10164.

126 Y. Wang, H. Cheng, J. R. He, Q. X. Yao, L. L. Li, Z. H. Liang and X. Li, *Catal. Lett.*, 2022, **152**, 1215–1223.

127 H. Zhao, *J. Chem. Technol. Biotechnol.*, 2016, **91**, 25–50.

128 B.-H. Xie, Z. Guan and Y.-H. He, *Biocatal. Biotransform.*, 2012, **30**, 238–244.

129 N. Sharma, U. K. Sharma, R. Kumar, N. Katoch, R. Kumar and A. K. Sinha, *Adv. Synth. Catal.*, 2011, **353**, 871–878.

130 K. S. Dalal, Y. A. Tayade, Y. B. Wagh, D. R. Trivedi, D. S. Dalal and B. L. Chaudhari, *RSC Adv.*, 2016, **6**, 14868–14879.

131 W. Hu, Z. Guan, X. Deng and Y.-H. He, *Biochimie*, 2012, **94**, 656–661.

132 J. Yu, X. Chen, M. Jiang, A. Wang, L. Yang, X. Pei, P. Zhang and S. G. Wu, *RSC Adv.*, 2018, **8**, 2357–2364.

133 Z.-Q. Liu, B.-K. Liu, Q. Wu and X.-F. Lin, *Tetrahedron*, 2011, **67**, 9736–9740.

134 W. Li, R. Li, X. Yu, X. Xu, Z. Guo, T. Tan and S. N. Fedosov, *Biochem. Eng. J.*, 2015, **101**, 99–107.

135 W. Li, S. N. Fedosov, T. Tan, X. Xu and Z. Guo, *ACS Catal.*, 2014, **4**, 3294–3300.

136 X. Garrabou, B. I. M. Wicky and D. Hilvert, *J. Am. Chem. Soc.*, 2016, **138**, 6972–6974.

137 M. Mogharabi-Manzari, M. Amini, M. Abdollahi, M. Khoobi, G. Bagherzadeh and M. A. Faramarzi, *ChemCatChem*, 2018, **10**, 1542–1546.

138 X. Liu, X. Li, Z. Wang, J. Zhou, X. Fan and Y. Fu, *ACS Sustainable Chem. Eng.*, 2020, **8**, 8206–8213.

139 T. Tokoroyama, *Eur. J. Org Chem.*, 2010, **2010**, 2009–2016.

140 S. C. Jha and N. N. Joshi, *ARKIVOC*, 2002, 167–196.

141 S. Witayakran and A. J. Ragauskas, *Eur. J. Org Chem.*, 2009, **2009**, 358–363.

142 J. Cai, Z. Guan and Y. He, *J. Mol. Catal. B: Enzym.*, 2011, **68**, 240–244.

143 B. Xie, Z. Guan and Y. He, *J. Chem. Technol. Biotechnol.*, 2012, **87**, 1709–1714.

144 Y. Yuan, L. Yang, S. Liu, J. Yang, H. Zhang, J. Yan and X. Hu, *Spectrochim. Acta, Part A*, 2017, **176**, 183–188.

145 J. Xu, F. Zhang, Q. Wu, Q. Zhang and X. Lin, *J. Mol. Catal. B: Enzym.*, 2007, **49**, 50–54.

146 J. Xu, F. Zhang, B. Liu, Q. Wu and X. Lin, *Chem. Commun.*, 2007, 2078–2080, DOI: 10.1039/b700327g.

147 L. Wu, L. Li, Y. Xiang, Z. Guan and Y. He, *Catal. Lett.*, 2017, **147**, 2209–2214.

148 B. List, *Angew. Chem., Int. Ed.*, 2010, **49**, 1730–1734.

149 E. Zandvoort, E. M. Geertsema, B.-J. Baas, W. J. Quax and G. J. Poelarends, *Angew. Chem., Int. Ed.*, 2012, **51**, 1240–1243.

150 Y. Miao, E. M. Geertsema, P. G. Tepper, E. Zandvoort and G. J. Poelarends, *ChemBioChem*, 2013, **14**, 191–194.

151 A. J. Boersma, R. P. Megens, B. L. Feringa and G. Roelfes, *Chem. Soc. Rev.*, 2010, **39**, 2083–2092.

152 S. Park and H. Sugiyama, *Angew. Chem., Int. Ed.*, 2010, **49**, 3870–3878.

153 S. Park and H. Sugiyama, *Molecules*, 2012, **17**, 12792–12803.

154 N. Duchemin, S. Aubert, J. V. de Souza, L. Bethge, S. Vonhoff, A. K. Bronowska, M. Smietana and S. Arseniyadis, *JACS Au*, 2022, **2**, 1910–1917.

155 P. M. Punt, M. D. Langenberg, O. Altan and G. H. Clever, *J. Am. Chem. Soc.*, 2021, **143**, 3555–3561.

156 H. Zhao and K. Shen, *RSC Adv.*, 2014, **4**, 54051–54059.

157 H. Zhao and K. Shen, *Biotechnol. Prog.*, 2016, **32**, 891–898.

158 K. Akagawa, R. Suzuki and K. Kudo, *Adv. Synth. Catal.*, 2012, **354**, 1280–1286.

159 K. Akagawa, T. Yamashita, S. Sakamoto and K. Kudo, *Tetrahedron Lett.*, 2009, **50**, 5602–5604.

160 K. Akagawa, R. Umezawa and K. Kudo, *Beilstein J. Org. Chem.*, 2012, **8**, 1333–1337.

161 E. Abdelraheem, B. Thair, R. F. Varela, E. Jockmann, D. Popadić, H. C. Hailes, J. M. Ward, A. M. Iribarren, E. S. Lewkowicz, J. N. Andexer, P.-L. Hagedoorn and U. Hanefeld, *ChemBioChem*, 2022, **23**, e202200212.

162 X. Yu and S.-M. Li, *ChemBioChem*, 2011, **12**, 2280–2283.

163 L. L. Kang Zhou and S.-M. Li, *J. Nat. Prod.*, 2015, **78**, 929–933.

164 X. Yu, A. Yang, W. Lin and S. Li, *Tetrahedron Lett.*, 2012, **53**, 6861–6864.

165 M. Liebhold, X. Xie and S. Li, *Org. Lett.*, 2012, **14**, 4882–4885.

166 E. E. Schultz, N. R. Braffman, M. U. Luescher, H. H. Hager and E. P. Balskus, *Angew. Chem., Int. Ed.*, 2019, **58**, 3151–3155.

167 J. Xue, J. Guo, Y. He and Z. Guan, *Asian J. Org. Chem.*, 2017, **6**, 297–304.

168 S. C. Hammer, J. M. Dominicus, P.-O. Syrén, B. M. Nestl and B. Hauer, *Tetrahedron*, 2012, **68**, 7624–7629.

169 S. Henche, B. M. Nestl and B. Hauer, *ChemCatChem*, 2021, **13**, 3405–3409.

170 R. B. Leveson-Gower, R. M. de Boer and G. Roelfes, *ChemCatChem*, 2022, **14**, e202101875.

171 A. Żądło-Dobrowolska, N. G. Schmidt and W. Kroutil, *ChemCatChem*, 2019, **11**, 1064–1068.

172 E. Siirola and W. Kroutil, *Top. Catal.*, 2014, **57**, 392–400.

173 S. Saranya, N. A. Harry, K. K. Krishnan and G. Anilkumar, *Asian J. Org. Chem.*, 2018, **7**, 613–633.

174 Z. Guan, J. Song, Y. Xue, D. Yang and Y. He, *J. Mol. Catal. B: Enzym.*, 2015, **111**, 16–20.

175 L. Wu, Y. Xiang, D. Yang, Z. Guan and Y. He, *Catal. Sci. Technol.*, 2016, **6**, 3963–3970.

176 D. Basavaiah, B. S. Reddy and S. S. Badsara, *Chem. Rev.*, 2010, **110**, 5447–5674.

177 S. Bjelic, L. G. Nivón, N. Çelebi-Ölçüm, G. Kiss, C. F. Rosewall, H. M. Lovick, E. L. Ingalls, J. L. Gallaher, J. Seetharaman, S. Lew, G. T. Montelione, J. F. Hunt, F. E. Michael, K. N. Houk and D. Baker, *ACS Chem. Biol.*, 2013, **8**, 749–757.

178 M. T. Reetz, R. Mondière and J. D. Carballeira, *Tetrahedron Lett.*, 2007, **48**, 1679–1681.

179 K. Asano and S. Matsubara, *Synthesis*, 2009, 3219–3226, DOI: 10.1055/s-0029-1216944.

180 N. Kato, T. Nogawa, R. Takita, K. Kinugasa, M. Kanai, M. Uchiyama, H. Osada and S. Takahashi, *Angew. Chem., Int. Ed.*, 2018, **57**, 9754–9758.

181 H. J. Kim, M. W. Ruszczycky, S. Choi, Y. Liu and H. Liu, *Nature*, 2011, **473**, 109–112.

182 A. Ichihara and H. Oikawa, *Curr. Org. Chem.*, 1998, **2**, 365–394.

183 H. Oikawa, K. Katayama, Y. Suzuki and A. Ichihara, *J. Chem. Soc., Chem. Commun.*, 1995, 1321–1322, DOI: 10.1039/C39950001321.

184 R.-R. Kim, B. Illarionov, M. Joshi, M. Cushman, C. Y. Lee, W. Eisenreich, M. Fischer and A. Bacher, *J. Am. Chem. Soc.*, 2010, **132**, 2983–2990.

185 G. Pohnert, *ChemBioChem*, 2003, **4**, 713–715.

186 J. M. Serafimov, H. C. Lehmann, H. Oikawab and D. Hilvert, *Chem. Commun.*, 2007, 1701–1703, DOI: 10.1039/B703177G.

187 J. M. Serafimov, D. Gillingham, S. Kuster and D. Hilvert, *J. Am. Chem. Soc.*, 2008, **130**, 7798–7799.

188 D. G. Gillingham, P. Stallforth, A. Adibekian, P. H. Seeberger and D. Hilvert, *Nat. Chem.*, 2010, **2**, 102–105.

189 M. J. Byrne, N. R. Lees, L.-C. Han, M. W. van der Kamp, A. J. Mulholland, J. E. M. Stach, C. L. Willis and P. R. Race, *J. Am. Chem. Soc.*, 2016, **138**, 6095–6098.

190 C. O. Marsh, N. R. Lees, L.-C. Han, M. J. Byrne, S. Z. Mbatha, L. Maschio, S. Pagden-Ratcliffe, P. W. Duke, J. E. M. Stach, P. Curnow, C. L. Willis and P. R. Race, *ChemCatChem*, 2019, **11**, 5027–5031.

191 D. J. Tantillo, *Org. Lett.*, 2010, **12**, 1164–1167.

192 M. Chandra and S. K. Silverman, *J. Am. Chem. Soc.*, 2008, **130**, 2936–2937.

193 B. Seelig and A. Jäschke, *Chem. Biol.*, 1999, **6**, 167–176.

194 T. M. Tarasow, S. L. Tarasow and B. E. Eaton, *Nature*, 1997, **389**, 54–57.

195 J. Xu, Q. Deng, J. Chen, K. N. Houk, J. Bartek, D. Hilvert and I. A. Wilson, *Science*, 1999, **286**, 2345–2348.

196 J. Chen, Q. Deng, R. Wang, K. Houk and D. Hilvert, *ChemBioChem*, 2000, **1**, 255–261.

197 M. Hugot, N. Bensel, M. Vogel, M. T. Reymond, B. Stadler, J.-L. Reymond and U. Baumann, *Proc. Natl. Acad. Sci. U. S. A.*, 2002, **99**, 9674–9678.

198 S. Müller, B. Appel, D. Balke, R. Hieronymus and C. Nübel, *F1000Research*, 2016, **5**, 1511.

199 M. R. Tremblay, T. J. Dickerson and K. D. Janda, *Adv. Synth. Catal.*, 2001, **343**, 577–585.

200 A. Serganov, S. Keiper, L. Malinina, V. Tereshko, E. Skripkin, C. Höbartner, A. Polonskaia, A. T. Phan, R. Wombacher, R. Micura, Z. Dauter, A. Jäschke and D. J. Patel, *Nat. Struct. Mol. Biol.*, 2005, **12**, 218–224.

201 M. Pohl, B. Lingen and M. Müller, *Chem.–Eur. J.*, 2002, **8**, 5288–5295.

202 A. S. Demir, P. Ayhan and S. B. Sopaci, *Clean*, 2007, **35**, 406–412.

203 F. Jordan, *Nat. Prod. Rep.*, 2003, **20**, 184–201.

204 M. Müller, G. A. Sprenger and M. Pohl, *Curr. Opin. Chem. Biol.*, 2013, **17**, 261–270.

205 S. Prajapati, F. R. von Pappenheim and K. Tittmann, *Curr. Opin. Struct. Biol.*, 2022, **76**, 102441.

206 M. Berheide, S. Kara and A. Liese, *Catal. Sci. Technol.*, 2015, **5**, 2418–2426.

207 D. Gocke, C. L. Nguyen, M. Pohl, T. Stillger, L. Walter and M. Müller, *Adv. Synth. Catal.*, 2007, **349**, 1425–1435.

208 I. F. Fernández, L. Hecquet and W.-D. Fessner, *Adv. Synth. Catal.*, 2022, **364**, 612–621.

209 P. P. Giovannini, P. Pedrini, V. Venturi, G. Fantin and A. Medici, *J. Mol. Catal. B: Enzym.*, 2010, **64**, 113–117.

210 M. Schapfl, S. Baier, A. Fries, S. Ferlaino, S. Waltzer, M. Müller and G. A. Sprenger, *Appl. Microbiol. Biotechnol.*, 2018, **102**, 8359–8372.

211 A. Kurutsch, M. Richter, V. Brecht, G. A. Sprenger and M. Müller, *J. Mol. Catal. B: Enzym.*, 2009, **61**, 56–66.

212 C. R. Müller, M. Pérez-Sáncheza and P. Domínguez de María, *Org. Biomol. Chem.*, 2013, **11**, 2000–2004.

213 P. Lehwald, O. Fuchs, L. A. Nafie, M. Müller and S. Lüdeke, *ChemBioChem*, 2016, **17**, 1207–1210.

214 M. Beigi, S. Waltzer, A. Fries, L. Eggeling, G. A. Sprenger and M. Müller, *Org. Lett.*, 2013, **15**, 452–455.

215 L. Wang, W. Song, B. Wang, Y. Zhang, X. Xu, J. Wu, C. Gao, J. Liu, X. Chen, J. Chen and L. Liu, *ACS Catal.*, 2021, **11**, 2808–2818.

216 K. Hernández, T. Parella, G. Petrillo, I. Usón, C. M. Wandtke, J. Joglar, J. Bujons and P. Clapés, *Angew. Chem., Int. Ed.*, 2017, **56**, 5304–5307.

217 X. Chen, Z. Wang, Y. Lou, Y. Peng, Q. Zhu, J. Xu and Q. Wu, *Angew. Chem., Int. Ed.*, 2021, **60**, 9326–9329.

218 Y. Li, N. Hu, Z. Xu, Y. Cui, J. Feng, P. Yao, Q. Wu, D. Zhu and Y. Ma, *Angew. Chem., Int. Ed.*, 2022, **61**, e202116344.

219 Y. Li, P. Yao, S. Zhang, J. Feng, H. Su, X. Liu, X. Sheng, Q. Wu, D. Zhu and Y. Ma, *Chem Catal.*, 2023, **3**, 100467.

220 C. S. Yeung and V. M. Dong, *Chem. Rev.*, 2011, **111**, 1215–1292.

221 V. Resch, J. H. Schrittwieser, S. Wallner, P. Macheroux and W. Kroutil, *Adv. Synth. Catal.*, 2011, **353**, 2377–2383.

222 W. Hüttel and M. Müller, *Nat. Prod. Rep.*, 2021, **38**, 1011–1043.

223 A. Präg, B. A. Grüning, M. Häckh, S. Lüdeke, M. Wilde, A. Luzhetskyy, M. Richter, M. Luzhetska, S. Günther and M. Müller, *J. Am. Chem. Soc.*, 2014, **136**, 6195–6198.

224 L. E. Zetzsche, J. A. Yazarians, S. Chakrabarty, M. E. Hinze, L. A. M. Murray, A. L. Lukowski, L. A. Joyce and A. R. H. Narayan, *Nature*, 2022, **603**, 79–85.

225 Z. Guo, P. Li, G. Chen, C. Li, Z. Cao, Y. Zhang, J. Ren, H. Xiang, S. Lin, J. Ju and Y. Chen, *J. Am. Chem. Soc.*, 2018, **140**, 18009–18015.

226 T. Katagiri and Y. Amao, *Green Chem.*, 2020, **22**, 6682–6713.

227 Q. Yang, X. Guo, Y. Liu and H. Jiang, *Int. J. Mol. Sci.*, 2021, **22**, 1890.

228 Y. Amao, S. Ikeyama, T. Katagiri and K. Fujita, *Faraday Discuss.*, 2017, **198**, 73–81.

229 T. Katagiri, K. Fujita, S. Ikeyama and Y. Amao, *Pure Appl. Chem.*, 2018, **90**, 1723–1733.

230 H. Hamby, B. Li, K. E. Shinopoulos, H. R. Keller, S. J. Elliott and G. Dukovic, *Proc. Natl. Acad. Sci. U.S.A.*, 2020, **117**, 135–140.

231 Y. Amao, *Chem. Lett.*, 2017, **46**, 780–788.

232 L. Castañeda-Losada, D. Adam, N. Paczia, D. Buesen, F. Steffler, V. Sieber, T. J. Erb, M. Richter and N. Plumeré, *Angew. Chem., Int. Ed.*, 2021, **60**, 21056–21061.

233 J. Zhou, X. Tian, Q. Yang, Z. Zhang, C. Chen, Z. Cui, Y. Ji, U. Schwaneberg, B. Chen and T. Tan, *Chem Catal.*, 2022, **2**, 2675–2690.

234 J. Yang, W. Song, T. Cai, Y. Wang, X. Zhang, W. Wang, P. Chen, Y. Zeng, C. Li, Y. Sun and Y. Ma, *Sci. Bull.*, 2023, **68**, 2370–2381.

235 V. P. Willers, M. Döring, B. Beer and V. Sieber, *Chem Catal.*, 2023, **3**, 100502.

236 T. Cai, H. Sun, J. Qiao, L. Zhu, F. Zhang, J. Zhang, Z. Tang, X. Wei, J. Yang, Q. Yuan, W. Wang, X. Yang, H. Chu, Q. Wang, C. You, H. Ma, Y. Sun, Y. Li, C. Li, H. Jiang, Q. Wang and Y. Ma, *Science*, 2021, **373**, 1523–1527.

237 B. Fu and E. P. Balskus, *Curr. Opin. Biotechnol.*, 2020, **65**, 94–101.

238 K. Yokoyama and E. A. Lilla, *Nat. Prod. Rep.*, 2018, **35**, 660–694.

239 F. Himo, *Biochim. Biophys. Acta*, 2005, **1707**, 24–33.

240 Y. Fu, H. Chen, W. Fu, M. Garcia-Borràs, Y. Yang and P. Liu, *J. Am. Chem. Soc.*, 2022, **144**, 13344–13355.

241 H. Pang, E. A. Lilla, P. Zhang, D. Zhang, T. P. Shields, L. G. Scott, W. Yang and K. Yokoyama, *J. Am. Chem. Soc.*, 2020, **142**, 9314–9326.

242 V. G. Dumas, L. A. Defelipe, A. A. Petruk, A. G. Turjanski and M. A. Marti, *Proteins*, 2014, **82**, 1004–1021.

243 M. Szaleniec and J. Heider, *Int. J. Mol. Sci.*, 2016, **17**, 514.

244 Y. Hai, M. Chen, A. Huang and Y. Tang, *J. Am. Chem. Soc.*, 2020, **142**, 19668–19677.

245 M. Liu, D. Wei, Z. Wen and J. Wang, *Front. Bioeng. Biotechnol.*, 2021, **9**, 653682.

246 K. Koch, R. J. F. van den Berg, P. J. Nieuwland, R. Wijtmans, H. E. Schoemaker, J. C. M. van Hest and F. P. J. T. Rutjes, *Biotechnol. Bioeng.*, 2008, **99**, 1028–1033.

247 M. Hashimoto, S. Watari, T. Taguchi, K. Ishikawa, T. Kumamoto, S. Okamoto and K. Ichinose, *Angew. Chem., Int. Ed.*, 2023, **62**, e202214400.

248 R. K. Zhang, K. Chen, X. Huang, L. Wohlschlager, H. Renata and F. H. Arnold, *Nature*, 2019, **565**, 67–72.

249 R. D. Shukla, B. Rai and A. Kumar, *Eur. J. Org Chem.*, 2019, **2019**, 2864–2868.

250 E. Busto, R. C. Simon and W. Kroutil, *Angew. Chem., Int. Ed.*, 2015, **54**, 10899–10902.

251 A. Chen, Z. Jiang and M. D. Burkart, *Chem. Sci.*, 2022, **13**, 4225–4238.

252 W. Li, G. C. Girt, A. Radadiya, J. J. P. Stewart, N. G. J. Richards and J. H. Naismith, *Open Biol.*, 2023, **13**, 220287.

253 H. Tang, M.-H. Wu, H.-Y. Lin, M.-R. Han, Y.-H. Tu, Z.-J. Yang, T.-C. Chien, N.-L. Chan and W.-c. Chang, *Proc. Natl. Acad. Sci. U.S.A.*, 2022, **119**, e2113770119.

254 C.-C. Chen, L. Zhang, X. Yu, L. Ma, T.-P. Ko and R.-T. Guo, *ACS Catal.*, 2020, **10**, 4717–4725.

255 E. T. Batchelar, R. B. Hamed, C. Ducho, T. D. W. Claridge, M. J. Edelmann, B. Kessler and C. J. Schofield, *Angew. Chem., Int. Ed.*, 2008, **47**, 9322–9325.